2019

Enhancing Aldehyde Detoxification as a Novel Therapy for Liver Fibrosis and Acetaminophen-Induced Liver Injury

Hereward John Wimborne
Medical University of South Carolina

Enhancing Aldehyde Detoxification as a Novel Therapy for Liver Fibrosis and Acetaminophen-Induced Liver Injury.

by

Hereward John Clifford Wimborne

A dissertation submitted to the faculty of the Medical University of South Carolina in partial fulfillment of the requirements for the degree of Doctor of Philosophy in the College of Graduate Studies

Program in Drug Discovery and Biomedical Sciences

2019

Approved by:

Chairman, Advisory Committee _____
Zhi Zhong

Co-Chairman, Advisory Committee _____
John J. Lemasters

_____
Don C.Rockey

_____
Craig C. Beeson

_____
Stephen Duncan

DEDICATION

This work is dedicated to my family, for all of their love and support:

To my wife, Layla: You have dealt with all of the frustrating challenges of my graduate career right along with me and encouraged me when the challenges seemed insurmountable. You have shown me courage in challenging me to continue and standing with me in the rain when things needed to be done. Together we succeeded and will continue to succeed.

For my daughters, Alia and Jenna: You have brightened the darkest days with laughter, fun, and a child's wonder and mischief. The best is yet to come.

For my father, Ward, who passed before I could complete my graduate training: You have been an inspiration and role model throughout my career. You set an almost impossible standard, and then expected me to rise to the challenge. While you never made me feel unworthy, I hope this dissertation and my life in general stand as an acceptable addition to your legacy and that of our fathers. We will keep moving forward.

ACKOWLEDGEMENTS

I would like to thank Dr. Zhi Zhong and Dr. John J. Lemasters, for overseeing this work, and well as Dr. Patrick Woster and Dr. Yuri Peterson for critical mentoring and moral support during this training period. I would further like to thank my committee members: Dr. Don Rockey, Dr. Craig Beeson, and Dr. Stephen Duncan for their contributions to the development and execution of this work. I would also like to thank Dr. Hartmut Jaeschke and Ms. Nga Nguyen for assistance with NAPQI adduct and JNK assays for the acetaminophen studies. Countless additional people have contributed advice, technical assistance, and moral support. I would like to directly thank my laboratory colleagues, including Dr. Kenji Takemoto, Dr. Jiangting Hu, Dr. David Dehart, and Dr. Li Li from Dr. Lemasters's Lab, Yasodha Krishnasamy from Dr. Zhong's Lab, and Dr. Loretta Jophlin, and Dr. Sweta Singh formerly of Dr. Rockey's Lab. All of these wonderful people have contributed directly to the research published herein.

Thanks are also due for assistance in learning background concepts and techniques that were instrumental in my graduate training. For this I thank Dr. Monika Gooz in the imaging core for her technical assistance, Gyda Beeson for her assistance with the Seahorse instrument, and Dr. Rick Schnellmann and members of his lab including Dr. Jenny Blakely, Mr. Rob Cameron, Dr. Sean Jesinkey, and Dr. Jay Stallons, for their assistance with laboratory techniques and procedures.

I have also benefitted from the support of friends and family outside the lab. I offer my heartfelt thanks to my mother- and father-in-law, Tahrir and Gihad, and my brothers- and sister-in-law John, Oday, Hamid, Hussam, Marianne, Zeyd, and Steve have been a

huge support for both Layla and me. I also thank my mother, Maree, and brother, Powell-Wesley, who have also been supportive.

This work was supported, in part, by the National Institutes of Health [grant numbers F31DK108570, T32DK083262, AA021191, AA025379, DK037034 and DK073336. The Cell & Molecular Imaging Core of the Hollings Cancer Center at the Medical University of South Carolina was supported by the National Institutes of Health [grant numbers 1P30 CA138313, and S10 OD018113, and provided instrumentation for microscopy.

TABLE OF CONTENTS

TABLE OF FIGURES

ABSTRACT

HEREWARD JOHN CLIFFORD WIMBORNE. Enhancing Aldehyde Detoxification as a Novel Therapy for Liver Fibrosis and Acetaminophen-Induced Liver Injury (under the direction of Zhi Zhong and John J. Lemasters).

Oxidative stress is a common component and important mediator in the pathogenesis of many liver injuries and of liver fibrosis. Although reactive oxygen species (ROS) are known to have effects on many important biological macromolecules and cell organelles, such as mitochondria, how oxidative stress causes liver injury/fibrosis has not been fully elucidated. ROS oxidize membrane lipids to form lipid radicals which undergo ß-scission to form aldehydes, such as malondialdehyde (MDA) and 4-hydroxynonenal (4-HNE). These aldehydes are highly reactive and readily form adducts with proteins and nucleic acids. Relatively little is known about the role of aldehydes in the pathogenesis of liver injury.

A key observation in the field is that aldehyde adducts appear to form on certain critical mitochondrial proteins. Since mitochondria are a major source of ROS in cells, I tested the hypothesis that activation of mitochondrial aldehyde dehydrogenase-2 (ALDH2) would accelerate aldehyde detoxification and thus attenuate liver injury and fibrosis. I examined the effects of Alda-1, a chemical chaperone and activator of ALDH2, in two animal models: acetaminophen (APAP) overdose, which causes acute liver failure, and bile duct ligation (BDL), which causes cholestatic liver injury and fibrosis leading to chronic liver failure. Previous studies have shown that oxidative stress plays an important role in the liver injury and fibrosis in these models.

In an APAP hepatotoxicity model, mice received Alda-1 (20 mg/kg, i.p.) or vehicle 30 minutes before administration of APAP (300 mg/kg, i.p.). 4-HNE protein adducts markedly increased after APAP treatment, demonstrating increased production of aldehydes, which Alda-1 decreased by 86%. Serum alanine aminotransferase (ALT) increased to 7594 U/L, and centrilobular necrosis occurred in 47% of liver tissue after APAP, indicating severe liver injury. Alda-1 decreased ALT and necrosis by 72% and 56% respectively. Previous studies have demonstrated that formation of *N*-acetyl-*p*-benzoquinone imine (NAPQI) protein adducts, activation of c-Jun-*N*-terminal kinase (JNK) and the mitochondrial permeability transition (MPT) are linked to APAP hepatotoxicity. After APAP treatment, NAPQI protein adducts and JNK phosphorylation increased six-fold, which Alda-1 did not alter. Without APAP, intravital microscopy revealed that no mitochondrial depolarization could be detected. At 6 h after APAP, 62% of tissue areas showed depolarization, which was decreased by nearly half with Alda-1 treatment. Therefore, Alda-1 decreased APAP hepatotoxicity not by alteration of APAP metabolism or blockade of JNK activation but by protecting against mitochondrial dysfunction.

Cholestasis in mice was induced by BDL. After BDL, 4-HNE adduct formation increased almost six-fold, which Alda-1 decreased to baseline levels. ALT increased to 537 U/L, and biliary infarcts occurred after BDL, consistent with the expected mechanism of liver injury. Alda-1 blunted ALT by half and decreased the area of biliary infarcts from 7.8% to 1.9%. Fibrosis occurred after BDL, as detected in liver sections by increased picrosirius red staining and second harmonic generation microscopy. Collagen-I mRNA also increased 12-fold after BDL. Alda-1 decreased each of these measures of fibrosis by approximately 50%. Expression of smooth muscle α-actin (α-SMA), a marker of activated

myofibroblasts, the cell type that produces collagen, increased ~19-fold after BDL, which Alda-1 limited to a 5-fold increase. Alda-1 also decreased macrophage infiltration by approximately 50% and expression of the proinflammatory and profibrotic protein osteopontin (OPN), by 64%.

Taken together, these data demonstrate that aldehydes are important mediators of liver injury caused by APAP intoxication and of both liver injury and fibrosis caused by cholestasis. Therefore, acceleration of aldehyde degradation by ALDH2 with Alda-1 is a potential new effective therapy to decrease liver injury/fibrosis related to high oxidative stress.

Chapter 1: Introduction and Background

OXIDATIVE STRESS, LIPID PEROXIDATION, AND ALDEHYDES

Introduction

Reactive oxygen species (ROS) play an important role in immune responses [1-4], maintenance of redox homeostasis [1-5], stem cell development [5], autophagy, apoptosis [1-5], and other processes under normal conditions. ROS are critical signaling molecules involved in multiple pathways, including nuclear factor kappa-light-chain-enhancer of activated B cells (NF-κB), mitogen-activated protein kinase (MAPK), Kelch-like ECH-associated protein 1-nuclear factor erythroid 2-related factor-antioxidant response element (Keap1-Nrf2-ARE), phosphoinositide 3-kinase-protein kinase B (PI3K-Akt), and protein kinases of ubiquitination/proteasome systems, as well as in regulation of calcium ion channels and the mitochondrial permeability transition pore (MPTP) [4]. Production of ROS can be increased by xenobiotics and various stress/disease situations [6]. Excessive ROS, such as superoxide anion ($O_2^{\bullet -}$), hydroxyl radical (•OH) and hydrogen peroxide (H_2O_2), can cause tissue damaging effects, such as lipid peroxidation and damage to DNA and protein [1-3, 5]. Oxidative stress associated with increased production of ROS is involved not only in the toxicity of xenobiotics and radiation damage but also in the pathophysiology of aging and in many diseases and injuries, including cancer, diabetes, atherosclerosis, Alzheimer's disease, various inflammatory diseases and ischemia/reperfusion injury in different organs [7-17].

Oxidative stress also plays an important role in the pathogenesis of numerous acute and chronic liver diseases/injuries, including alcoholic and non-alcoholic fatty liver diseases, cholestatic liver diseases, hepatotoxicity of drugs and chemicals (e.g., acetaminophen, paraquat, etc), inflammatory liver diseases, liver fibrosis, liver cancer,

liver injury due to hereditary diseases (e.g., hereditary hemochromatosis and Wilson's disease), and hepatic ischemia/reperfusion injury (e.g., trauma, hemorrhagic shock, and primary liver graft non-function after liver transplantation) [18-28]. Massively increased ROS may cause cell destruction by lipid peroxidation. However, in many cases, ROS work by alteration of signal transduction pathways, thus affecting redox-sensitive enzymes, organelles (e.g., mitochondria) and transcription factors. Examples of redox sensitive signaling includes hypoxia-inducible factor-1 alpha (HIF1-α), which increases transcription of proteins adapted to low-oxygen conditions, mammalian target of rapamycin (mTOR) activation, which regulates cellular growth, and NF-κB, which is a key regulator of cell survival and inflammation [2, 5]. Despite extensive research, how oxidative stress causes liver injury is not fully understood. In this project, I focused on the role of aldehydes generated by lipid peroxidation in mitochondria in the pathogenesis of liver injury and fibrosis [3, 29].

The chemistry of reactive oxygen species

ROS are generated by many cellular/enzymatic sources. Resident macrophages (e.g., Kupffer cells in the liver), infiltrating monocytes and polymorphonuclear leukocytes (neutrophils, PMN) produce $O_2^{\bullet-}$ via the action of NADPH oxidase (NOX) [13]. ROS can also be produced intracellularly in almost every liver cell type via various enzymes and organelles, including P450 enzymes, xanthine oxidase, NOX, endoplasmic reticulum, peroxisomes, and mitochondria [2, 4, 30].

The primary free radical generated by single-electron reduction of oxygen is $O_2^{\bullet-}$ [1, 3, 4]. This occurs in Complex I and III of the mitochondrial electron transport chain and by enzymatic reactions catalyzed by NOX, cytochrome P450, xanthine oxidase and others

[3, 4]. $O_2^{\bullet-}$ is moderately reactive under physiological conditions, but its diffusion-limited reaction with nitric oxide (described below) yields highly reactive peroxynitrite [3]. $O_2^{\bullet-}$ is converted to H_2O_2 and water by superoxide dismutase (SOD) [1-3, 5]. H_2O_2 is a longer-lived species than H_2O_2 and can diffuse across membranes [1-3, 5]. In the presence of transition metals such as iron and copper, the Haber-Weiss/Fenton reaction occurs, in which ferrous iron (Fe^{2+}) or cuprous copper (Cu^{+}) reacts with H_2O_2 to produce ferric iron (Fe^{3+}) or cupric copper (Cu^{2+}), respectively, and •OH and hydroxide ion (OH^-) [1-3, 31]. $O_2^{\bullet-}$ then reacts with Fe^{3+} (or Cu^{2+}) to regenerate Fe^{2+} (or Cu^{2+}). The iron-catalyzed Haber-Weiss reaction is also called the Fenton reaction. •OH is much more reactive than $O_2^{\bullet-}$ and consequently is extremely short-lived (10^{-9} s). •OH reacts with virtually the first thing it collides with other than water and thus is damaging to cellular components, including proteins, lipids, and nucleic acids.

H_2O_2 can also react with chloride ion (Cl^-) to produce hypochlorous acid [1-3]. This reaction commonly occurs in neutrophils and is catalyzed by myeloperoxidase [2, 3]. The reactions yielding ROS as mentioned above are summarized in **Figure 1-1**.

Interaction of Reactive Oxygen Species with Reactive Nitrogen Species

Investigations into redox homeostasis and oxidative stress have also uncovered the importance of reactive nitrogen species (RNS), which originate with the production of nitric oxide ($NO^{\bullet}$) [2, 3]. Nitric oxide is produced by nitric oxide synthases (NOS), including endothelial (eNOS), inducible (iNOS), and neuronal (nNOS) [3]. eNOS and nNOS are “constitutively” active and localized largely to endothelial and neuronal cells, respectively. In contrast, iNOS expression is widespread and is stimulated is by inflammatory cytokines and lipopolysaccharide [2, 3]. $NO^{\bullet}$ reacts with $O_2^{\bullet-}$ to form peroxynitrite ($ONOO^-$).

Peroxynitrite is a strong oxidant that reacts with thiol groups and iron centers in proteins; thus, it reacts readily with antioxidant defenses [3]. Peroxynitrite is a dangerous species in excess because it damages proteins through tyrosine nitration, undergoes lipid peroxidation with membranes forming aldehydes, damages nucleic acids, and causes cellular damage and mitochondrial dysfunction through all of these means [3]. Further, peroxynitrite can decompose into highly reactive radicals [3]. The reactions of NO in RNS formation are summarized in **Figure 1-1.**

Non-enzymatic and enzymatic defenses against oxidative stress

The presence of so much ROS means cells have extensive antioxidant defenses. Non-enzymatic antioxidant defenses include all-trans retinol 2 (vitamin A), ascorbic acid (vitamin C), α-tocopherol (vitamin E), ß-carotene, and glutathione (GSH), which act as free radical scavengers [1]. Enzymatic defenses include superoxide dismutase (SOD) which catalyzes the conversion of $O_2^{\bullet-}$ to H_2O_2 and O_2, two less damaging species. In mammals and most chordates, there are three isoforms of SOD: SOD1, a copper-zinc (Cu-Zn) SOD in the cytosol. SOD2, a manganese (Mn) SOD in the mitochondrial matrix, and SOD3, a Cu-Zn SOD in the extracellular space [1, 3, 4]. H_2O_2 must also be detoxified, not only because it can cause cellular damage when converted to •OH by transition metals, but also because, unlike $O_2^{\bullet-}$, it can cross membranes [3, 4]. H_2O_2 is detoxified by catalase or glutathione peroxidase [1, 3, 4]. Thioredoxin, peroxiredoxin and the glutathione system among others all support antioxidant defense [1, 3, 4].

GSH and its maintenance system are key antioxidant defenses in cells, but GSH also participates in iron-sulfur cluster biogenesis, protein disulfide bond reduction, and toxic electrophile detoxification [32]. GSH contains a thiol group that can donate a reducing

equivalent and reacts with other GSH molecules to form glutathione disulfide (GSSH), the oxidized form of GSH [32]. GSH is used as a substrate for the glutaredoxin (Grx), glutathione-S-transferases (Gst) and glutathione peroxidases (Gpx). GSSH is restored to GSH by the glutathione reductase (Glr) using NAD(P)H as an electron donor [32].

Mitochondria as sources of oxidative stress

Mitochondria are a major source of ROS in the cell [33, 34]. Mitochondria contain or generate electrons, free radicals, O_2 and iron, which is a dangerous combination of materials in a high redox environment. During mitochondrial respiration, some electrons escape the electron transport chain prematurely to form $O_2^{\bullet-}$ [33, 34]. Complex I and Complex III can produce $O_2^{\bullet-}$, and this electron leak is increased if electron flow is interrupted or if respiration is activated [35, 36]. Mitochondrial SOD2 (MnSOD) scavenges $O_2^{\bullet-}$ to produce O_2 and H_2O_2. Increased ROS production promotes pathological processes in many diseases and in aging [33]. The dangers of ROS are compounded by RNS. Increased RNS production in mitochondria also occurs in cancer, inflammatory diseases, aging, and many liver disease [37-43].

Lipid peroxidation and aldehyde formation

Since mitochondria are a major source of ROS, the two phospholipid membranes of mitochondria are primary targets of lipid peroxidation, especially the mitochondrial inner membrane with its high content of unsaturated phospholipids [29]. Lipid peroxidation occurs when free radicals react with polyunsaturated lipids to form unstable lipid radicals, which then react with O_2 to form lipid-peroxyl radicals that propagate via free radical chain reactions forming lipid peroxides (**Figure 1-1**) [3]. While some lipid peroxides continue to

propagate the free radical chain reactions, others undergo ß-scission to form aldehydes, which form adducts with biomolecules including proteins and DNA.

Many different aldehydes are formed from lipid peroxidation, including malondialdehyde (MDA) (3 carbons, 2 carbonyl groups), acrolein (3-carbons, 1 carbonyl group, and 4-hydroxy-2-nonenal (4-HNE, 9 carbons, one carbonyl group), among others [3, 44]. As chain length increases, the aldehydes become more lipophilic, and aliphatic aldehydes with 8 carbons (octanals) or more are considered fatty aldehydes. Cyclization of aldehydes can also occur. Aldehydes are generated under oxidative stress and so are suspected to play a role in multiple ROS-associated pathologies, including in heart and liver diseases [29, 45-53]. Acrolein, 4-HNE, and MDA, for example, can form 1,4-Michael adducts with nucleophiles, including proteins and DNA, to inhibit enzyme function and cause genotoxicity [44]. Lipid peroxidation is summarized in **Figure 1-1**.

Common aldehydes of biological/pathological importance

Acrolein is a three-carbon aldehyde with one carbonyl group [44] (**Figure 1-2)**. Acrolein reacts much more readily with the thiol groups of cysteine residues in protein and depletes GSH during its detoxification. Acrolein is detected in plasma of patients with neurodegenerative disorders, atherosclerosis and chronic obstructive lung disease [54-57] .

Malondialdehyde (MDA) is a three-carbon aldehyde with two carbonyls [44] (**Figure 1-2**). A product of lipid-peroxidation, MDA forms adducts with nucleic acids and lysine residues of proteins. Acetaldehyde, a product of ethanol metabolism, and MDA react together to form hybrid proteins adducts called MAA adducts. MAA adducts exist in

low levels in normal situations but increase markedly after alcohol consumption [44]. MAA adducts are shown to cause inflammatory, fibrogenic, and immune responses [44].

4-HNE (**Figure 1-2)** displays high biological activity and its adducts are measurable in blood or tissues in a wide variety of ROS-related diseases, including metabolic diseases, I/R injury in many different organs, alcoholic liver disease, cardiovascular diseases, various chronic inflammatory diseases, and Alzheimer's disease [25, 44-48, 50, 52, 58-61]. In addition, 4-HNE promotes onset of the MPT, mitophagy, and other mitochondrial stress responses [53, 58, 59].

Aldehyde dehydrogenases and aldehyde dehydrogenase-2

Aldehyde dehydrogenases (ALDH) are NAD(P^+)-dependent enzymes that catalyze the oxidation of aldehydes to carboxylic acids. They also serve multiple biological functions beyond aldehyde detoxification, including roles in embryogenesis and maintaining the cornea of the eye [62, 63]. Humans express nineteen different ALDH genes (**Table 1-1**), but many are cell-type and tissue specific [62, 63]. Two isoforms are expressed in high levels in the liver: ALDH1 localized to cytosol and ALDH2 localized to the mitochondrial matrix [64].

ALDH2 was originally studied in terms of alcohol metabolism, but as aldehydes and their biological effects in many diseases have come to light, ALDH2 has become increasingly important as a key enzyme in detoxifying aldehydes in environments with high oxidative stress, including I/R in different organs (e.g., heart, liver, brain, lung), chronic ethanol consumption, and radiation-induced dermatitis [61, 63, 65-68]. Mitochondria are a major source of ROS generation and have phospholipid membranes vulnerable to lipid peroxidation. As a result, aldehyde production is likely high in mitochondria. Therefore,

mitochondrial ALDH2 plays a crucial role for detoxification of oxidative stress-produced aldehydes. Previous studies show that the decreases and increases of ALDH2 activity increase and decreases, respectively, protein adducts of acrolein, MDA, or 4-HNE, demonstrating that all these three aldehydes are substrates for ALDH2, although with increasing K_m as chain-length increases [69].

There are two common ALDH2 polymorphisms, ALDH2*1 and ALDH2*2 (also known as the rs671 polymorphism) [61, 70-72]. The active form (wild-type) of ALDH2 is a homotetramer of ALDH2*1 gene products with NAD+ as its cofactor [73]. The gene product of ALDH2*2 has low affinity for binding of the NAD^+ cofactor [73]. Any copy of the ALDH2*2 gene product in a ALDH tetramer decreases the activity of the enzyme by 60% vs. wild-type, whereas homotetramers of all ALDH2*2 gene products only have 10% activity compared to wild-type [61]. The decreased activity due to the ALDH2*2 polymorphism is responsible for development of Asian flushing syndrome due to impaired clearance of acetaldehyde [61]. The east Asian population with a high incidence of ALDH2*2 polymorphism show increased incidence of cancer, susceptibility to alcohol related liver injury, and a higher risk of epilepsy after stroke [74-77]. Moreover, ALDH2 insufficiency is also associated with higher risk of cancer in the digestive system, environment-induced and smoking-induced lung cancers, osteoporosis and impaired recovery from heart attack and stroke [70-72, 78-80]. ALDH2 knockout mice are more susceptible to ethanol-induced liver injury, inflammation and fibrosis [81-83].

Aldehyde dehydrogenase-2 activation by Alda-1

A collaboration between Dr. Daria Mochley-Rosen's group at Stanford University and Dr. Thomas Hurley's group at Indiana University, utilizing a high throughput screen,

discovered a small molecule activator of ALDH2, Alda-1, which increases activity of both wild-type ALDH2*1 and ALDH2*2 in *vitro* and in an *ex vivo* heart I/R model [61].

ALDH2 is a flavin-dependent homotetramer that has a substrate binding site and nicotinamide binding cleft forming a tunnel through the enzyme. The ALDH2 activator Alda-1 binds near this substrate binding tunnel with its hydrophobic bezodioxol attracted by a group of hydrophobic aromatic amino acids [73]. Alda-1 binding causes a conformational change that restores cofactor binding by correcting the conformational defect in the ALDH2*2 enzyme. In wild type ALDH2, Alda-1 binding increases the rate of the oxidation of the acyl-enzyme intermediate by improving the orientation of the catalytic centers [73]. Alda-1 increases homotetrameric ALDH2*2 activity from less than 10% activity to roughly 30%, restores the activity of heterotetramers of ALDH2*2 and ALDH2*1 to almost 100% of the wild-type, and doubles wild-type (homoteramers of ALDH2*1) ALDH2 activity [61].

Alda-1 shows beneficial effects in a number of models of injury related to ROS and lipid peroxidation, including I/R injury in several organs (heart, lung, brain, intestinal, liver), radiation-induced dermatitis, and alcohol-induced liver steatosis [65-67, 84-88]. However, the role of aldehydes in many other liver diseases remains unclear. In this study, I used Alda-1 as a tool to examine the role of aldehydes in drug hepatotoxicity and liver fibrosis and to evaluate the possibility of enhancing aldehyde detoxification by ALDH2 activation as a treatment modality for liver injury.

MITOCHONDRIAL BIOLOGY

Introduction

Mitochondria are best known for their metabolic functions, such as ATP synthesis by oxidative phosphorylation, but mitochondria also play important roles in signaling that regulates cell death, cell cycle, cell growth and differentiation, inflammation and fibrosis. [89]. Understanding how mitochondria work is critical to understanding their role in oxidative stress and liver injury.

Structure of Mitochondria

The mitochondrion is a dual-bilayer system, as detailed in **Figure 1-3**. The outer mitochondrial membrane (OMM) is a composed of phospholipid bilayer with embedded proteins. The types and proportions of specific proteins present in the two mitochondrial membranes vary with the species of animals and differentiation of cells. OMM can interface with the endoplasmic reticulum (ER) at mitochondria-associated ER membranes (MAM) [90]. These MAM play a role in regulation of calcium homeostasis, lipid synthesis and transport, autophagy and mitophagy, and apoptosis [90].

OMM also has proteins responsible for transport of molecules in and out of mitochondria. The translocase of the outer membrane (TOM) complex, together with translocase of the inner membrane complex (TIM), is responsible for import of nuclear-encoded mitochondrial proteins and signaling molecules (e.g. transcription factors) into mitochondria [91]. There are also other proteins that serve as channels or specific translocation receptors for metabolites, ions, and precursor proteins. The most abundant of these are the voltage-dependent anion channel (VDAC) [92]. VDAC forms a barrel

enclosing a ~2.5 nm aqueous channel. Except for a relatively few small membrane-permeant lipophilic compounds, most substrates and metabolites of mitochondrial metabolism (e.g., NADH, ATP, ADP, Pi, long-chain acyl CoA, cholesterol, ureagenesis substrates, some ions, etc.) that enter and leave mitochondria must cross the OMM through VDAC [93-95]. VDAC is generally assumed to be open during mitochondrial metabolism. However, under certain circumstances VDAC can close, thus inhibiting metabolite exchange [96-99]. Therefore, VDAC is considered as a 'governator' of global mitochondrial function [92, 98, 100]. In addition, VDAC closure can lead to steatosis by suppression of entry of long-chain fatty acids into mitochondria for β-oxidation and can also increase mitochondrial oxidative stress by decreasing entry of GSH into mitochondria. There are three VDAC isoforms in humans [101]. Functionally, all three VDAC isoforms transfer metabolites. VDAC2 possibly also plays a role in the import of apoptotic BCL-2 family proteins [102]. Cysteine residues of VDAC3 are often modified by ROS and may serve a signaling role in oxidative stress and mitophagy [92, 101, 103].

Invaginations in the inner mitochondrial membrane (IMM) give rise to the cristae [104]. The complexes of the electron transport chain (ETC) are embedded in the cristae membrane, and proteins necessary for the maintenance of ETC proteins and electron carriers for the ETC are resident in the cristae. IMM also contains a numbers of transporters, such as the TIM complexes, the mitochondrial calcium uniporter (MCU) complex, the adenine nucleotide translocator (ANT) and the mitochondrial citrate transporter (CIC) [104].

Inside of the IMM is the mitochondrial matrix which contains enzymes and substrates feeding into the ETC and responsible for a wide variety of other metabolism

(e.g., citric acid cycle, urea cycle, and beta-oxidation reactions). Moreover, mitochondrial DNA (mtDNA) in the matrix space codes for 37 genes, including 13 protein subunits of various enzymes required for oxidative phosphorylation [105]. Due to the lack of histones, mtDNA is more vulnerable to ROS attack [106]. Mitochondrial ribosomes translate mRNA to protein that can be integrated directly into the IMM [107]. The matrix also contains enzymes necessary for DNA replication, transcription, and translation, but these proteins are encoded by nuclear DNA and are imported from the cytosol by TIM and TOM complexes. Between the OMM and IMM is the intermembrane space (IMS) [104]. Pro-apoptotic proteins such as apoptosis inducing factor (AIF), Smac/Diablo, and cytochrome *c* exist in IMS, and can stimulate cell death upon release [104, 108-112]. IMM and OMM are attached physically to one another at contact sites [113].

Mitochondrial Metabolism and the Electron Transport Chain

Catabolism of carbohydrates, fatty acids, and proteins converge on acetyl-coenzyme A (acetyl-CoA) [114]. Pyruvate formed by glycolysis is imported into the matrix where it is oxidized by pyruvate dehydrogenase to form acetyl-CoA [115, 116]. Fatty acids are bound to coenzyme A (CoA) by CoA ligase enzymes. Short chain fatty acids diffuse freely across the mitochondrial membranes, but long chain fatty acids enter mitochondria through VDAC and the carnitine shuttle for transport into mitochondrial matrix. Inside mitochondria, ß-oxidation of acyl-CoAs cleaves 2 carbons at time to form acetyl-CoA [117-119]. Finally, amino acid catabolism can produce pyruvate, acetyl-CoA, or other metabolic substrates which enter mitochondrial metabolism as either pyruvate or as a substrate for enzymes in the citric acid cycle. Acetyl-CoA is the “fuel” for the citric acid cycle and begins

the cycle through the reaction with oxaloacetate. Of importance, succinate and NADH generated from the citric acid cycle then drive the ETC.

Five integral inner membrane protein complexes comprise the enzymes of oxidative phosphorylation. Complex I (NADH dehydrogenase) and Complex II (succinate dehydrogenase) oxidize NADH and succinate, respectively, and deliver reducing equivalents (electrons) to ubiquinone, which further passes electrons to Complex III (cytochrome bc_1 complex) and then to cytochrome *c* (cyt *c*). Cyt *c* transfers electrons to Complex IV (cytochrome *c* oxidase), which then reduces O_2 to water [120, 121]. Energy gained from the transfer of electrons down the ETC is used to pump protons from the mitochondrial matrix into the IMS at Complex I, III, and IV, thus creating an electrochemical proton gradient across the IMM [120]. This proton electrochemical gradient or protonmotive force (Δp) is comprised of an alkaline inside pH gradient (ΔpH) and negative inside mitochondrial membrane potential ($\Delta\Psi_M$). Δp in turn drives ATP synthase coupled to the movement of protons through Complex V (F_1F_O-ATP synthase) back into the matrix. Suppression of the activity of Complexes I-IV decreases ATP production. However, uncoupling molecules also decrease ATP production by allowing futile entry of protons into the matrix and using the energy of Δp to produce only heat [122, 123]. The dynamic regulation of ATP generation is of particular importance to oxidative stress. Uncoupling, inhibition and activation of different enzymes of the ETC or feeding into the ETC can all result in electron leakage leading to ROS formation. In all, 11 distinct mitochondrial sites can leak electrons to oxygen to produce $O_2^{\bullet-}$ and/or H_2O_2 [124]. The 11 sites of mitochondrial electron leakage are summarized in **Figure 1-4**.

Mitochondria and Pathogenesis of Liver Injury

In liver tissue, energy supply is crucial for maintaining cell survival and function. Therefore, liver is very vulnerable to insults that causes mitochondrial dysfunction. Lack of energy production suppresses many liver functions, inhibits liver regeneration, and causes cell death. Unfortunately, mitochondria are particularly susceptible to oxidative injury due to their role as sites of ROS formation [29]. Abundant membranes containing polyunsaturated phospholipids provide ample substrates for propagation of lipid peroxidation reactions [29]. Moreover, mtDNA is easily attacked by ROS, since mtDNA lacks the protection of histones [125]. As a result, mitochondrial alterations frequently occur in many diseases where oxidative stress is high [126]. For example, megamitochondria, deletions of mtDNA, mitochondrial depolarization, and a mitochondrial respiratory burst with decreased ATP production all occur in the liver in vivo after oral intake of ethanol [127-132]. In rodent models and humans with non-alcoholic fatty liver disease (NAFLD) or non-alcoholic steatohepatitis (NASH), maladaptation of mitochondrial oxidative flux is a central event of the transition from simple steatosis to NASH [133]. Mitochondrial dysfunction also occurs in cholestatic liver injury and I/R injury [134-137]. In addition, mitochondria actively participate in many signaling pathways, thus regulating various physiological or pathological processes, such as immune responses, cell proliferation, cell death, stress responses, calcium homeostasis, and nuclear epigenetics [138]. Mitochondrial stress/dysfunction can cause alterations of signaling pathways, thus leading to liver injury. Below the relation of mitochondria with cell death and inflammation is discussed.

Mitochondria and Cell Death

Mitochondria play a key role in cell death [109, 139]. Apoptosis is caspase-mediated programmed cell death that is a part of normal tissue development and cell turnover [112]. However, markedly increased apoptosis can occur from exposure to insults, leading to injury. There are two primary pathways of apoptosis, the extrinsic and intrinsic pathways, which converge on the release of cytochrome *c* from mitochondria and the formation of the apoptosome, a heptameric complex, through interaction with apoptotic protease activating factor-1 (Apaf-1). The apoptosome activates caspase-9, which leads to a full caspase cascade [140]. The signaling of both apoptotic pathways is summarized in (**Figure 1-5**).

The intrinsic pathway is initiated by the mitochondria in response to intracellular stimuli and is regulated by the BCL-2 family of proteins [112, 141]. The interactions of the BCL-2 protein family exert pro- and anti-apoptotic control of mitochondria [141]. BAX and BAK translocation to mitochondria increases the permeability of the OMM and causes formation of a large pore, allowing the release of cytochrome *c* and other proapoptotic factors which triggers apoptosis [112, 141]. BCL-2, BCL-XL, and MCL-1 are anti-apoptotic factors that prevent membrane permeabilization by sequestering the proapoptotic factors [112, 141]. Some BH3 molecules, such as tBID, promote apoptosis by activating BAX and BAK, while others, such as BAD, inactivate the anti-apoptotic BCL-2 proteins [112, 141].

In the extrinsic pathway, extracellular signals activate one or more types of transmembrane receptors in the cell membrane, leading to an apoptotic response [141, 142]. Macrophages release TNF-α, which activates tumor necrotic factor receptor 1 (TNFR1), which is a trimeric protein. Similarly, cytotoxic T cells release Fas ligand (FasL), which activates the Fas receptor, which trimerizes [143]. Non-immune cells release TNF-

related apoptosis-inducing ligand (TRAIL) [143]. On their intracellular domains, these three death receptors act as scaffolds for the formation of signaling complexes that eventually cleave caspases and effect apoptosis. FasL and TRAIL form complexes including the Fas-associated protein with death domain (FADD) protein, which cleave procaspase 8 [143]. Caspase 8 directly cleaves proapoptotic caspase 3, leading to apoptosis. Moreover, caspase 8 also cleaves the Bcl-2 protein BH3 interacting-domain death agonist (BID) to its truncated form (tBID), a BH3 molecule that activates BAX and BAK leading to cytochrome *c* release from mitochondria [141, 142]. Therefore, there is a crosstalk between the extrinsic and intrinsic pathways.

In contrast to apoptosis, necrosis is caspase-independent [109, 139]. Necrosis is often related to mitochondrial dysfunction caused by suppression/damage of the ETC or onset of the MPT. Many factors, such as ROS, RNS, Ca^{++}, Pi, JNK activation, p53 activation, etc, cause onset of the MPT [23, 144-150]. As mentioned above, mitochondrial oxidative phosphorylation depends on Δp across IMM, Impermeability of IMM to protons is crucial for maintaining Δp. When IMM permeability increases, mitochondrial membranes depolarize, which compromises ATP production, leading to oncotic cell death. The MPT can also causes apoptosis since the MPT leads to mitochondrial swelling, rupture of the OMM, and subsequent release of proapoptotic factors such as cytochrome *c* [151]. The MPT onset is caused by opening of MPT pores (mPTP), a "megachannel" in the IMM that nonspecifically transport aqueous solutes up to a molecular weight of about 1500 Da [12–16]. Despite extensive work, the exact molecular composition of mPTP remains unclear [152, 153]. In one theory, mPTP are composed of the voltage dependent anion channel (VDAC) in OMM, the adenine nucleotide translocator (ANT) in IMM, cyclophilin D (CypD)

from the matrix which inhibits the opening of mPTP, and other ancillary proteins such as hexokinase II and glycogen synthase kinase-3β [17]. Cyclosporin A (CsA) and its non-immunosuppressive analog NIM811 are potent blockers of the MPT by binding to CypD [154]. In an alternative theory, mPTP are formed by aggregation of misfolded and damaged membrane proteins caused by various stressors (e.g. ROS). CypD and other molecular chaperones close nascent pores whereas Ca2+ opens these pores [23]. CsA inhibits the MPT when the number of chaperones exceeds misfolded aggregates (regulated MPT) [153]. When the number of misfolded protein aggregates exceeds the number of available chaperones, the MPT occurs which is independent of Ca2+ and cannot be inhibited by CsA (unregulated MPT) [153]. The MPT plays important roles in cell death in many liver injury including I/R injury, drug toxicity (e.g., APAP), cholestatic liver injury, etc. [31, 151, 155-160].

In recent years, a new form of cell death has been identified, namely necroptosis [161]. Necroptosis exhibits the pathological phenotype of necrosis but is initiated with TNFα binding to death receptors, recruitment of TRADD and subsequent recruitment of receptor-interacting serine/threonine-protein kinase (RIPK1 and RIPK3). Under conditions in which caspase-8 activation is inhibited, phosphorylation of RIPK1 and RIPK3 leads to the formation of necrosomes, which then activates the pro-necroptotic protein mixed lineage kinase domain-like protein (MLKL). MLKL executes necrosis by inserting into the membranes of organelles and plasma membrane [162]. Necrosome formation has been shown to cause mitochondrial damage (e.g., adenine nucleotide translocase (ANT) inhibition, onset of the MTP, and decreased cellular ATP levels), leakage of lysosomal

digestive enzymes into the cytoplasm, and plasma membrane rupture [162]. In conclusion, mitochondrial dysfunction is a key player in cell death.

Mitochondria and Inflammation

In recent years, mitochondria have emerged as an important regulator for inflammatory processes. According to the endosymbiotic theory, mitochondria originated as prokaryotic bacteria and have evolved in symbiosis with eukaryotic cells [104, 107, 111, 163]. This theory is widely accepted due to structural similarities of circular mtDNA to bacteria [107]. When mtDNA, mitochondrial formyl peptides encoded by mtDNA, and other mitochondrial components are released by injured cells, they become mitochondrial damage-associated molecular patterns (mtDAMPs), causing an immune response similar to pathogen associated molecular patterns (PAMPS) which are recognized by the immune system after bacterial infiltration [164, 165]. This response includes activation of toll-like receptors (TLRs) and p38 MAPK pathways as well as formyl peptide receptor 1 (FPR1) which activate neutrophils and participate in neutrophil chemotaxis [165]. Circulating mtDNA increases in patients and laboratory animals with a variety of liver diseases, including NASH, sepsis, acute liver failure, hepatic I/R, and alcoholic liver injury [132, 164, 166-169].

Mitochondria are also involved in inflammasome activation. Inflammasomes are large protein complexes composed of NOD-like receptor proteins (NLRP), an apoptosis-associated speck-like CARD-domain-containing (ASC) protein and the caspase-1 (Casp-1) protein [170]. In response to danger signals detected by the pattern-recognition domains of the NOD-like receptors, NLRP is activated and interacts with pro–caspase-1, leading to the activation of caspase-1, which subsequently promotes the formation of

mature proinflammatory cytokines IL-1β and IL-18 [171, 172]. NLRP3 is colocalized with ER and mitochondria, and the danger signals from mitochondria due to stress, damage, and infection promote the formation of inflammasomes [171, 173]. Danger signals released from hepatocytes can trigger inflammasome activation in immune cells, but inflammasome activation can also occur in hepatocytes [174, 175]. Inflammasome activation plays a role in development of alcoholic steatohepatitis, NASH, chronic HCV infection, I/R and APAP-induced liver injury [176]. Moreover, mitochondrial stress/damage are also involved in development of liver fibrosis, which will be discussed below.

ACETAMINOPHEN INDUCED LIVER INJURY

Epidemiology and Clinical Treatment of Acetaminophen Hepatotoxicity

Acetaminophen (N-acetyl-p-aminophenol, paracetamol, Tylenol®, APAP) is widely used throughout the United States and worldwide as an effective over-the-counter analgesic and antipyretic in adults and children. It is estimated that about 60 million Americans consume APAP on a weekly basis [177]. APAP is available as a standalone product, in many remedies for cough, cold, and flu, and combined with opioids by prescription. APAP intoxication can be caused by accidental overdose, abuse, and suicidal attempts. Reports estimate that between 50% and 60% of ingestions are attempts at self-harm. [177-180]. About 6% of Americans are prescribed more than the recommended 4 g APAP per day [180, 181]. While APAP causes toxic effects in many organs/tissues, such as the liver, kidney, gastrointestinal tracts, etc., its hepatotoxicity is the most common and serious side effect. APAP overdose is a leading cause of drug-induced liver injury (DILI) in Europe and the United States [181]. APAP hepatotoxicity

accounts for 40-50% of overdose-related acute liver failure (ALF) cases in the US and 40-70% in the UK [179]. In the US, APAP is responsible for more than 100,000 calls to poison control centers, 56,000 emergency room visits, 2600 hospitalization, and roughly 450 deaths due to ALF [179]. Hepatotoxicity after accidental overdose is associated with worse outcomes when treatment is delayed. APAP combination drugs have been implicated as a key factor in the prevalence of accidental overdose, since the presence of APAP is not easily recognized. In one study, opioid-acetaminophen combinations accounted for 55% of accidental overdose cases [178, 181].

In severe cases, APAP hepatotoxicity results in fulminant liver failure (also known as acute liver failure or ALF). Although just a small fraction of APAP hepatotoxicity patients develop outright liver failure, APAP hepatotoxicity is the most frequent cause of ALF in the US and other Western countries [182]. More than 40% of cases of ALF are associated with APAP overdose. Overdose of APAP alone and APAP in combination products represent the fourth and sixth highest causes of fatalities from substance poisoning [180, 182].

APAP hepatotoxicity has four clinical stages. Stage I occurs within 24 hours and is characterized by nonspecific symptoms such as nausea, vomiting, and lethargy [179, 183]. Stage II follows with improvement of stage I symptoms, but elevations of the liver enzymes alanine aminotransferase (ALT) and aspartate aminotransferase (AST) are evident [179, 183]. Stage III is marked by the return of stage I symptoms plus lactic acidosis and encephalopathy [179, 183]. Liver function tests continue to rise. Stage IV is recovery, although histological recovery can be longer than clinical recovery, especially if biopsies are performed during acute toxicity [179, 183]. In full blown ALF, patients will

develop encephalopathy with changes of mental status [182]. The underlying pathophysiology is linked to cerebral edema, which may progress to brain ischemia, herniation, and even death [182]. ALF patients may also present with jaundice, impaired gluconeogenesis/glycogenolysis, increased intracellular lactate, diminished lactate uptake, and impaired renal function [182]. ALF patients may require liver transplantation, which has a 70% 1-year survival rate, but many patients with APAP mediated ALF do not receive donor organs and are not transplanted [182]. In the US, 450 annual deaths are attributed to ALF after APAP overdose [179].

Mechanisms of Acetaminophen Hepatotoxicity

APAP causes liver injury in a dose-dependent, threshold manner characterized by fulminant centrilobular necrosis that is associated with the generation of *N*-acetyl-*p*-benzoquinone imine (NAPQI) [159, 179, 180, 183-185]. At therapeutic doses (up to 4 g/day in adults), the primary pathways of metabolism are glucuronidation and sulfation, which account for about 90% of metabolites [159, 179, 183]. The remainder of metabolites are the result of oxidation by cytochrome P450 enzymes to form NAPQI [159, 179, 183]. NAPQI is detoxified by GSH conjugation and further metabolism [159, 179, 183]. Liver toxicity occurs at high doses of APAP as glucuronidation and sulfation pathways become saturated with a higher proportion of metabolism occurring via CYP450 to form NAPQI [159, 179, 183]. Excess NAPQI depletes available GSH, allowing NAPQI to form adducts with proteins and nucleic acids [159, 179, 183]. Many events beyond the point of GSH depletion then occur, and the relative contribution of each of these events to liver injury is less clear. However, oxidative stress, activation of *c*-jun *N*-terminal kinase (JNK), and

mitochondrial dysfunction all appear to contribute importantly to cell death caused by APAP [159, 179, 183-185].

Oxidative stress and lipid peroxidation have been reported in experimental APAP hepatoxicity models since the 1970s and were at the center of one of the two major mechanistic hypotheses of the time, the other being the protein binding theory [156]. Essentially, one theory placed ROS generated from CYP450 activity as primary event that leads to cell death, while the other placed the formation of protein adducts of NAPQI, the metabolic product of CYP450 and APAP, as the primary event leading to cell death through protein and mitochondrial dysfunction and the resulting oxidative stress [156]. The focus of APAP hepatotoxicity mechanisms is the mitochondria [186-188]. Comparison of nontoxic (in mice) AMAP to APAP metabolism demonstrated that the primary difference between the two was protein binding, i.e. mitochondrial protein-NAPQI adducts formed in APAP metabolism, but mitochondrial proteins were unmodified in AMAP administration [156, 186, 188, 189]. Further, toxicity correlated with the amount of protein-NAPQI adducts formed [156, 190]. NAPQI forms adducts with mitochondrial proteins including ATP synthase α subunit, glutathione peroxidase, ALDH (due to its localization we can assume this is ALDH2), and glutathione-S transferase [156, 191]. Finally, nitrotyrosine adducts to proteins were observed in *in vitro* APAP hepatotoxicity models [156, 189, 192]. Nitrotyrosine adducts are a product of peroxynitrite oxidation of proteins and signify formation of RNS [156, 189, 192]. As previously described, nitric oxide radicals are formed by the three NOS isoforms, including iNOS, which is induced by cellular stress [2, 3]. Nitric oxide radicals then react with $O_2^{\bullet-}$ to form peroxynitrite. Nitrotyrosine adducts form with additional proteins, including MnSOD (SOD2), and directly damage DNA [2, 3, 193].

Peroxynitrite scavenging with delayed GSH treatment improved recovery during APAP toxicity [156, 194, 195].

ROS increase phosphorylation and activation of JNK through the ROS-sensitive apoptosis signal-regulating kinase 1 (ASK1) and mixed-lineage kinase 3 (MLK3) pathways. JNK is a well-established regulator of apoptosis and necrosis [155, 159, 185]. JNK activation after APAP has been confirmed *in vitro* and *in vivo* in both animal models and humans [196-199]. Mitochondrial dysfunction is also considered as a critical contributor for cell death after APAP overdose [31, 199-201]. Further, NAPQI adduct formation is associated with loss of $\Delta\Psi_M$ and onset of the MPT, leading to cell death [155].

Risk Factors for Acetaminophen Toxicity

The maximum daily recommended dose of APAP is 4 g/day in adults for the general population, but conditions that increase patient susceptibility to APAP hepatotoxicity may make this recommended dose unsafe for certain populations. Factors that favor CYP2E1 metabolism of APAP, such as CYP2E1 induction by chronic alcohol consumption, drugs and environmental factors, or mutations of enzymes in glucuronidation and sulfation pathways may increase NAPQI generation and the resultant hepatotoxicity [179, 180, 183]. Further, any situations that lead to depletion of GSH, including fasting, malnutrition, obesity, chronic liver disease, or steatosis, decrease the ability of the liver to clear NAPQI and increase the risk of hepatotoxicity [179, 180, 183]. Use of APAP in patients with chronic alcohol consumption is associated with high risk of APAP hepatotoxicity due to both CYP2E1 induction and decreased GSH stores by alcohol [179, 180, 183]. Herbal and pharmaceutical medications (e.g., isoniazid, rifampicin, phenobarbital, St. John's wort) can induce expression of CYP2E1, while others (e.g.

zidovudine, trimethoprim-sulfamethoxazole) can interfere with glucuronidation, leading to increased NAPQI production [179, 180, 183, 202]. Likewise, patient age and nutritional status as well as chronic liver disease all increase susceptibility to APAP hepatotoxicity through a combination of impaired detoxification through glucuronidation and sulfation and decreased availability of GSH [179, 180, 183].

Current Treatment of Acetaminophen Hepatotoxicity

Currently the primary treatment for APAP hepatotoxicity is *N*-acetyl cysteine (NAC). NAC is a cell-membrane permeable precursor of GSH which decreases APAP hepatotoxicity by increasing GSH thus enhancing NAPQI detoxification [179, 180, 183]. NAC to boost GSH detoxification of APAP is most effective when administered within 8 h of the overdose in humans [202]. Therefore, identification of APAP overdose early is critical for successful treatment with NAC.

Other serum biomarkers for APAP hepatotoxicity include APAP-protein adducts, glutamate dehydrogenase (GDH), nuclear DNA (nDNA), mtDNA, and high mobility group B1 (HMGB1) [183]. GSH analogs, polyphenol free radical scavengers, CsA, its analog NIM811, and other MPT inhibitors have all been successful in animal models of APAP hepatotoxicity, but these have not yet been clinically proven [31, 155, 203-205]. If APAP hepatotoxicity develops to ALF, patients may require liver transplantation [179, 182].

Animal Models of Acetaminophen Induced Liver Injury

APAP administration to fasted mice (12-16 h) in the range of 200-600 mg/kg by i.p. injection is the most common model of APAP induced liver injury [206]. Injury begins at doses of 150 mg/kg. In this model, typical centrilobular necrosis is observed when 200-

300 mg/kg is given, and decreased survival is observed when the dose is increased to ~600 mg/kg [206-208].

Key advantages of using mice are the ease of the model and the applicability of the model to clinical and mechanistic human studies [206, 209]. APAP administration in mice causes hepatotoxicity in a similar range to human doses and replicates most of the pathogenesis processes and pathology in human APAP hepatotoxicity, including formation of NAPQI and NAPQI-protein adducts, ROS generation, JNK activation, mitochondrial damage, and necrosis [206]. Genetic knockout mice make it easier to examine the role of various proteins in APAP hepatotoxicity. Conversely, experiments in rats do not show the same level of NAPQI-protein adduct formation or oxidative stress, even at much higher doses, and mitochondrial dysfunction does not occur, making it a poor model for human hepatotoxicity [206, 208].

Although mice are a good model for human APAP hepatotoxicity, limitations must be considered when using this model. First, hepatotoxicity peaks at 12-24 hours in mice vs. 24-72 hours in humans [206]. Second, modification of P450 expression or activity must be avoided to preserve the bioactivation of APAP into NAPQI. Many therapeutics and even common drug vehicles such as dimethyl sulfoxide (DMSO) are CYP450 inhibitors or inducers [142, 206, 210, 211]. Likewise, mouse strain and source must be considered. For example, the nicotinamide nucleotide transhydrogenase gene (*Nnt)* transfers protons between NAD^+ and $NADP^+$ and can run in both directions [206, 212]. When the ETC is under stress more NADH is produced, which feeds the ETC producing more ROS increasing APAP hepatotoxicity [206, 212]. C57Bl/6J have a mutation that only allows the enzyme to transfer hydrogens from NADH to $NADP^+$. This offers partial protection from

hepatotoxicity in C57Bl/6J mice [206, 212]. Similar variations between strains may falsely implicate signaling processes and molecules, such as toll like receptor 4 (TLR4) [206, 213]. A mutation in the *Tlr4* gene makes C3H/HeJ mice, which are resistant to APAP toxicity, less responsive to endotoxin, though whether Tlr4 is relevant as a mediator of APAP hepatotoxicity is debated [206, 213].

LIVER FIBROSIS/CIRRHOSIS

Clinical Definitions and Treatment of Liver Fibrosis

Liver fibrosis is a dysregulated scarring process where excess extracellular matrix (ECM) is formed in the liver [214-216]. Fibrosis is a response to injury, such as viral infection, toxic chemical exposure, cholestasis, and others [214-216]. As fibrosis progresses, parenchymal cells are replaced with collagen fibers. As the structure of the liver is distorted, blood and bile flow are reduced, exacerbating liver injury and leading to loss of liver function [214-217]. Patients with cirrhosis are at higher risk for hepatocellular carcinoma, and this risk is amplified if the initial insult is due to viral hepatitis infection [218]. The only effective treatment for advanced liver fibrosis (cirrhosis) is transplantation [214, 215].

The onset of liver fibrosis is not noticed by many patients until it reaches an advanced state [214]. Structural remodeling of parenchyma and changes to endothelial cells during cirrhosis lead to chronic liver failure, disruption of hepatic blood flow, portal hypertension, and many severe or even fatal complications, such as ascites, varices and gastrointestinal bleeding, hepatorenal syndrome, hepatic hydrothorax, hepatopulmonary syndrome, spontaneous bacterial peritonitis, and hepatic encephalopathy [215].

While non-invasive methods of detecting and grading liver fibrosis and cirrhosis are being investigated, the gold-standard for evaluating fibrosis remains histological examination of liver biopsy tissue [217]. In 1977, the histopathology of cirrhosis was defined by Anthony *et al.* with features of "parenchymal necrosis, regeneration, and diffuse fibrosis resulting in disorganization of the lobular architecture throughout the whole liver." [217]. Nodular appearance, whether micro- or macronodular, is characteristic, and areas of liver adjacent to fibrotic areas grow at different rates and show nodular remodeling [217].

Epidemiology, Morbidity and Mortality of Liver Fibrosis

Using data from The National Health and Nutrition Examination Survey (NHANES) from 1999-2010, Scaglione *et al.* estimated the prevalence of advanced liver fibrosis (cirrhosis) to be approximately 633,323 adults in US [219]. Globally, cirrhosis accounts for approximately 1.2 million deaths yearly [220]. Many of the patients (69%) reported that they were unaware of having liver disease, which delays treatment [219]. In the National Vital Statistics Reports article, "Deaths: Final Data for 2015", chronic liver disease and cirrhosis ranked as the 12th leading cause of death in the United States above hypertension (13th) [221]. The crude death rate for chronic liver disease and cirrhosis in the US including both males and females is 12.5 per 100,000 [219]. Gender disparities of mortality due to chronic liver disease and cirrhosis exists with males exceeding females (1.9 male deaths per female) [219].

Pathophysiology of Fibrosis

Aspects of fibrosis are similar in many different organs [215]. Rockey *et al.* suggest that injury to epithelial cells (hepatocytes in the liver) leads to inflammation [215]. Both the

injury to the epithelium and the resulting recruitment of inflammatory cells causes activation of effector cells, which share a number of similarities in various tissues. Gene expression is modified in these effector cells, and they begin to proliferate and produce ECM [215, 222].

In the liver, many injuries, typically leading to inflammation, give rise to fibrosis, including alcoholic steatohepatitis (ASH) and nonalcoholic steatohepatitis NASH, drug toxicity, viral infection, cholestasis, and metabolic diseases [214, 222]. Fibrosis is primarily a wound-healing response that becomes dysregulated and eventually alters the structure and function of the liver [214, 215, 223]. Many molecules and signaling pathways are associated with fibrosis progression. These are summarized in **Table 1-2**. Key factors include TGF-ß, TNF-α, IL-10, and IL-1ß that are shared among multiple types of liver disease [214, 222]. The primary effector cell of fibrosis in the liver is the hepatic stellate cell (HSC), which is sensitive to cytokines and chemokines that come from hepatocytes, Kupffer cells, cholangiocytes, and infiltrating leukocytes, and even HSCs themselves [214, 222]. Although portal myofibroblasts and bone marrow cells also have fibrogenic potential, their lineage and contribution to fibrosis is debated and may vary between liver diseases [214, 224, 225]. Whatever their lineage, hepatic collagen-producing cells undergo a change in gene expression and take on a distinctly myofibroblast phenotype, including the characteristic expression of smooth muscle α-actin (α-SMA), which can be used to identify myofibroblasts in the liver [224].

Activated HSCs (i.e., myofibroblasts) deposit ECM, including fibrillar collagens I, III, and IV [224]. Tissue inhibitors of metalloproteinase (TIMPs) are also expressed in liver injury; these in turn inhibit matrix metalloproteinase enzymes (MMPs), thus stabilizing

excreted ECM [224]. A critical point is that activated HSCs, activated Kupffer cells, and infiltrating inflammatory cells, all contribute to the pro-inflammatory/pro-fibrogenic signaling cascades found in liver injury, with TGF-ß and TNF-α, chemokine (C-C motif) ligand 5 (CCL5), IL-8 and IL-10 being prominent for as long as the injury remains unresolved [224]. Eventually, fibrosis replaces large areas of the parenchymal tissue, and gross remodeling takes place, which causes an impairment in liver function [224]. Patients with advanced disease present with portal hypertension and impaired liver function, progressing to ascites, bleeding varices, and finally end-stage liver disease and encephalopathy that currently can be treated only with liver transplantation [215].

A substantial body of evidence demonstrates that ROS and mitochondrial stress/dysfunction also play important role in pathogenesis of fibrosis. ROS are activators of HSC [25, 26]. In experimental cholestasis, impaired bile flow, ROS have been shown to be generated in hepatocytes due to bile acid exposure, but of more importance is the ROS generated by neutrophils recruited in the inflammatory component of the injury [226]. Mitochondrial oxidative stress promotes formation/activation of potent profibrogenic cytokine TGF-β and expression of proinflammatory and profibrotic protein osteopontin (OPN) [227, 228]. IL-1β, which is produced during inflammasome activation, not only mediates inflammation, but also promotes fibrosis [229]. Succinate released from mitochondria can stimulate HSC activation through binding to the GPR91 succinate receptor in HSC [230]. Free radical scavengers, mitochondrial targeted antioxidants and overexpression of mitochondrial SOD inhibit HSC activation in vitro and/or decrease fibrosis in vivo [27, 28, 231].

Treatment of Liver Fibrosis

For many years, cirrhosis has been thought to reflect irreversible pathological change in the liver. However, in recent years, cirrhosis regression has been observed in patients with many different forms of liver disease, including chronic viral hepatitis, hemochromatosis, and secondary biliary cirrhosis [222, 232]. For example, due to the development of novel direct-acting antiviral therapies, cirrhosis reversion occurs in some hepatitis C patients, which leads to improvement of clinical outcomes, decreases of portal pressure and reduced mortality [233, 234]. However, for liver diseases in which there is not effective primary therapy, anti-fibrotic therapies would be highly desirable.

Significant progress in uncovering the cellular and molecular basis of hepatic fibrosis has stimulated the efforts to develop antifibrotic strategies. Many mechanism-based pharmaceutical antifibrotic treatment modalities have been attempted for liver fibrosis. Among these are angiotensin-converting enzyme (ACE) inhibitors and angiotensin-receptor blockers (ARB), colchicine, interferon, pioglitazone, and farglitazar [215]. Unfortunately these and other anti-fibrotic treatments have been shown to be ineffective in clinical trials [215]. Clinical trials of antioxidant therapies have also been disappointing. Vitamin E, which was proven to be effective in animal studies, did not decrease fibrosis in patients with non-alcoholic hepatitis [215, 235, 236]. However, one trial demonstrated that treatment with a silybin-vitamin E-phospholipid complex reduced liver fibrosis in patients with chronic hepatitis C treated with pegylated interferon α and ribavirin [237].

Animal Models of Liver Fibrosis

Research into the cellular processes of fibrosis has been conducted in cell lines and using isolated primary cells [238, 239]. Primary cells that may be isolated from the

liver include hepatocytes [240], HSC [239], endothelial cells [241], and Kupffer cells [241], and co-culture may reproduce some aspects of *in vivo* biology. Primary cultures of HSC or human HSC cell lines (e.g. LX-2 cells) have been widely used to examine the effects of pro-fibrotic and antifibrotic reagents [242-245]. While the contributions of the various cell types to fibrotic processes may be replicated in culture using cell lines or primary cells, the gold-standard for fibrotic research, especially translational research, is the use of animal models [238].

Animal models are more effective than *in vitro* models in replicating the complexities of fibrotic pathogenesis in the liver, especially in pathologically complex fibrogenesis involving multiple cell types [238]. Infectious models include parasitic infection and hepatitis viral infection in immune-compromised mice [238]. Chemical models include carbon tetrachloride (CCl_4), thioacetamide, and dimethylnitrosoamine. These chemical models result in reproducible fibrosis [83, 231, 246-250]. Intraperitoneal (IP) administration of CCl_4 has also been used but may lead to peritonitis.

Dietary models have also be used to induce fibrosis, most with the goal of replicating non-alcoholic fatty liver disease (NAFLD) or non-alcoholic steatohepatitis (NASH). The major limitations of these models include that it takes months to generate fibrosis, and fibrosis is typically very mild [238].

Genetic models can also produce fibrosis. For example, multi-drug resistance-associated protein 2-deficient mice have been reported to develop biliary fibrosis at 8 weeks and HCC at 4-6 months. *Alms1 Fat ausi* mutant mice fed a high fat diet begin to show injury after 24 weeks with fibrosis proceeding thereafter [239]. However, the pathogenetic process of fibrosis caused by genetic manipulation may not be reversible,

relevant to human disease, or suitable for evaluation of the effects of potential therapeutic agents [239].

Bile duct ligation (BDL) is a widely used and well-established surgical cholestatic model of fibrosis [239]. Liver fibrosis occurs in many cholestatic liver diseases in humans [239]. Therefore, this model is also of clinical relevance. Ligating the common bile duct leads to cholestasis, cytokine secretion by biliary epithelial cells, ductular reactions (e.g. proliferation of biliary epithelial cells), hepatocellular necrosis (biliary infarcts), and inflammation [251]. Portal fibroblasts become activated, and HSC lose their retinoid-containing fat droplets, begin expressing α-SMA, and transform to a myofibroblast phenotype [251]. Fibrotic markers including TIMP-1 and TGF-ß are also expressed [239]. Activated myofibroblasts express collagens, and fibrosis may be observed at 10 days and is pronounced by 14 days after surgery [251]. However, surgical complications (e.g., due to bile leakage), which occur occasionally, may lead to variation in fibrotic responses or death [239].

Rationale and Project Goals

Previous studies have shown that oxidative stress, in particular mitochondrial oxidative stress, occurs in many liver diseases and plays an important role in liver disease pathogenesis. However, though many effects of ROS are known, how ROS leads to liver injury is not fully elucidated (**Figure 1-6**). Since lipid peroxidation produces reactive aldehydes, in this study I tested the central hypotheses that aldehydes are important mediators of liver injury and fibrosis and that acceleration of aldehyde degradation by activation of mitochondrial ALDH2 would decrease liver injury and fibrosis. I examined the role of aldehydes in liver injury in APAP-induced liver injury, which causes ALF, and

cholestatic liver fibrosis which causes chronic liver failure. I expected that success of this study will elucidate the role of aldehydes in oxidative stress-related liver injury and fibrosis, thus identifying a new therapeutic target. I further expected that this study will determine whether ALDH2 activation is an effective treatment modality for liver diseases that cause both acute and chronic liver failure.

FIGURES

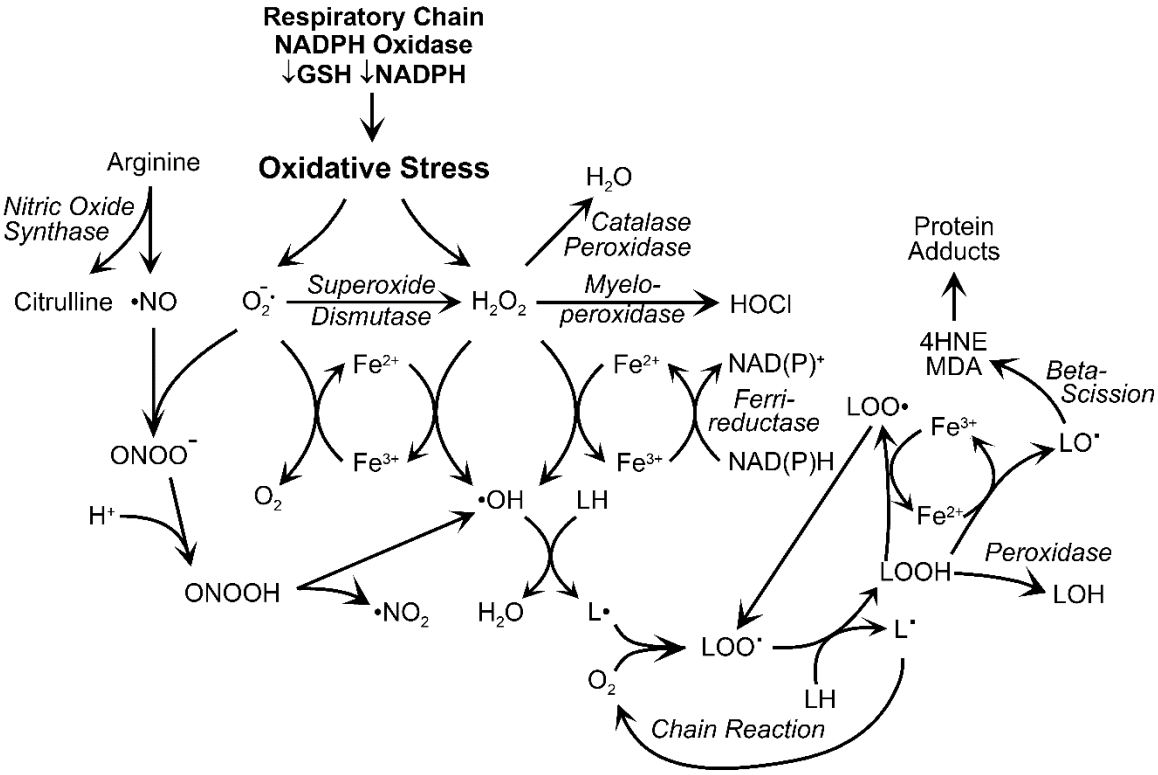

Figure 1-1. Common reactive oxygen species and their sources

ROS are produced from the respiratory chain and NADPH Oxidase, which deplete glutathione (GSH) stores and NADPH. Superoxide ($O_2^{\cdot-}$) can interact with nitric oxide (•NO) to produce peroxynitrite ($ONOO^-$), which can be protonated, leading to decomposition to nitrogen dioxide (•NO2) and hydroxyl radical (•OH). Superoxide can also be reduced to hydrogen peroxide (H_2O_2) by superoxide dismutase enzyme. H_2O_2) can be detoxified to water (H_2O) by catalase and peroxidase enzyme or serve as a substrate for myeloperoxidase enzyme to form hypochlorous acid. Fenton chemistry forms •OH and

(Fe^{3+}) from ferrous iron (Fe^{2+}) and (H_2O_2). Free radicals form peroxyl radical (LOO•) and lipid peroxides (LOOH), which also undergo a number of lipid chain reactions. Lipid alkoxyl radicals undergo ß-scission to form aldehydes such as malondialdehyde (MDA) and 4-hydroxynonenal (4-HNE).

Source: Image kindly provided by Lemasters, JJ

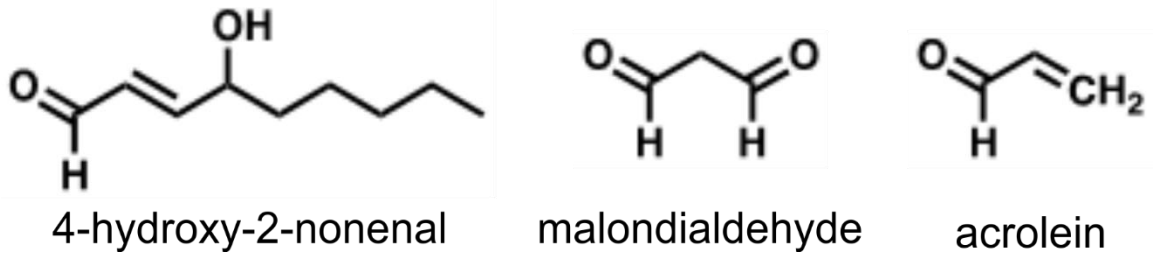

Figure 1-2. Structures of three aldehydes of biological significance

See text.

Source: Image kindly provided by Woster, PM

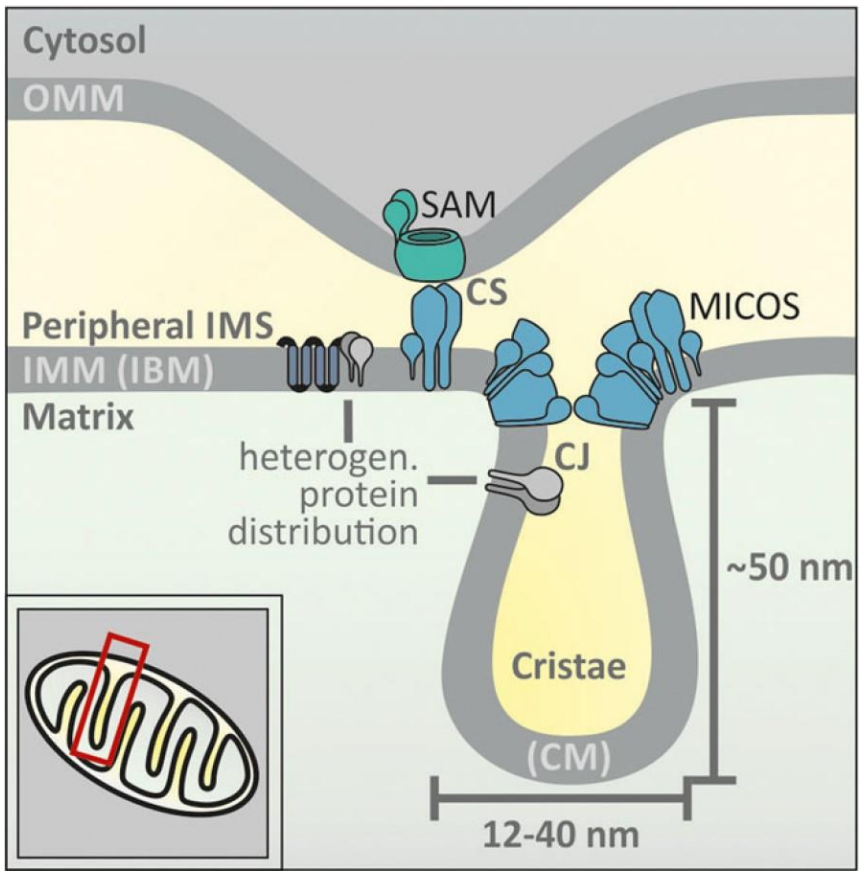

Figure 1-3. The overall structure of mitochondria.

Shown are the outer mitochondrial membrane (OMM), inner mitochondrial membrane (IMM), and the invaginations forming the cristae and christae membrane (CM). Also seen are the sorting and assembly machinery (SAM) of OMM at a contact site (CS) with the mitochondrial contact site and cristae organizing system (MICOS), and cristae junctions (CJ).

Source: [104] M. Habich, S.L. Salscheider, J. Riemer, Cysteine residues in mitochondrial intermembrane space proteins: more than just import, Br J Pharmacol 176(4) (2019) 514-531.

Used with permission.

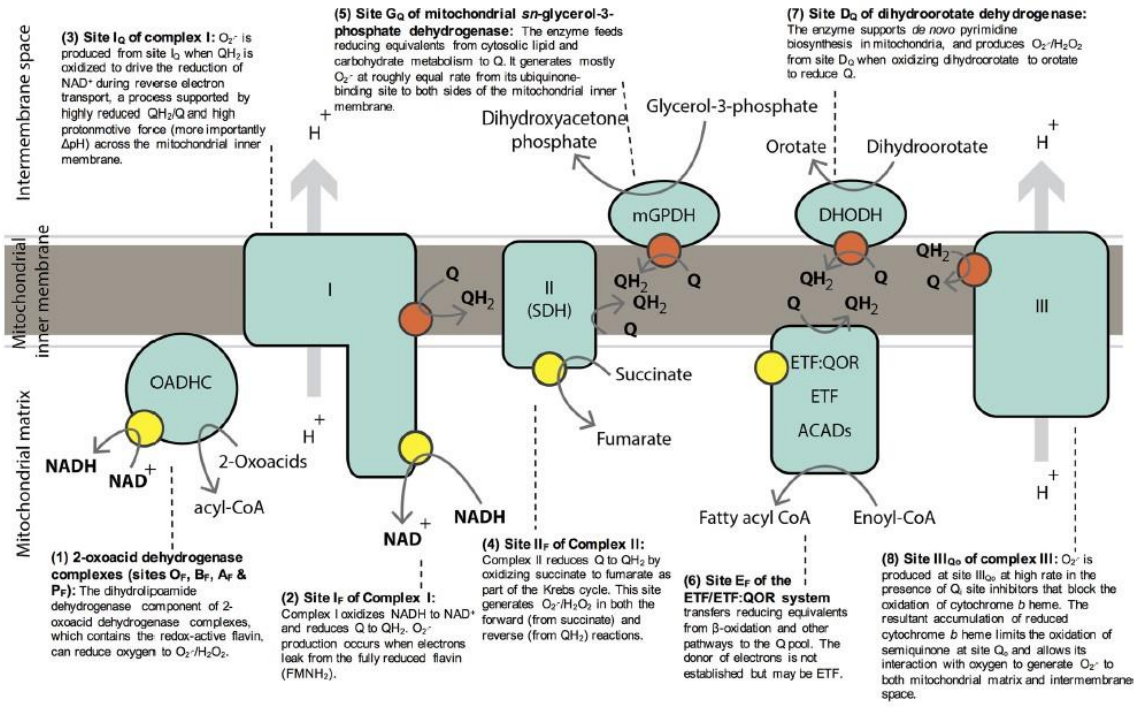

Figure 1-4. The electron transport chain, showing 11 sites of electron leak.

Source: [124] This research was originally published in the Journal of Biological Chemistry. H.S. Wong, P.A. Dighe, V. Mezera, P.A. Monternier, M.D. Brand, Production of superoxide and hydrogen peroxide from specific mitochondrial sites under different bioenergetic conditions, J Biol Chem 292(41) (2017) 16804-16809.

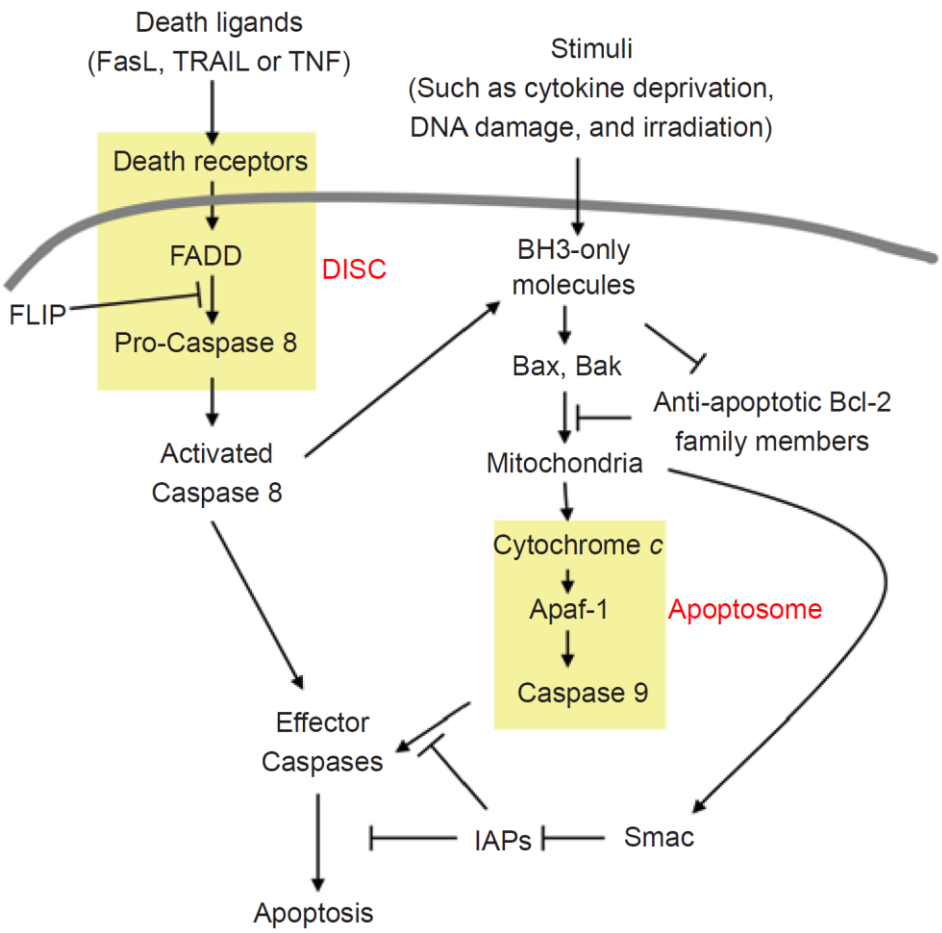

Figure 1-5. Extrinsic and intrinsic apoptosis signaling.

The left side shows extrinsic (receptor mediated) apoptotic signaling pathway, in which signals from cell membrane receptors lead to cleavage of cleaved caspase 8 and initiation of the caspase cascade. The right side shows intrinsic apoptotic signaling. See text. Source: [252] G. Xu, Y. Shi, Apoptosis signaling pathways and lymphocyte homeostasis, Cell Res 17(9) (2007) 759-71.

Used with permission.

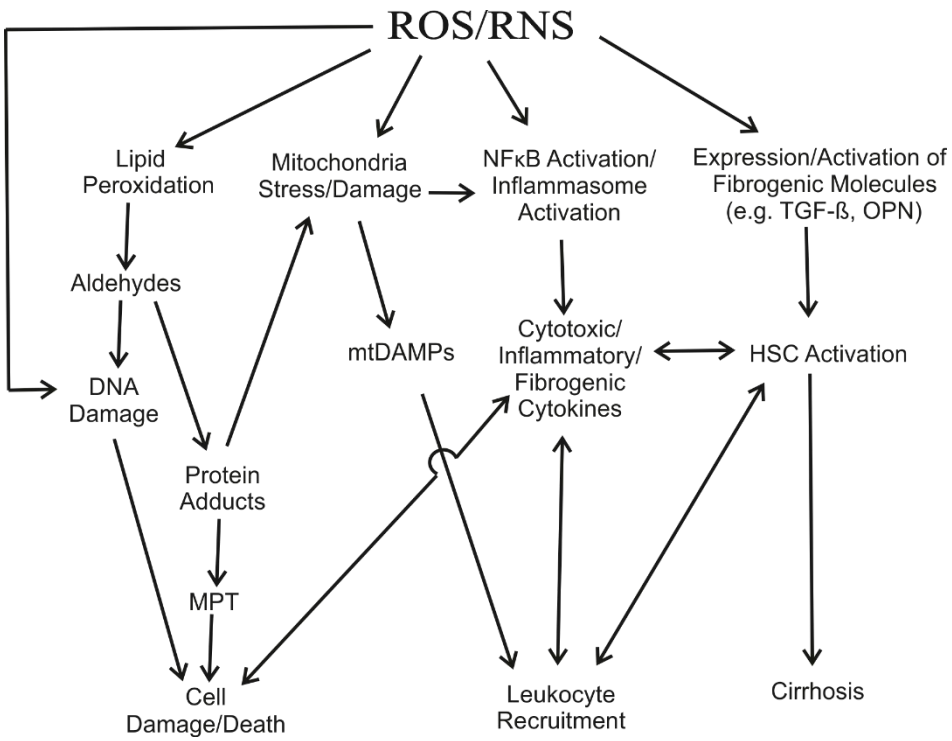

Figure 1-6. Role of reactive oxygen species and aldehydes in liver injury, inflammation and fibrosis.

Reactive oxygen species cause lipid peroxidation, mitochondrial stress, and stress signaling, many of which converge on cell death, inflammation, and fibrosis as final outcomes. We hypothesize that aldehyes generated from lipid peroxidation mediate many detrimental effects caused by ROS.

Source: Original work.

ALDH	Subcellular Location	Preferred Substrate	Disease, Mutational Phenotypes, Functions	Chromosome	GeneBank Accession No.
ALDH1A1	Cytosol	Retinal	Alcohol sensitivity, alcoholism, Parkinsonism with ALDH2 double knockout animal (334)	9q21.13	NM_000689
ALDH1A2	Cytosol	Retinal	Increased risk for neural tube defect	15q22.1	NM_003888
ALDH1A3	Cytosol	Retinal	Embryonic lethal in knockout animal	15q26.2	NM_000693
ALDH1B1	Mitochondria	Aliphatic aldehydes	Unknown	9q11.1	NM_000692
ALDH1L1	Cytosol	10-Formyl tetrahydrofolate	Low fertility and decreased hepatic folate in knockout animal	3q21.2	NM_012190
ALDH1L2	Unknown	Unknown	Unknown	12q23.3	NM_001034173
ALDH2	Mitochondria	Acetaldehyde, 4-HNE and MDA	See Figure 4 in this review	12q24.2	NM_000690
ALDH3A1	Cytosol, nucleus	Aromatic, aliphatic aldehydes	Cataracts in knockout animal	17p11.2	NM_000691
ALDH3A2	Microsomes, peroxisomes	Fatty aldehydes	Sjögren-Larsson syndrome	17p11.2	NM_000382
ALDH3B1	Cytosol	Unknown	Unknown, locus linked to paranoid schizophrenia	11q13.2	NM_000694
ALDH3B2	Unknown	Unknown	Unknown	11q13.2	NM_000695
ALDH4A1	Mitochondria	Glutamate γ-semi-aldehyde	Type II hyperprolinemia	1p36.13	NM_003748
ALDH5A1	Mitochondria	Succinate semi-aldehyde	γ-Hydroxybutric aciduria	6p22.2	NM_001080
ALDH6A1	Mitochondria	Malonate semi-aldehyde	Development delay, metabolic abnormality, methylmalonic aciduria	14q24.3	NM_005589
ALDH7A1	Cytosol, nucleus, mitochondria	α-Aminoadipic semi-aldehyde	Pyridoxine-dependent seizures, locus linked to osteoporosis (107)	5q31	NM_001182
ALDH8A1	Cytosol	Retinal	Unknown	6q23.2	NM_022568
ALDH9A1	Cytosol	γ-Aminobutyr-aldehyde	Unknown	1q23.2	NM_000696
ALDH16A1	Unknown	Unknown	Unknown	19q13.33	NM_153329
ALDH18A1	Mitochondria	Glutamic γ-semi-aldehyde	Hyperammonemia, hypoprolinemia, neurodegeneration, cataract	10q24.3	NM_002860

Table 1-1. The nineteen ALDH enzymes expressed in humans.

See Text

Source: [64] C.H. Chen, J.C. Ferreira, E.R. Gross, D. Mochly-Rosen, Targeting aldehyde dehydrogenase 2: new therapeutic opportunities, Physiol Rev 94(1) (2014) 1-34.

Used with permission.

Genetic and nongenetic factors associated with fibrosis progression in different types of chronic liver diseases

Type of liver disease	Candidate genes	Candidate genes (full name)	Nongenetic factors
Chronic HCV infection	*HFE*	Hereditary hemochromatosis gene	Alcohol intake
	Angiotensinogen	Angiotensinogen	Coinfection HIV and/or hepatitis B virus
	TGF-β1	Transforming growth factor β1	Age at time of acute infection
	TNF-α	Tumor necrosis factor α	Liver transplantation
	ApoE	Apolipoprotein E	Diabetes mellitus
	MEH	Microsomal epoxide hydroxylase	No response to therapy
	MCP-1	Monocyte chemotactic protein type 1	
	MCP-2	Monocyte chemotactic protein type 2	
	Factor V	Factor V (Leiden)	
Alcohol-induced	*IL-10*	Interleukin 10	Alcohol intake
	IL-1β	Interleukin 1β	Episodes of alcoholic hepatitis
	ADH	Alcohol dehydrogenase	
	ALDH	Aldehyde dehydrogenase	
	CYP2E1	cytochrome P450, family 2, subfamily e, polypeptide 1	
	TNF-α	Tumor necrosis factor α	
	CTLA-4	Cytotoxic T lymphocyte antigen type 4	
	TAP2	Transporter-associated antigen-processing type 2	
	MnSOD	Manganese superoxide dismutase	
NASH	*HFE*	Hereditary hemochromatosis gene	Age
	Angiotensinogen	Angiotensinogen	Severity of obesity
	TGF-β1	Transforming growth factor β1	Diabetes mellitus
			Hypertriglyceridemia
PBC	*IL-1β*	Interleukin 1β	
	TNF-α	Tumor necrosis factor α	
	ApoE	Apolipoprotein E	
Autoimmune hepatitis	*HLA-II*	Human leukocyte antigen type II haplotypes	Type II autoimmune hepatitis
			No response to therapy

Table 1-2. Factors Associated with Progression of Fibrosis

See Text

Source: [214] R. Bataller, D.A. Brenner, Liver fibrosis, Journal of Clinical Investigation 115(2) (2005) 209-218.

Used with permission.

CHAPTER 2: Aldehyde Dehydrogenase-2 Activation Decreases Acetaminophen Hepatotoxicity by Prevention of Mitochondrial Depolarization

ABSTRACT

Background and Aim: Acetaminophen (APAP) hepatotoxicity is a leading cause of acute liver failure worldwide. Previous studies show that oxidative stress contributes to APAP hepatotoxicity. Since lipid peroxidation produces reactive aldehydes, we investigated whether accelerating aldehyde detoxification by activation of mitochondrial aldehyde dehydrogenase (ALDH2) with Alda-1 decreases liver injury after APAP.

Methods: Male C57Bl/6J mice fasted overnight received Alda-1 (20 mg/kg, i.p.) or vehicle 30 minutes before administration of APAP (300 mg/kg, i.p.). Food was returned to the animals 30 minutes after APAP administration. Blood and livers were collected 2 or 24 h after APAP. Intravital multiphoton microscopy of rhodamine 123 (Rh123) and propidium iodide (PI) fluorescence was conducted 6 h after APAP administration to detect mitochondrial polarization status and cell death.

Results: 4-HNE protein adducts were present in 0.1% of tissue area without APAP treatment but increased to 7% and 19% after 2 and 24 h treatment with APAP, respectively. Alda-1 blunted 4-HNE adduct formation to 1% and 2.4% at 2 and 24 h. Serum alanine aminotransferase (ALT) increased to 7594 U/L at 24 h after APAP, and this increase was blunted 72% by Alda-1. Alda-1 also decreased centrilobular necrosis at 24 h after APAP from 47% of lobular areas to 21%. *N*-acetyl-*p*-benzoquinone imine (NAPQI) protein adducts formation increased significantly with APAP, which Alda-1 did not alter. JNK phosphorylation also increased after APAP as expected, but Alda-1 also did not alter. Without APAP, no mitochondrial depolarization was detected by intravital microscopy. At 6 h after APAP, 62% of tissue area showed depolarization, which decreased by nearly half to 33.5% with Alda-1 treatment. Cell death as detected by PI labeling increased from

0 to 6.8 cells per 30x field 6 h after APAP, which decreased to 0.6 cells by Alda-1 treatment.

Conclusion: Aldehydes are important mediators of APAP hepatotoxicity. Accelerated aldehyde degradation by ALDH2 with Alda-1 decreases APAP hepatotoxicity by protection against mitochondrial dysfunction.

INTRODUCTION

Acetaminophen (*N*-acetyl-*p*-aminophenol, paracetamol, Tylenol®, APAP) is a widely used effective over-the-counter analgesic and antipyretic. In cases of overdose, APAP metabolism produces a hepatic injury that can lead to acute liver failure requiring transplantation and is the primary cause of acute liver failure worldwide [159, 179, 180, 183-185]. Sensitivity to APAP toxicity can be increased by various conditions, including chronic alcohol use, poor nutrition, use of herbal or other medications that affect APAP metabolism, chronic liver injury, and age [179, 180, 183]. While the glutathione (GSH) precursor, N-acetylcysteine (NAC), is currently used as an antidote to treat APAP-induced liver injury, NAC becomes ineffective at longer periods after APAP overdose, and additional approaches to improve therapy of APAP hepatotoxicity are needed.

APAP is metabolized by glucuronidation and sulfation, producing roughly 90% of metabolites. Cytochrome P450s, primarily Cyp2E1, also metabolize APAP to form a N-acetyl-p-benzoquinone imine (NAPQI) intermediate, which accounts for roughly 10% of metabolites [159, 179, 180, 184]. Conjugation with GSH is the principal route of NAPQI detoxification. At high APAP doses, glucuronidation and sulfation pathways become saturated, and a greater proportion of APAP is converted to NAPQI. Excessive NAPQI depletes GSH After GSH depletion, NAPQI forms adducts with proteins and nucleic acids, leading to cell damage [159, 180, 183, 184, 202]. Mitochondrial NAPQI-protein adduct formation increases superoxide formation from the respiratory chain, thus increasing mitochondrial oxidative stress [159, 185, 192]. Lipid peroxidation damages the mitochondrial membrane and forms aldehydes [29]. Previous studies also show that the mitochondrial permeability transition (MPT) occurs after APAP overdose and that the MPT

inhibitors cyclosporin A and NIM811 decrease APAP hepatotoxicity [155, 253]. Activation of c-Jun *N*-terminal kinase (JNK) pathway is also implicated in APAP hepatotoxicity [159, 183, 185]. Activation of apoptosis signal-regulating kinase 1 (ASK1) and mixed-lineage protein kinase 3 (MLK3) by reactive oxygen species (ROS) is possibly responsible for JNK activation [159, 185].

Although it is well accepted that ROS play a role in APAP hepatotoxicity, whether aldehyde formation subsequent to lipid peroxidation contributes to APAP hepatotoxicity remains unclear. Alda-1 (N-(1,3-benzodioxol-5-ylmethyl)-2,6-dichlorobenzamide) is an activator of mitochondrial aldehyde dehydrogenase (ALDH2) responsible for aldehyde degradation. Previous studies show that Alda-1 decreases injury in high-ROS environments, such as experimental radiodermatitis and experimental ischemia-reperfusion injury in multiple organs [61, 65-68, 73, 84-86, 88]. Therefore, Alda-1 provides a powerful tool to determine whether aldehydes play a role in the pathogenesis of hepatotoxicity. Here, we show that Alda-1 pretreatment markedly decreases mitochondrial dysfunction and liver injury in a mouse model APAP toxicity.

EXPERIMENTAL PROCEDURES

Synthesis of Alda-1. Alda-1 was synthesized as previously described [254]. The product was shown to be >99% pure by HPLC chromatography, and the structure was verified by NMR spectroscopy.

Acetaminophen and Alda-1 Administration. Male C57BL/6 mice (20-22g) were purchased from the Jackson Laboratory (Bar Harbor, MA) and maintained on a 12-h light/dark cycle with *ad libitum* food and water. All animal procedures followed the NIH "Guide for the Care and Use of Laboratory Animals" and were preapproved by the

Institutional Animal Care and Use Committee at the Medical University of South Carolina. After fasting overnight (15-18 h), Alda-1 (20 mg/kg) or equal volume of vehicle (Neobee M-5, Stephan Lipid Nutrition, Maywood, NJ) was administered intraperitoneally. APAP (300 mg/kg i.p.) dissolved in saline (20 mg/ml) was injected 30 min later. Food was returned to the animals 30 min after APAP treatment. Vehicle control animals were fasted and received saline and Neobee M-5 injections.

Tissue Harvest and Histology. At 2 h and 24 h after APAP administration, blood and liver were harvested under pentobarbital anesthesia (100 mg/kg, ip). Blood was collected from the inferior vena cava. Livers were perfused with 5 mL normal saline via the portal vein before removal of left lateral lobes. Half of each left lateral lobe was snap frozen in liquid nitrogen for storage at -80^{o}C for biochemical analysis. The remainder was trimmed, washed in PBS and fixed in 10% formalin for 24 h. After processing and embedding in paraffin, 5-µm sections were cut on a rotary microtome. Xylene and alcohol were used to deparaffinize and rehydrate sections before H&E staining. Images were captured using a 10x objective. Necrotic areas were identified from ten random 10x fields, and necrotic areas were quantified using ImageJ (FIJI, Madison, WI) [255].

Serum Alanine Aminotransferase Measurement. Serum alanine aminotransferase (ALT) was measured using an ALT kit (Pointe Scientific, Canton, MI) according to the manufacturer's instructions [256].

NAPQI-Protein Adducts Assay. NAPQI-protein adducts in liver tissue were measured by HPLC as previously described [208].

Immunoblotting. JNK and phospho-JNK immunoblotting was performed as previously described [257, 258]. Primary antibodies were rabbit anti-JNK (cat. no. 9252,

Cell Signaling Technology, Danvers, MA), rabbit anti-phospho-JNK (cat. no. 4668) and rabbit anti ß-actin (cat. no 4967). Secondary antibody was an HRP-conjugated anti-rabbit IgG (1:5000, Santa Cruz Biotechnology, Dallas TX). Chemiluminescence was imaged using a LICOR Odyssey imaging system (LICOR Biosciences, Lincoln NE).

Immunohistochemistry. Liver sections were deparaffinized and rehydrated, followed by blocking in 2.5% normal horse serum supplied in a Vector IMMPress HRP polymer Kit (MP-7401, Vector Laboratories, Burlingame CA). Primary antibody was Alpha Diagnostics rabbit anti-4-HNE (4-hydroxynonenal, HNE11-S Alpha Diagnostics, San Antonio, TX), applied at 1:600 in PBS at 4^{o}C overnight. Vector IMMPress HRP polymer secondary antibody (Vector Laboratories, Burlingame, CA) was applied, and the sections were incubated for 30 minutes at room temperature. Cy3-conjugated anti-HRP antibody (1:500 in PBS, 123-165-021, Jackson Immunoresearch, West Grove, PA) was incubated with sections for 1 h before coverslipping with VectaShield Hard Set with DAPI mounting media (Vector Laboratories). Ten random images were collected using a 20x objective. 4-HNE immunofluorescence images were converted to 8-bit grayscale in Adobe Photoshop CS4 (Adobe, San Jose CA), and non-tissue background areas were set to a pixel value of 5 to normalize black levels. All images were then rescaled to the same levels. The images were then analyzed in ImageJ using thresholding of pixel values 35-255. Pixels within the threshold range were counted. Non-tissue regions in the image were excluded from analysis.

Intravital multiphoton microscopy. At 6 h after vehicle or APAP administration, mice were anesthetized with ketamine and xylazine (100 and 10 mg/kg, i.p., respectively), intubated a 20-gauge catheter inserted into the trachea and connected to a small animal

ventilator. Rhodamine 123 (Rh123, 2 μmol/mouse), a green-fluorescing mitochondrial polarization indicator, and propidium iodide (PI, 0.4 μmol/mouse), which labels the nuclei of non-viable cells, were infused via the femoral vein using polyethylene-10 tubing over 10 min.

After midline laparotomy, the liver was gently withdrawn from the abdominal cavity and placed over a no. 1.5 glass coverslip mounted on the stage of an Olympus Fluoview 1200 MPE multiphoton microscope (Olympus, Center Valley, PA) equipped with a Spectra Physics Mai Tai Deep Sea tunable multiphoton laser (Newport, Irvine, CA). Rh123 and PI fluorescence was imaged simultaneously using 820-nm multiphoton excitation and a 30x 1.05 N.A. silicon oil objective lens. The respirator was turned off for 5-10 sec to eliminate breathing artifacts during imaging. Ten or more random images were collected for each mouse. Bright punctate Rh123 fluorescence signified hepatocytes with polarized mitochondria, whereas dimmer diffuse cytosolic fluorescence signified cells with depolarized mitochondria. Percent area of mitochondrial depolarization was analyzed using ImageJ distributed by Fiji [255]. Nonviable, PI-positive cells were counted in 10 random images per animal.

Statistics. Differences between two groups were analyzed by the Student's *t*-test. One-way ANOVA followed by the Bonferroni post-hoc test was used for comparison of differences of 3 groups. $p < 0.05$ was considered statistically significant. Groups sizes were 3 or more.

RESULTS

Alda-1 decreases serum alanine aminotransferase release after acetaminophen treatment. After 24 h, vehicle-treated control animals without APAP exposure had serum ALT levels of 26 ± 5 U/L (**Figure 2-1**). After APAP, ALT increased to 7594 ± 1255 U/L ($p<0.001$ vs vehicle). Pretreatment with Alda-1 before APAP decreased serum ALT by more than two-thirds to 2132 ± 883 U/L compared to APAP alone ($p<0.01$ vs APAP) (**Figure 2-1**).

Alda-1 decreases centrilobular necrosis after acetaminophen treatment. Necrosis was assessed in H&E-stained liver sections 24 h after APAP treatment (**Figure 2**). Vehicle-treated control mice without APAP treatment showed no necrosis (**Figure 2-2A**). By contrast after 24 h, animals receiving APAP showed widespread centrilobular necrosis in 47.1 ± 2.8% of cross-sectional area (**Figure 2-2B and D**). Alda-1 treatment decreased necrosis to 20.7 ± 6.0% ($p<0.01$ vs APAP) (**Figure 2-2C and D**).

Alda-1 does not alter formation of NAPQI-protein adducts after APAP. The NAPQI intermediate of APAP metabolism is detoxified by conjugation with glutathione, but after the glutathione pool becomes depleted, NAPQI forms adducts with proteins [156, 159, 179, 180, 183-185]. Accordingly, we measured NAPQI adducts to cysteine residues of proteins after APAP**.** As expected, NAPQI-protein adducts were undetectable in animals not given APAP (**Figure 2-3**). After APAP, NAPQI-protein adducts increased to 0.34 ± .03 ng/mg protein ($p<0.01$ vs no APAP, **Figure 2-3**). With Alda-1 pretreatment before APAP, NAPQI-protein adducts remained high at 0.38 ± .03 ng/mg protein, which was not significantly different from APAP alone.

Alda-1 does not decrease JNK activation after APAP. Previous studies show that JNK activation is involved in cell death after acetaminophen overdose [159, 183, 185]. Accordingly, we assessed JNK and phospho-JNK (p-JNK) by immunoblotting. With vehicle only treatment, p-JNK was almost undetectable, and the ratio of p-JNK to JNK was 0.10 ± 0.03 (**Figure 2-4**). This ratio increased to 0.63 ± 0.06 after APAP treatment ($p<0.01$ vs no APAP, **Figure 2-4**). Alda-1 treatment did not significantly change JNK activation after APAP, with p-JNK/JNK averaging 0.56 ± 0.06.

Alda-1 decreases 4-hydroxynonenal-protein adduct formation after APAP. Lipid peroxidation produces aldehydes including 4-HNE. 4-HNE forms adducts with proteins that can be detected by immunohistochemistry. Without APAP, 4-HNE immunostaining was weak and corresponded to 0.13 ± 0.07% of the cross-sectional area (**Figure 2-5A and D**). 2 h after APAP, adducts increased to 7.3 ± 1.7% of area ($p<0.01$ vs vehicle) (**Figure 2-5B and D)**. At this timepoint, Alda-1 treatment decreased 4-HNE adducts to 1.0 ± 0.3% of area ($p<0.05$ vs APAP) (**Figure 2-5C and D**).

Alda-1 decreases mitochondrial depolarization and cell death after APAP. The mitochondrial permeability transition leads to mitochondrial depolarization and cell death after APAP overdose [31, 155, 156, 159]. Accordingly, we measured mitochondrial depolarization and cell death using intravital microscopy of Rh123 and PI fluorescence. In mice without APAP treatment, green Rh123 fluorescence was punctate in virtually every hepatocyte, indicating mitochondrial polarization, and red PI labeling of nuclei was absent (**Figure 2-6A**). After APAP treatment, depolarization increased 62.3 ± 2.0% of cross-sectional area ($p<.001$ vs. vehicle only) (**Figure 2-6B and D**), and the number of PI-labeled calls per 30x field increased to 6.8 ± 2.3 ($p<0.01$ vs. vehicle) **Figure 2-6B and E**).

With Alda-1 pretreatment, the area of mitochondrial depolarization after APAP decreased to 33.5 ± 3.4% ($p<0.01$ vs APAP alone) (**Figure 2-6C and D**), and the number of PI-labeled cells per field decreased to 0.6 ± 0.1 ($p<0.05$ vs APAP) (**Figure 2-6C and E).**

DISCUSSION

Aldehydes are important mediators of acetaminophen hepatotoxicity

Despite the introduction of NAC treatment, APAP hepatotoxicity is still the most common cause of liver failure worldwide [159, 179, 183-185]. NAC, a glutathione precursor, is most effective in early stages of APAP hepatotoxicity. When administered at later stages, the therapeutic effect of NAC markedly decreases, although some protection can still be achieved, possibly through the antioxidant effect of NAC [179]. Additional studies are needed to further elucidate the mediators of APAP hepatotoxicity so that new therapeutic targets can be identified. While previous studies have demonstrated that ROS play a role in APAP hepatotoxicity, the specific contribution of aldehydes, products of lipid peroxidation, remains unclear. Free aldehydes readily form adducts with proteins and nucleic acids, disrupting their function [68]. The electron transport chain of mitochondria is a main source of ROS underlying oxidant stress. The mitochondrial isoform of aldehyde dehydrogenase, ALDH2, detoxifies aldehydes including acetaldehyde, malondialdehyde, and 4-hydroxynonenal (4-HNE) among others [61, 69, 73]. In this study, we investigated the role of aldehydes in APAP hepatotoxicity by using Alda-1, an ALDH2 activator, to enhance detoxification of aldehydes in mice that receive an overdose of APAP.

Our results demonstrate that 4-HNE protein adducts increased as early as 2 h after APAP administration and continued to increase through 24 h (**Figure 2-5**). Notably, Alda-1 markedly blunted this increase of 4-HNE protein adducts after APAP at both timepoints (**Figure 2-5**). These data are consistent with the hypothesis that oxidative stress after APAP increases generation of toxic aldehydes and that activation of ALDH2 accelerates degradation of these aldehydes. Serum ALT also increased markedly after APAP, an

increase strongly blunted by Alda-1 pretreatment (**Figure 2-1**). Moreover, centrilobular necrosis occurring after APAP overdose was decreased by more than half with Alda-1 pretreatment (**Figure 2-2**). These data clearly demonstrate that APAP hepatotoxicity is associated with markedly increased reactive aldehyde production and that acceleration of aldehyde degradation effectively decreases APAP hepatotoxicity. Therefore, aldehydes are important mediators of APAP hepatotoxicity and a novel therapeutic target.

Acceleration of aldehyde detoxification decreases acetaminophen hepatotoxicity by protecting against mitochondrial dysfunction but not by altering acetaminophen metabolism or JNK activation

We explored how Alda-1 protects against APAP hepatotoxicity. Many events after APAP intoxication help mediate the pathogenesis of liver injury, such as NAPQI protein adduct formation, JNK activation, and onset of the MPT [156, 159, 179, 180, 183-185]. Previous studies show that APAP overdose increases the proportion of APAP metabolized to NAPQI by cytochrome P450 [159, 179]. Once GSH is depleted and can no longer detoxify NAPQI, NAPQI begins to form adducts with proteins and nuclear acids, altering their functions. This NAPQI adduct formation is a crucial step in APAP induced liver injury [159, 179, 183-185]. Therefore, we explored whether Alda-1 decreases APAP hepatotoxicity by alteration of APAP metabolism. We showed that NAPQI-protein adduct formation markedly increased after APAP treatment, but NAPQI-protein adduct formation was not decreased by Alda-1 (**Figure 2-3**). Therefore, Alda-1 protection is not due to alteration of APAP metabolism (**Figure 2-7**).

JNK activation is also linked to APAP hepatotoxicity [159, 185], and previous studies show that JNK inhibitors decrease APAP-induced liver injury [155]. NAPQI forms adducts with mitochondrial proteins of the electron transport chain, leading to increased ROS production. Apoptosis signal-regulating kinase 1 (ASK1, MAP3K5) and mitogen-activated protein kinase kinase kinase 11 (MLK3, MAP3K11) are the upstream kinases that activate JNK and are themselves activated by increased ROS [159, 185]. JNK activation is associated with prevention of apoptosis but potentiation necrosis [259]. This may explain why the dominant form of cell death is necrosis rather than apoptosis in APAP hepatotoxicity. Furthermore, persistent JNK activation can also increase ROS production thus further exacerbating necrosis [259]. Since JNK activation is associated with ROS formation, we explored whether aldehydes mediate JNK activation, JNK activation increased as early as 2 h after APAP administration. However, Alda-1 did not alter JNK activation (**Figure 2-4**). These data showed that Alda-1 protection against APAP hepatotoxicity is not due to inhibition of JNK activation (**Figure 2-7**). A possible explanation for this phenomenon is that ASK1 and MLK3 are activated by ROS but not by aldehydes.

Previous studies demonstrate that onset of the MPT plays a critical role in APAP hepatotoxicity [31, 155, 156, 158, 159]. The MPT is caused by opening of permeability transition (PT) pores in the mitochondrial inner membrane, leading to collapse of mitochondrial membrane potential, decreased ATP production and necrotic cell death [151, 155, 156, 158, 159]. The MPT can also trigger apoptosis by causing release of proapoptotic factors such as cytochrome *c* [151]. APAP causes onset of the MPT in both cultured hepatocytes and *in vivo* [155, 158]. The MPT inhibitors cyclosporin A and NIM811 decrease APAP-induced necrotic cell death [155, 158]. ROS, JNK activation and

mitochondrial translocation, and iron translocation from lysosomes to mitochondria all help trigger the MPT [31, 155, 158]. The present study confirmed that mitochondrial depolarization occurs after APAP, indicating onset of the MPT (**Figure 2-6**). Importantly, Alda-1 decreased mitochondrial depolarization and subsequent cell death (**Figure 2-6**). These results show that aldehydes contribute to initiating the onset of the MPT, thus leading to liver injury after APAP overdose (**Figure 2-7**). Aldehydes including 4-HNE are previously reported to promote MPT in isolated liver mitochondria and to be involved in the pathogenesis of cardiovascular diseases [49, 50].

Taken together, this study demonstrates that aldehydes are important mediators of APAP hepatotoxicity, and that acceleration of aldehyde degradation is a promising approach to decrease APAP-induced liver injury. Moreover, this study demonstrates that Alda-1 protection is not due to decreased APAP metabolism or inhibition of JNK activation but is mediated by prevention of aldehyde-induced mitochondrial dysfunction after APAP overdose (**Figure 2-7**). Mitochondria are at particular risk of lipid peroxidation due to active production of ROS from the respiratory chain and the high content of unsaturated phospholipids in mitochondrial membranes. Therefore mitochondria are likely exposed to high levels of reactive aldehydes [260]. Overall, activation ALDH2 to increase the rate of aldehyde detoxification is a promising therapeutic strategy to prevent mitochondrial dysfunction and protect cells in high ROS environments, such as occurs in APAP hepatotoxicity.

FIGURES

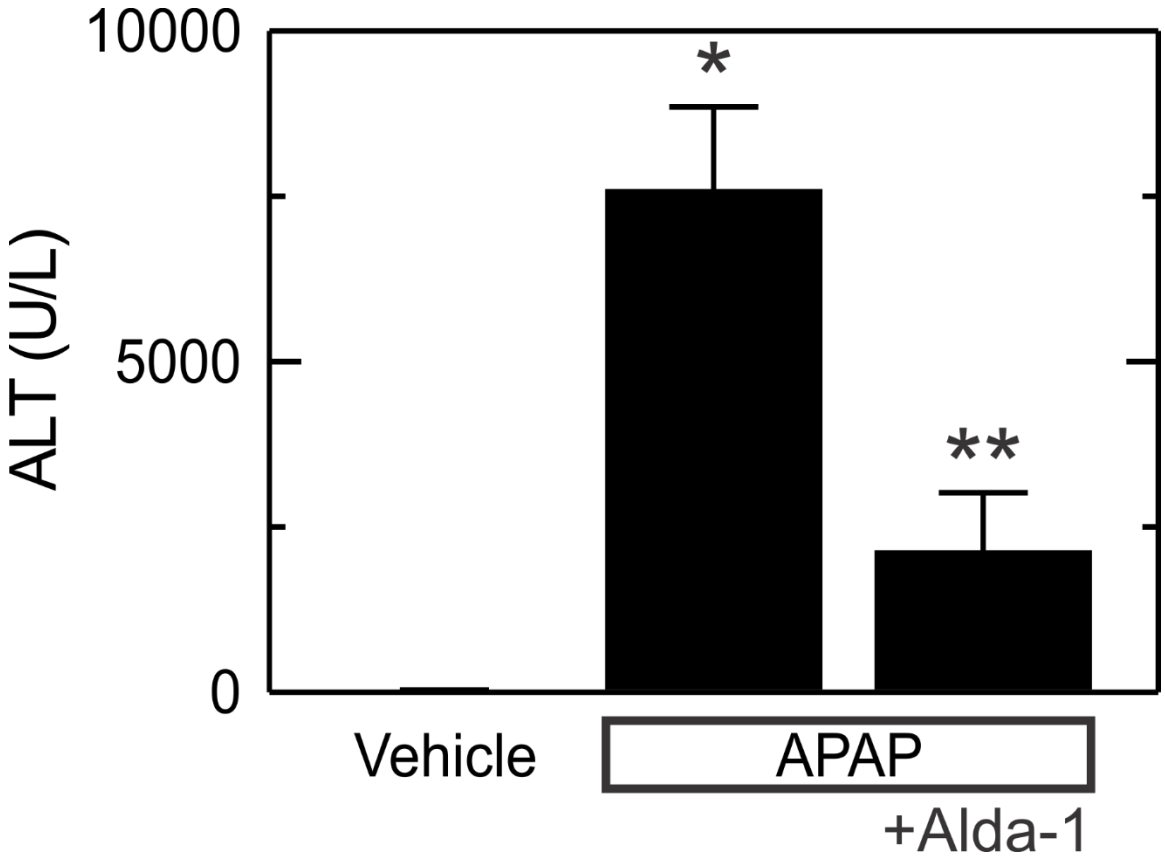

Figure 2-1. Alda-1 decreases alanine aminotransferase release after acetaminophen overdose.

Serum ALT was measured 24 h after treatment with vehicle only, APAP, and APAP plus Alda-1. Values are means ± SEM (n = 4 per group). *, $p<0.01$ vs. Vehicle; **, $p<0.01$ vs. APAP.

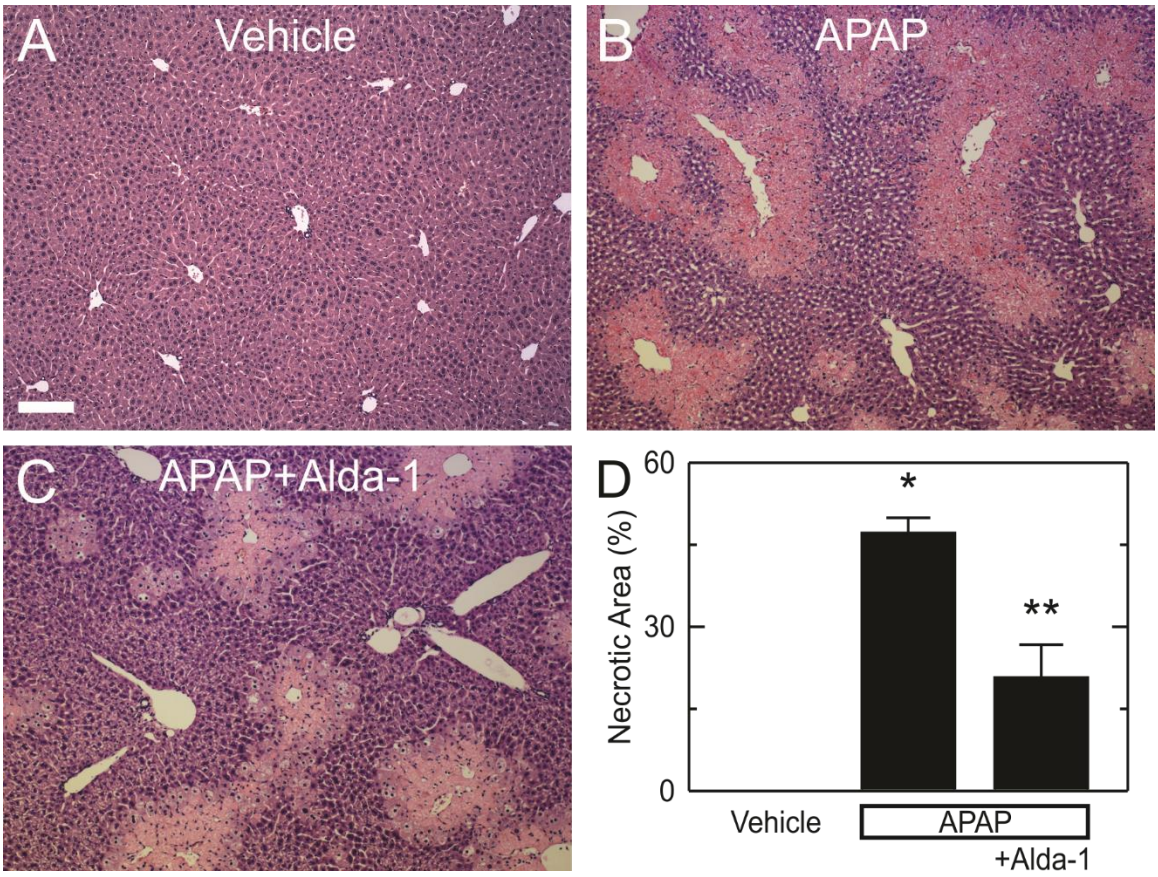

Figure 2-2. Alda-1 decreases centrilobular necrosis after acetaminophen overdose.

Livers were harvested for H&E histology 24 h after treatment with vehicle only (**A**), APAP (**B**) and APAP plus Alda-1 (**C**) (representative images are shown). Ten random images were collected per slide using a 10x objective, and necrotic areas were quantified (**D**). Values are means ± SEM (n = 4, 3 and 4, respectively, for Vehicle, APAP and APAP plus Alda-1. Bar is 200 µm. *, $p<0.01$ vs. Vehicle; **, $p<0.01$ vs. APAP.

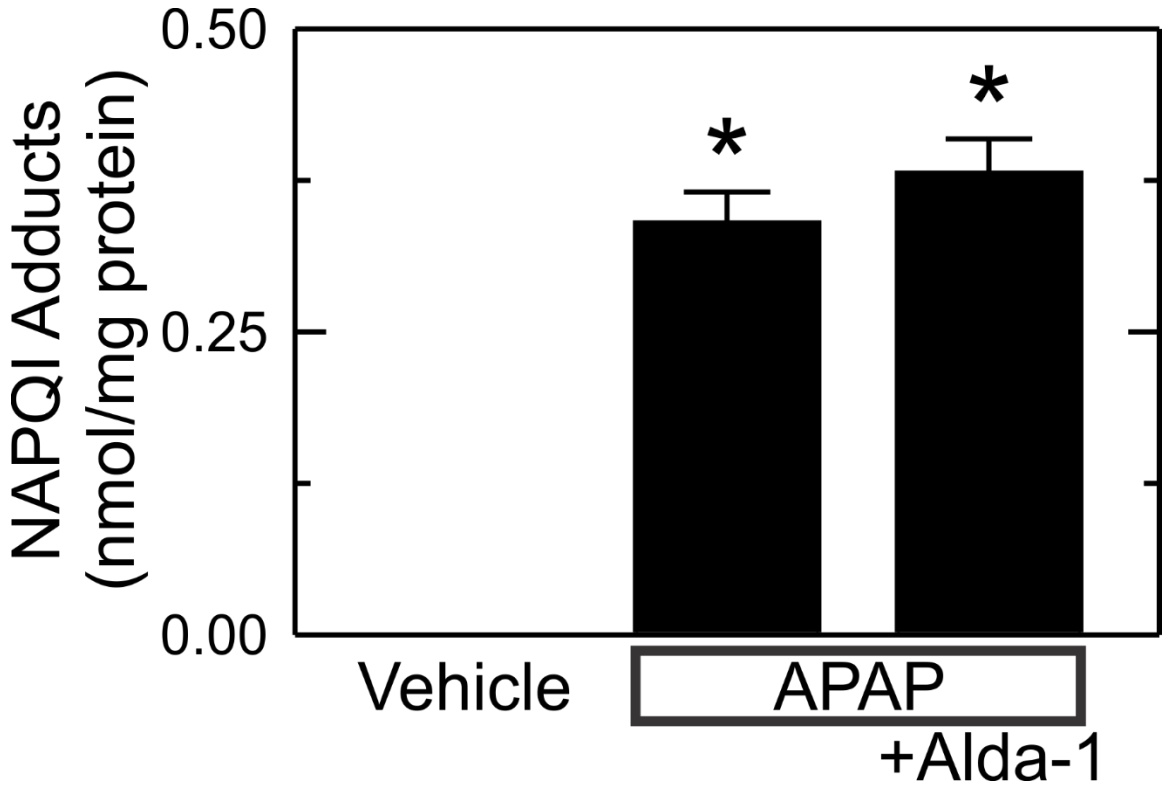

Figure 2-3. Alda-1 does not alter formation of NAPQI-protein adducts after acetaminophen.

Livers were harvested 2 h after vehicle only, APAP and APAP plus Alda-1 treatments. NAPQI-protein adducts were measured by HPLC. Values are mean ± SEM (n = 5/group). *, $p<0.01$ vs. Vehicle.

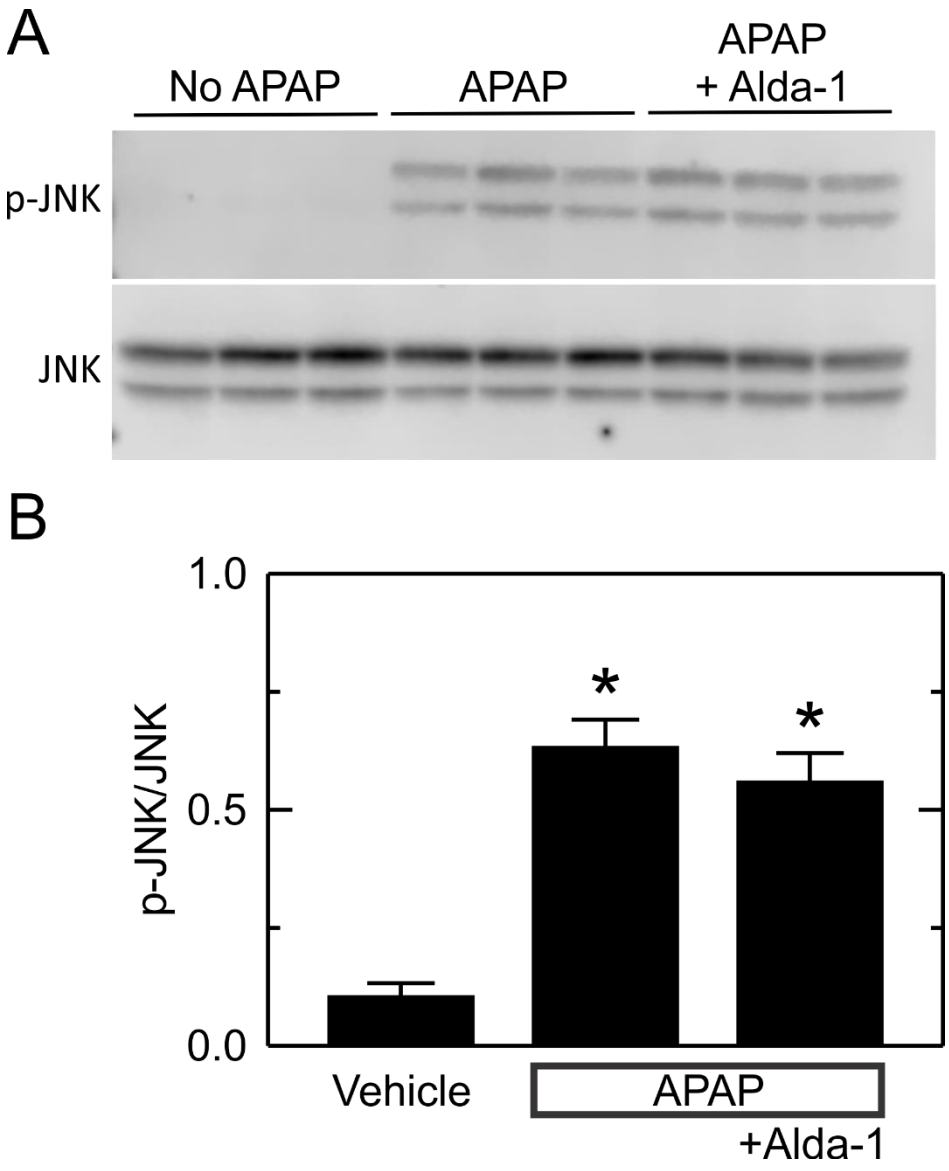

Figure 2-4. Alda-1 does not alter JNK activation after acetaminophen.

Livers were harvested 2 h after vehicle with vehicle only, APAP or APAP plus Alda-1. JNK and p-JNK were detected by immunoblotting, quantified by densitometry and reported as p-JNK/JNK ratios. **A** shows representative images of p-JNK and JNK

immunoblots (n=3/group). **B** shows quantified values as means ± SEM (n = 5/group). *, $p<0.05$ vs. Vehicle.

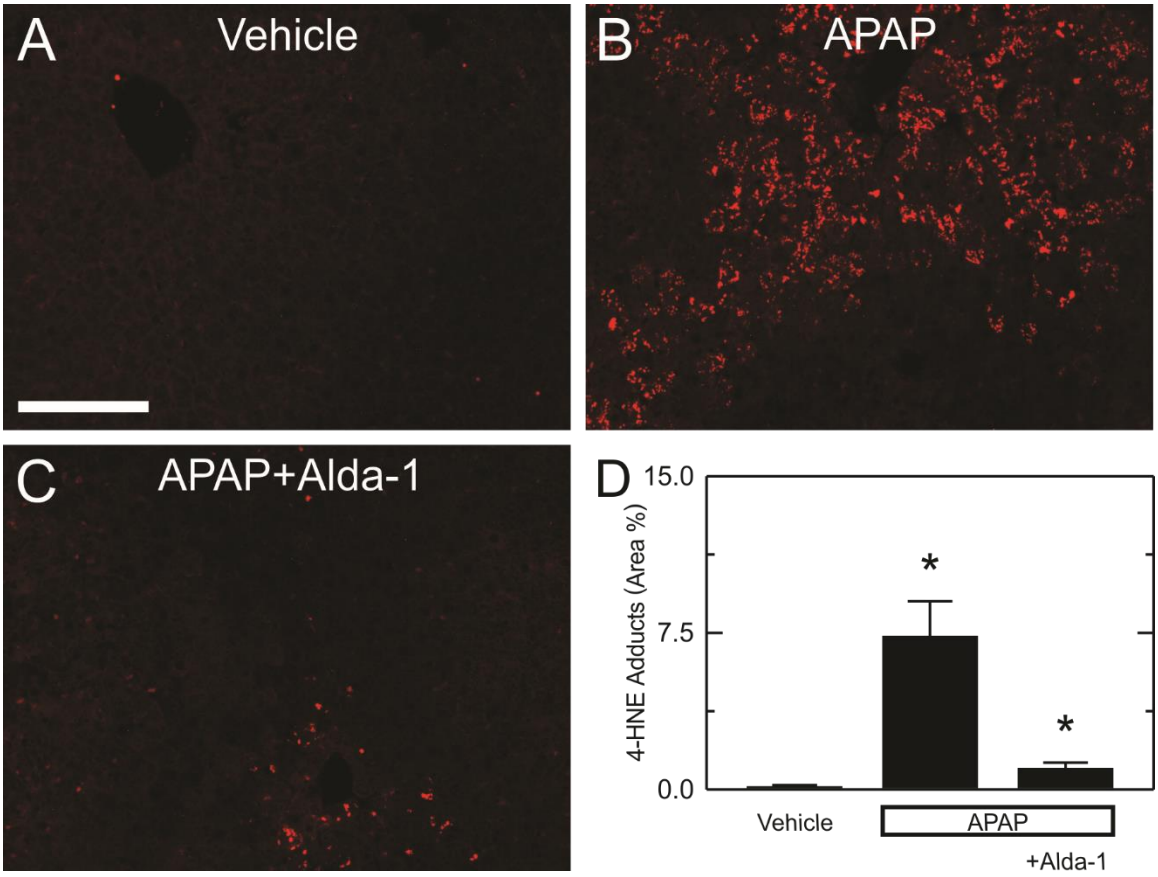

Figure 2-5. Alda-1 decreases 4-HNE adducts after acetaminophen overdose.

Livers were harvested 2 h after treatment with vehicle only **(A)**, APAP (**B**), and APAP plus Alda-1 (**C**), and immunohistochemistry was performed to detect 4-HNE as in Methods (representative images are shown). The scale bar = 100 µm. Ten random images were collected per slide using a 10x objective, and 4-HNE positive areas were quantified (**D**) using histomorphometry as in Methods. Values are means ± SEM (n = 5/group). *, $p<0.05$ vs. vehicle alone; **, $p<0.05$ vs. APAP.

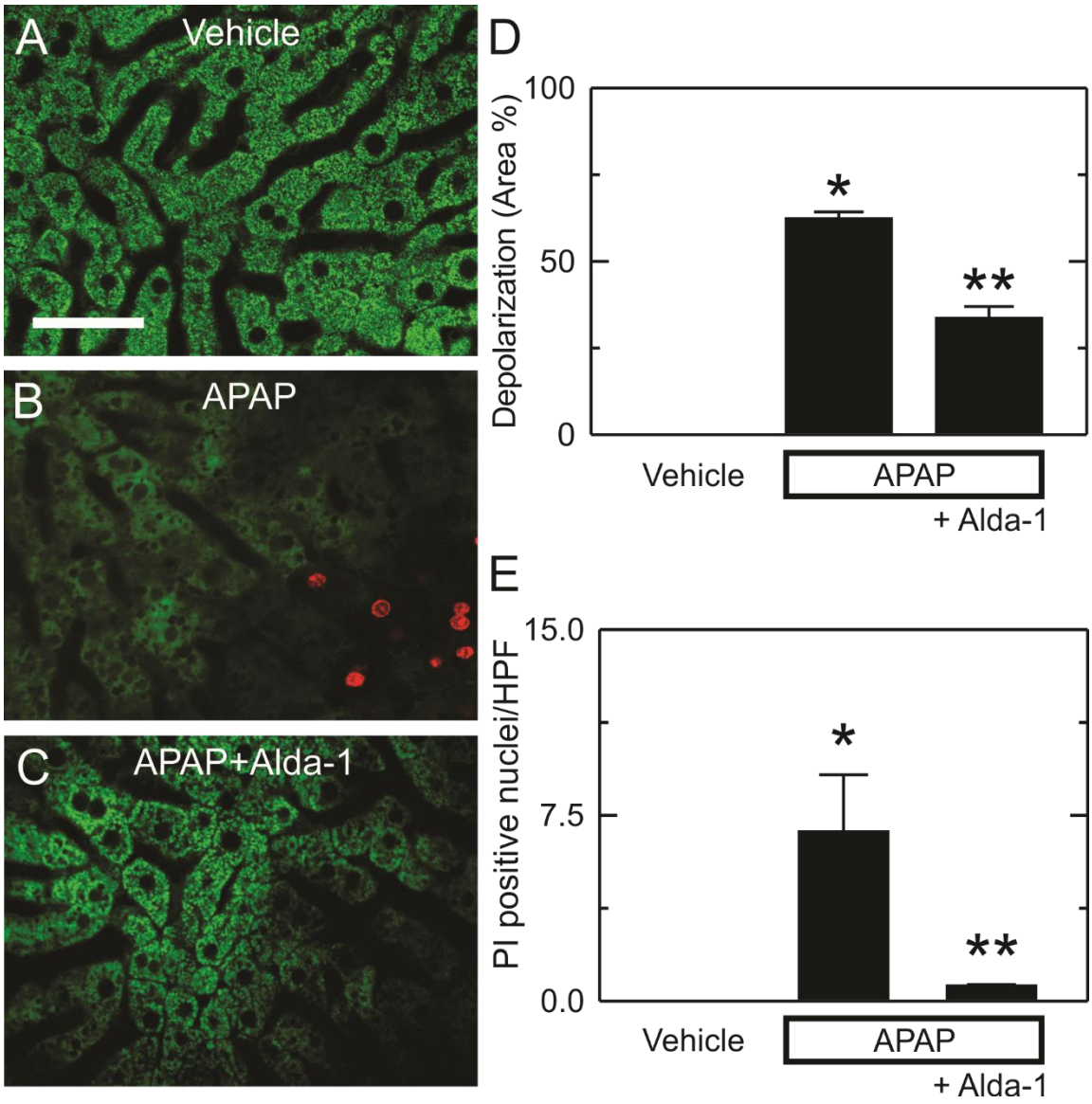

Figure 2-6. Alda-1 decreases mitochondrial depolarization and cell death after APAP overdose.

Animals were infused with rhodamine 123 (green) and PI (red) 6 h after treatment with vehicle only (**A**), APAP (**B**), and APAP plus Alda-1 (**C**). Livers were imaged 10 min

later using two-photon intravital microscopy. Shown are representative images. Bar is 50 μm. For each liver imaged, 10 random images were obtained using a 30x objective lens and quantified for depolarized area (**D**) and PI-positive nuclei per high power field (**E**). Values are means ± SEM (n = 3/group). *, $p<0.05$ vs. Vehicle; **, $p<0.05$ vs. APAP.

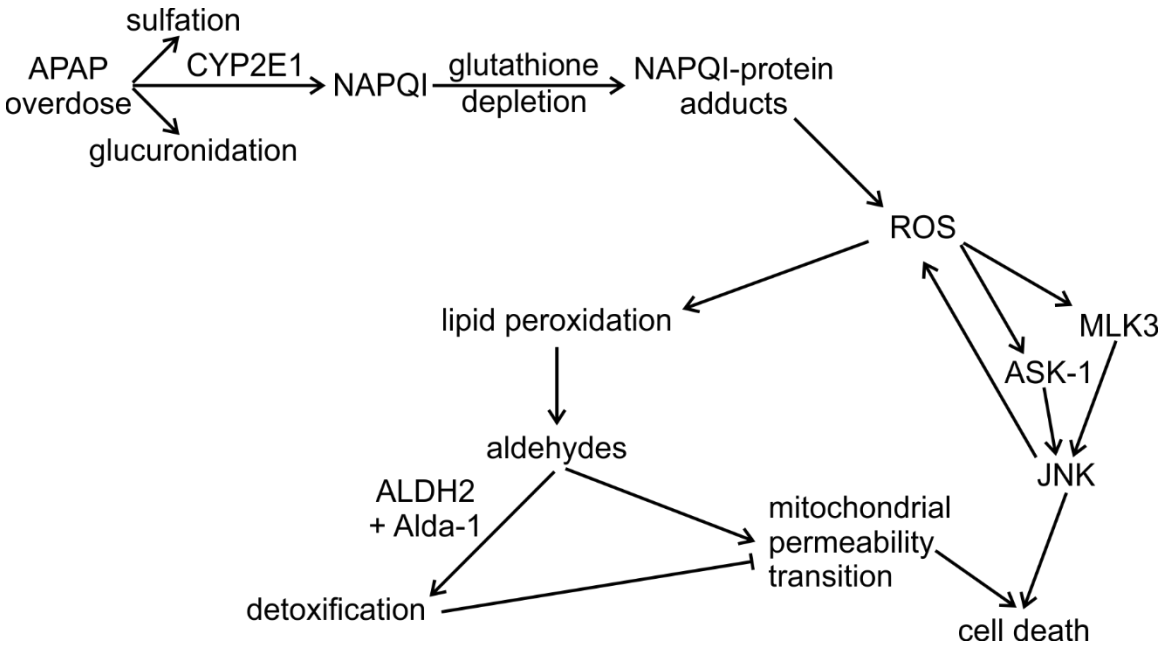

Figure 2-7. Aldehyde dehydrogenase-2 activation by Alda-1 decreases acetaminophen hepatotoxicity by detoxifying aldehydes and preventing the mitochondrial permeability transition.

An overdose of APAP saturates the sulfation and glucuronidation pathways causing a greater proportion of APAP to be metabolized to NAPQI. Excess NAPQI causes depletion of GSH, leading to the formation of NAPQI protein adducts in mitochondria. The resulting increased ROS formation causes JNK activation via the ASK1 and MLK3 pathways, as well as aldehyde formation by lipid peroxidation. These aldehydes promote onset of the MPT and cell death. Detoxification of aldehydes by ALDH2 activated by Alda-1 decreases cell death by preventing the MPT.

CHAPTER 3: Aldehyde Dehydrogenase-2 Activation by Alda-1 Decreases Necrosis and Fibrosis After Bile Duct Ligation in Mice

ABSTRACT

Background and Aim: Liver fibrosis is a leading cause of morbidity and mortality worldwide. Oxidative stress is a key component in the pathogenesis of liver fibrosis. We investigated the role of aldehydes resulting from lipid peroxidation in cholestatic liver injury and fibrosis.

Methods: C57Bl/6J mice underwent bile duct ligation (BDL) or sham operation. One hour after surgery and daily thereafter, mice were given Alda-1 (20 mg/kg s.c.), an aldehyde dehydrogenase-2 activator, or an equivalent volume of vehicle. Blood and livers were collected after 3 and 14 days.

Results: Serum alanine aminotransferase (ALT) increased to 537 U/L 3 days after BDL, and Alda-1 reduced this increase by 48%. Biliary infarcts with a periportal distribution developed in an area of 7.8% 14 days after BDL *versus* 0% area after sham operation. Alda-1 treatment during BDL decreased the biliary infarct area to 1.9%. Fibrosis detected by picrosirius red morphometry increased from an area of 1.6% in sham to 7.3% after BDL, which decreased to 3.8% with Alda-1. Alda-1 mediated suppression of fibrosis was additionally confirmed by second harmonic generation microscopy. After BDL, collagen-I mRNA increased 12-fold compared to sham, which decreased to 6-fold after Alda-1 exposure. Smooth muscle α-actin, a marker of activated myofibroblasts, increased from 1% area in sham to 18.7% after BDL, which decreased to 5.3% after Alda-1. Macrophages increased from 33.4 cells/field in sham to 132 cells/field after BDL and were decreased to 65 cells/field with Alda-1. Finally, 4-hydroxynonenal adduct (4-HNE) immunofluorescence was expressed in an area of 2.5% in sham, 14.1% after BDL, and 2.2% after Alda-1.

Conclusion: Accelerated aldehyde degradation by Alda-1 decreases BDL-induced liver necrosis, inflammation, and fibrosis, implying that aldehydes play an important role in the pathogenesis of cholestatic liver injury and fibrosis.

Keywords: 4-hydroxynonenal, Alda-1, aldehyde dehydrogenase-2, aldehydes, fibrosis, hepatic stellate cells, inflammation, macrophages, osteopontin, oxidative stress.

INTRODUCTION

Chronic liver disease and cirrhosis are leading causes of morbidity and mortality with 40,326 deaths (12.5 per 100,000 population) in the US in 2015 [217, 221, 223, 231, 261]. Fibrotic transformation is the result of a wound healing process that fails to self-regulate, which is stimulated by chronic injury to the liver, including viral infection, alcoholic and non-alcoholic liver disease, cholestasis, toxic chemical exposure, and others [262-265]. As fibrosis progresses, structural changes and loss of liver function become irreversible and can only be remedied by liver transplantation. While an understanding of fibrotic processes has increased over the past twenty years, effective treatments for fibrosis have not yet become available [223, 266].

Previous studies in our and other laboratories have demonstrated that reactive oxygen species (ROS) play a role in the pathogenesis of liver injury and fibrosis [25-28, 51, 226, 267]. ROS directly attack macromolecules and alter mitochondrial function, leading to liver injury. ROS also stimulate inflammation and fibrosis [226]. Antioxidant therapy, such as green tea polyphenols, decreases fibrosis after cholestasis [27]. Moreover, mitochondria are prone to damage by ROS. Overexpression of superoxide dismutase-2, the mitochondrial isoform, shows greater efficacy than overexpression of cytosolic superoxide dismutase-1 in decreasing liver injury, fibrotic signaling, and fibrosis after bile duct ligation (BDL), which indicates an important role of mitochondrial ROS in stimulation of injury and fibrosis [28]. MitoQ, a mitochondrially targeted antioxidant, also markedly decreases carbon tetrachloride induced liver injury and fibrosis [231].

ROS lead to lipid peroxidation, resulting in damage to lipid membranes [226]. Moreover, peroxidized lipids undergo ß-scission to form aldehydes like malondialdehyde

(MDA) and 4-hydroxynonenal (4-HNE). Free aldehydes are reactive and readily form adducts with proteins, nucleic acids and other lipids. Such adduct formation disrupts protein function and can lead to mitochondrial dysfunction, apoptotic signaling, and necrosis [68]. Aldehydes are detoxified by the aldehyde dehydrogenase family. The mitochondrial isoform, aldehyde dehydrogenase-2 (ALDH2), detoxifies a multitude of aldehydes at physiological concentrations, with increasing K_m and decreasing K_{cat} as chain length increases [69]. Recently, an activator of ALDH2, Alda-1 (N-(1,3-benzodioxol-5-ylmethyl)-2,6-dichlorobenzamide) was discovered and has proven to decrease experimental radiodermatitis and experimental ischemia-reperfusion injury in multiple organs [61, 65-68, 73, 84-86, 88].

Although oxidative stress correlates with fibrosis [25, 51], the role of aldehydes in the pathogenesis of fibrotic liver injury is not well understood. Alda-1 provides a tool to examine whether accelerated aldehyde detoxification through activation of ALDH2 ameliorates fibrosis in liver. Here, we investigated the role of aldehydes in the pathogenesis of fibrosis using an experimental cholestasis model in mice. We demonstrate that treatment with Alda-1 decreases biliary infarct, inflammation and fibrosis after BDL.

EXPERIMENTAL PROCEDURES

Synthesis of Alda-1. Alda-1 was synthesized in one step by coupling 2.5 g 2,6 dichlorobenzoic acid to 4g benzo[*d*][1,3]dioxol-5-ylmethanamine in N,N-dimethylformamide under standard peptide coupling conditions with 5.5 g [(1-[bis(dimethylamine)methylene]-1H-1,2,3-triazolo[4,5-b]pyridinium 3-oxid hexafluorophosphate (HATU), 5 g N-ethyl-N-isoproylpropan-2-amine (DIPEA), Upon completion, the reaction mixture was washed with five 25 mL portions dichloromethane. The dichloromethane solution was then washed with two 25 mL portions of saturated sodium chloride and dried over anhydrous magnesium sulfate. The solution was then filtered, the solvent was removed by rotary evaporation, and the residue was purified by silica gel chromatography using a Teledyne Combiflash (Teledyne Isco, Lincoln NE). Fractions containing the product were pooled, and the solvent removed to afford pure Alda-1 as an amorphous solid. The product was shown to be certified 99+% pure by HPLC chromatography, and the structure was verified by NMR spectroscopy using a Bruker Nanobay 400 (9.4T) operating at 400MHz.

Bile Duct Ligation and Alda-1 Administration. Male C57BL/6 mice (23-27g) were purchased from the Jackson Laboratory (Bar Harbor, MA) and maintained on a 12-h light/dark cycle with *ad libitum* food and water. All animal procedures followed the NIH "Guide for the Care and Use of Laboratory Animals" and were approved by the Institutional Animal Care and Use Committee at the Medical University of South Carolina. Under isoflurane anesthesia, a midline abdominal incision was performed and the common bile duct isolated. The common bile duct was ligated three times with 6-0 silk suture and bisected between the middle and distal ligature. Sham animals had the bile duct isolated

without ligation, and the abdomen was then closed. One hour after surgery and daily thereafter, BDL animals received 20 mg/kg Alda-1 or an equivalent volume of DMSO vehicle subcutaneously. Sham-operated mice received vehicle only.

Tissue Harvest and Processing. At 3 and 14 days after surgery, mice were anesthetized with pentobarbital (80 mg/kg, i.p.). A laparotomy was performed, and blood was collected from the inferior vena cava. The liver was perfused with 5 mL normal saline via the portal vein. The left lateral lobe was then removed. Half of the lobe was snap frozen in liquid nitrogen and stored at -80^{o}C for biochemical analysis. The edges of the other half of the lobe were trimmed and the lobe bisected before fixation in 10% neutral buffered formalin for 24 h before washing in water and processing for paraffin embedding. Sections (5-µm) were cut on a rotary microtome. Slides were deparaffinized and rehydrated through an alcohol series before staining with hematoxylin and eosin (H&E) or picrosirius red. Area analysis of ten random 10X fields was performed using ImageJ (FIJI, Madison, WI) [255]. For analysis, biliary infarcts were identified from ten random 10x fields per animal, with areas recorded as the number of pixels in each region of interest. Picrosirius red stained images were converted to 8-bit RGB stacks, and the green channel was used for thresholding using pixel values 0-75, and the number of pixels in the range was recorded.

Serum Alanine Aminotransferase Measurement. Serum alanine aminotransferase (ALT) was measured using an ALT kit (Pointe Scientific, Canton, MI) according to the manufacturer's instructions [256].

Immunohistochemical staining. Osteopontin (OPN), alpha-smooth muscle actin (α-SMA), cluster of differentiation 68 (CD68) and 4-HNE adducts were detected by immunohistochemistry in rehydrated 5-µm deparaffinized sections, as described in Table

1. Ten random images were collected using 10X or 20X objective lenses, and The FIJI distribution of ImageJ was used for analysis [255]. For OPN and α-SMA, the color deconvolution tool was used to isolate stained regions. The number of pixels in these regions were counted by the software. CD68 positive cells were counted in 20x random fields. 4-HNE immunofluorescence images were processed in Adobe Photoshop CS4. Images were converted to 8-bit grayscale images. Non-tissue background areas were set to a pixel value of 5 to normalize black levels. All images were then rescaled to the same range of 0-100, improving brightness and contrast for analysis. The images were then analyzed in ImageJ using thresholding of pixel values 35-255 and the pixels within this range were counted. Non-tissue regions in the image were excluded from analysis.

Detection of fibrosis by second harmonic generation microscopy. Second-harmonic generation (SHG) microscopy was performed with an Olympus FluoView 1200MPE laser scanning multiphoton microscope (Center Valley, PA) using a 30x UPLSAPO30XS silicone oil immersion objective and 900-nm excitation. SHG was detected through a 450-nm interference filter [268].

Real-time PCR. mRNA for collagen-I (COL-I) were assessed by two-step qPCR as previously described [269]. Briefly, total RNA was isolated using QIAzol lysis reagent (QIAGEN, Hilden, Germany) and quantified with a spectrophotometer. RNA (2µg) was reverse-transcribed into cDNA with a SuperScript III kit (Invitrogen, Carlsbad CA). qPCR was performed with a Bio-Rad MyiQ Single-Color Real-Time PCR Detection System using iQ SYBR Green Supermix (Bio-Rad, Hercules, CA). COL1 cDNA was normalized to cDNA for glyceraldehyde phosphate dehydrogenase (GAPDH) by the ΔΔ*Ct* method using Ct values obtained with MyiQ software. Col.1α1 primers were

TCAGCCACCTCAAGAGAAGTC (forward) and CTGCGGATGTTCTCAATCTGC (reverse). GAPDH primers were TGCACCACCAACTGCTAAGC (forward) and GGCATGGACTGTGGTCATGAG (reverse).

Statistics. Differences between two groups were analyzed by the Student's *t*-test. One-way ANOVA followed by the Bonferroni post-hoc test was used for comparison of the difference of 3 groups. $p < 0.05$ was considered statistically significant. Groups sizes were 4 or more.

RESULTS

Alda-1 decreases serum alanine aminotransferase after bile duct ligation. Three days after sham surgery, serum ALT was 39.8 ± 10.5 U/L (Figure 1). After BDL with vehicle treatment, ALT increased 13.5-fold to 537 ± 78.9 ($p<0.01$). Treatment with Alda-1 after BDL decreased serum ALT to 281.0 ± 37.2 ($p<0.01$ vs BDL plus vehicle), which was a 7.1-fold increase compared to sham (Figure 1).

Alda-1 decreases biliary infarct area after bile duct ligation. Necrosis was assessed in H&E-stained liver sections after 14 days (Figure 2). In livers of sham animals, no necrosis was observed (Figure 2A). By contrast, at 14 days after BDL with vehicle treatment, areas of focal necrosis (biliary infarcts) developed in 7.8% ± 0.6% of cross-sectional area (Figure 2B and D). Alda-1 treatment decreased biliary infarct area to 1.9% ± 1.0% ($p<0.01$) (Figure 2C and D). The number of biliary infarcts per 10x field after BDL plus vehicle was 1.26 ± 0.16 and did not change after BDL plus Alda-1 (0.92 ± 0.53, $p>0.10$ vs. BDL plus vehicle).

Alda-1 decreases fibrosis after bile duct ligation. Picrosirius red staining was performed to visualize collagen deposition and morphometric analysis was used to quantitate fibrosis expression. In sham mice, picrosirius red staining occurred primarily in portal tracts and around large vessels – and was present in 1.6% ± 0.5% of cross-sectional area of the liver (Figure 3A and D). After BDL, picrosirius red staining increased in portal and periportal areas and was 7.3% ± 2.7% of the cross-sectional area of the liver ($p<0.01$) (Figure 3B and D). Treatment with Alda-1 decreased picrosirius red staining after BDL to 3.8% ± 0.5% ($p<0.05$ vs. BDL plus vehicle) (Figure 3C and D).

Fibrosis was also visualized in paraffin sections by SHG microscopy, which directly visualizes elongated fibrous structures, such as collagen fibrils [231, 270]. In sham mice, SHG signals were confined to portal tracts and around large vessels (Figure 4A). After BDL, SHG signals became more intense and widely distributed (Figure 4B). Alda-1 treatment after BDL attenuated the fibrotic changes (Figure 4C). These results confirmed the findings by picrosirius red staining.

COL-I mRNA was measured to assess collagen expression. In BDL mice after vehicle treatment, COL-I mRNA increased 12 ± 1.4-fold compared to sham. By contrast, in Alda-1 treated BDL mice, COL-I mRNA increased only 6.1 ± 1.4-fold, ($p<0.05$ vs BDL plus vehicle) (Figure 5).

Alda-1 leads to a reduction of stellate cell activation after bile duct ligation. In fibrosis, collagen-producing cells of various origins transdifferentiate into myofibroblast-like cells expressing both α-SMA and collagen; in the liver these cells have been shown to be hepatic stellate cells [223, 266, 271]. Accordingly, we used α-SMA immunohistochemistry and morphometric analysis to identify and quantitate changes in α-SMA expression, respectively. In sham animals, the α-SMA positive area was 1% ± 0.1%, primarily identified in the vasculature – as expected (Figure 6A and D). After BDL with vehicle treatment, α-SMA expression markedly increased to 18.7% ± 2.2% of area with intense staining in the portal, periportal and perisinusoidal regions (Figure 6B and D). With Alda-1 treatment after BDL, α-SMA staining decreased to 5.3% ± 1.7% ($p<0.01$ vs BDL plus vehicle) (Figure 6C and D).

Alda-1 decreases inflammatory infiltrates after bile duct ligation. Previous studies show that BDL causes infiltration of inflammatory cells [251]. Accordingly, we

quantified macrophage infiltration by immunohistochemical staining for the macrophage marker CD68. In sham mice, the number of CD68-positive cells was 33.4 ± 4.8 per 20X field (Figure 7A and D). After BDL with vehicle treatment, CD68-positive cells increased to 134.5 ± 8.6 per field (Figure 7B and D). Alda-1 treatment after BDL decreased this infiltration to 64.9 ± 4.0 per field ($p<0.01$ vs BDL plus vehicle) (Figure 7C and D).

Alda-1 decreases osteopontin expression after bile duct ligation. OPN is a mediator of inflammation and fibrosis after BDL [272]. In sham mice, OPN was present principally in cholangiocytes, and OPN immunoreactivity was 0.4% ± 0.1% of cross-sectional area (Figure 8A and D). After BDL with vehicle treatment, OPN expression markedly increased primarily in cholangiocytes and to a lesser extent in periportal parenchymal cells to 2.5% ± 0.3% of area (Figure 8B and D). With Alda-1 treatment after BDL, OPN-positive area decreased to 0.9% ± 0.3% ($p<.01$ vs BDL plus vehicle), and OPN expression became nearly absent in the parenchyma (Figure 8C and D).

Alda-1 decreases 4-hydroxynonenal adduct formation after bile duct ligation. 4-HNE adducts were detected by immunohistochemistry. In the livers of sham mice, 4-HNE adducts were present in 2.5% ± 1.1% of cross-sectional area, which increased to 14.1% ± 3.5% after BDL ($p<0.01$ vs. sham) (Figure 9A, B and D). Alda-1 treatment after BDL decreased 4-HNE immunoreactivity to 2.2% ± 1.0% ($p<0.01$ vs. BDL plus vehicle) (Figure 9C and D).

DISCUSSION

Liver fibrosis and cirrhosis are major causes of morbidity and mortality in the US and worldwide, but effective therapy is lacking. Identification of novel therapeutic targets is critical to the development of anti-fibrotic treatments beyond treating the underlying injury. Previous studies show that oxidative stress plays an important role in cholestatic liver injury and fibrosis [25-28, 51, 226, 267]. However, whether reactive aldehydes produced by oxidative stress mediate injury and fibrosis remains unclear. In this study, we investigated the role of aldehydes in the pathogenesis of liver fibrosis by using Alda-1, an ALDH2 activator, to decrease aldehyde load in mice that have undergone BDL surgery.

Our results showed a strong anti-necrotic and anti-fibrotic effect by Alda-1. ALT increased after BDL but was decreased with Alda-1 treatment (Figure 1). Necrotic biliary infarcts increased after BDL but were decreased markedly in size but not number by Alda-1 treatment (Figure 2). Picrosirius red staining and second-harmonic generation showed increased collagen deposition after BDL, which was blunted by Alda-1 treatment (Figure 3 and 4). Furthermore, Alda-1 treatment decreased COL-I mRNA expression after BDL (Figure 5). After BDL, myofibroblast-like cells began to express α-SMA, and CD68-positive macrophages infiltrated, events that Alda-1 treatment decreased (Figure 6 and 8).

A characteristic ductular reaction with proliferation of cholangiocytes occurred after BDL consistent with previous reports (Figure 2) [251, 272-274]. The expression of OPN in cholangiocytes also increased, and OPN expression was also observed in the parenchyma after BDL. While the ductular reaction was present after BDL with Alda-1, OPN expression decreased to a smaller area and became nearly absent in the parenchyma (Figure 8). In addition, 4-HNE adducts, formed by an aldehyde associated

with lipid peroxidation reacting with proteins, were increased by BDL and decreased by Alda-1 treatment after BDL (Figure 9), Taken together, these data are consistent with the conclusion that aldehydes formed after oxidative stress play an important role in the pathogenesis of necrotic liver injury and fibrosis in cholestatic liver disease. Previous studies by others demonstrated that Alda-1 is protective in other settings of high oxidative stress, such as ischemia-reperfusion injury to heart and other organs and radiation-induced dermatitis, which also indicates that aldehydes are important mediators of oxidative stress-induced injury [51, 61, 65-69, 73, 84-86, 88]. Although 4-HNE is a product of oxidative stress, the formation of 4-HNE adducts interferes with the mitochondrial electron transport chain, leading to further increase of oxidative stress and lipid peroxidation. [50, 53].

In this study, we showed that activation of ALDH2 with Alda-1 to accelerate degradative metabolism of reactive aldehydes decreases cell death after BDL (Figure 2). How aldehydes cause cell death is incompletely understood. One possibility is that aldehydes promote mitochondrial dysfunction. Previous studies show that 4-HNE mediates cardiac ischemia/reperfusion injury by modifying mitochondrial proteins such as cytochrome *c* oxidase [46, 47]. HNE adducts also form on succinate dehydrogenase leading to inhibition [275]. 4-HNE was also reported to be a strong promotor of the mitochondrial permeability transition (MPT), which could lead to both necrosis and apoptosis after BDL [49, 50]. Therefore, acceleration of aldehyde degradation likely accounts for protection by Alda-1 against cell death after BDL.

How Alda-1 inhibits fibrosis remains uncertain. Although fibrosis after BDL is usually believed to be stimulated by cell injury and death [26, 214, 215, 225, 231, 239], another

study showed that the cyclosporin A analog NIM811, an inhibitor of the MPT, markedly decreases cell death after BDL but does not block fibrosis [276]. Thus, it is possible that aldehydes may stimulate fibrosis by a mechanism other than cell death mediated inflammatory changes. Nonetheless, hepatic stellate cells (HSC) are resistant to direct activation by aldehydes [277]. The role of exogenous or endogenous aldehydes on cholangiocytes and Kupffer cells remains unclear. Aldehydes are linked to secretion of HSC activators like OPN from cholangiocytes and TNF-α from Kupffer cells, though whether the aldehydes are generated within the cholangiocytes and Kupffer cells after BDL, or released from hepatocytes that are under oxidative stress will require further study [277, 278].

In liver fibrosis, oxidative stress stimulates inflammatory processes [26, 214, 223, 231, 266]. Here, Alda-1 decreased macrophage infiltration after BDL, indicating suppression of inflammation (Figure 7). This finding is consistent with the conclusion that aldehydes promote inflammation after BDL. Inflammation amplifies liver injury and stimulates fibrosis [214, 223, 226, 231, 251, 265-267, 279], and a recent study shows that intraperitoneal injection of 4-HNE exacerbates colonic inflammation in a mouse model of dextran sulfate sodium-induced inflammatory bowel disease, leading to enhanced activation of toll-like receptor 4 signaling [52]. Cell injury and death also lead to release damage-associated molecular pattern molecules that stimulate inflammation, whereas infiltrating leukocytes produce toxic cytokines and reactive oxygen and nitrogen species to damage cells and promote fibrosis [214, 223, 266, 279]. Together, the processes of inflammation and cell injury create a vicious cycle, which reactive aldehydes enhance. Moreover, infiltrating inflammatory cells, resident Kupffer cells and injured hepatocytes

activate HSCs by releasing cytokines and growth factors to promote fibrosis [278-281]**.** Thus, inhibition of inflammation can prevent the cell death and inflammatory cascades that promote fibrogenesis. Oxidative stress also stimulates inflammasome activation, leading to formation of proinflammatory IL-1 [282]. Aldehydes may also promote these reactions, since 4-HNE increases inflammasome activation and IL-1β production in cultured ARPE-19 retinal pigment epithelial cells [283].

OPN is a multifunctional protein produced in many tissues and exists in all body fluids. OPN is involved in diverse biological and pathological processes, including inflammation and fibrosis [284]. OPN promotes recruitment and retention of leukocytes in inflamed sites and is implicated in autoimmune diseases [285, 286]. Relevant to hepatic fibrosis, OPN increases HSC activation, migration, and production of TGF-ß and collagen [272, 287, 288], although other studies show that OPN has anti-inflammatory effects through downregulation of Stat-1 phosphorylation resulting in downregulation of iNOS expression [289-293]. Oxidative stress and mitochondrial dysfunction increase OPN expression [284, 294, 295]. Interestingly, we observed a marked increase of OPN expression after BDL, which Alda-1 decreased (Figure 7). These data suggest that aldehydes may also mediate increased expression of OPN as a pro-inflammatory and profibrotic mediator after BDL.

Taken together, the present study shows that reactive aldehydes produced by oxidative stress are important mediators of cholestatic liver injury, inflammation, and fibrosis. Mitochondria are an important source of ROS and target for lipid peroxidation due to their high content of membranes [260]. Thus, increasing the clearance of aldehydes in mitochondria by activation of ALDH2 is a promising anti-fibrotic therapy.

FIGURES

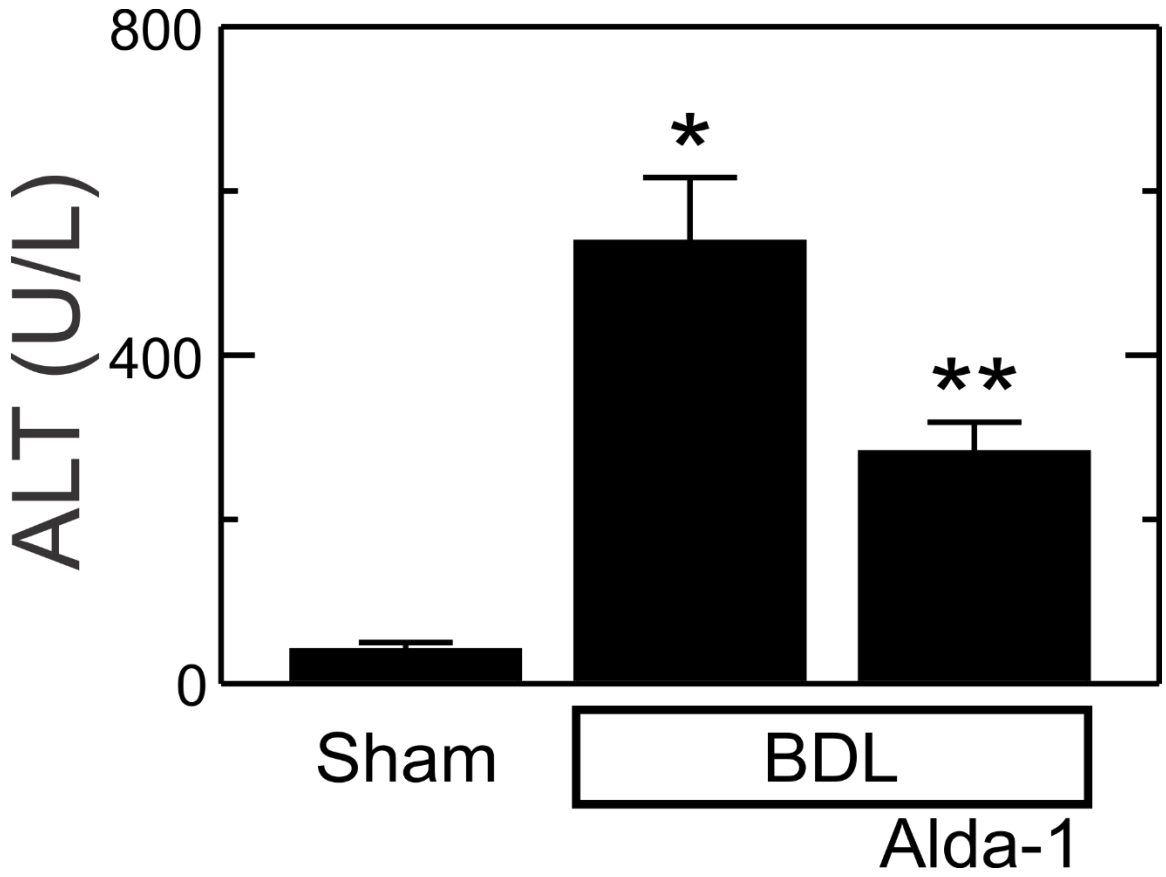

Figure 3-1. Alda-1 decreases alanine aminotransferase release after bile duct ligation.

Serum ALT was measured 3 days after sham operation plus vehicle treatment, BDL plus vehicle treatment, and BDL plus Alda-1 treatment. Values are means ± SEM (n = 5, 4 and 5, respectively, for sham, BDL and BDL plus Alda-1; *, $p<0.01$ vs. sham; **, $p<0.01$ vs. sham and BDL).

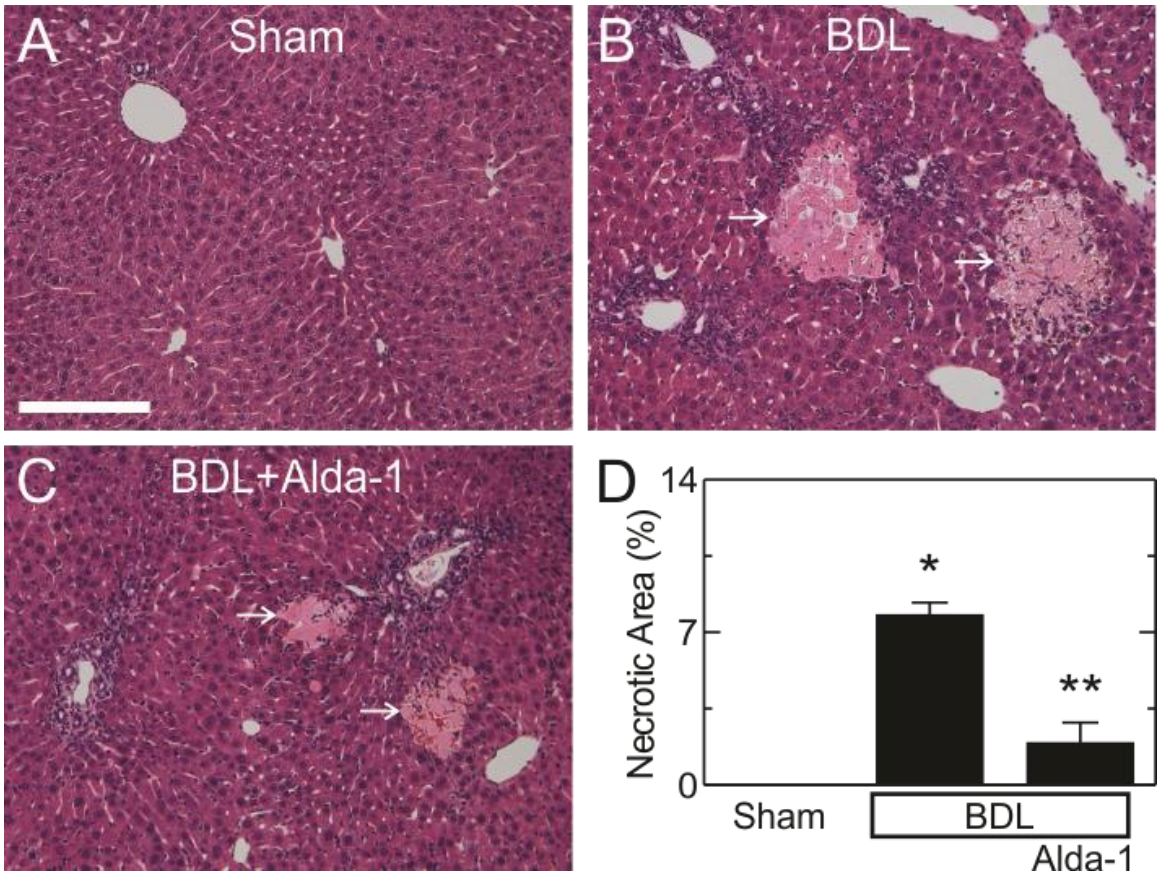

Figure 3-2. Alda-1 decreases biliary infarct size after bile duct ligation.

Livers were harvested 14 days after sham operation plus vehicle treatment (**A**), BDL plus vehicle treatment (**B**) and BDL plus Alda-1 treatment (**C**), fixed, and subjected to H&E histology. Representative images are shown. The scale bar = 200 microns. Ten random images were collected per slide using a 10x objective, and necrotic areas (arrows) were quantified (**D**). Values are means ± SEM (n = 6, 5 and 6, respectively, for sham, BDL and BDL plus Alda-1; *, $p<0.01$ vs. sham; **, $p<0.01$ vs. sham and BDL).

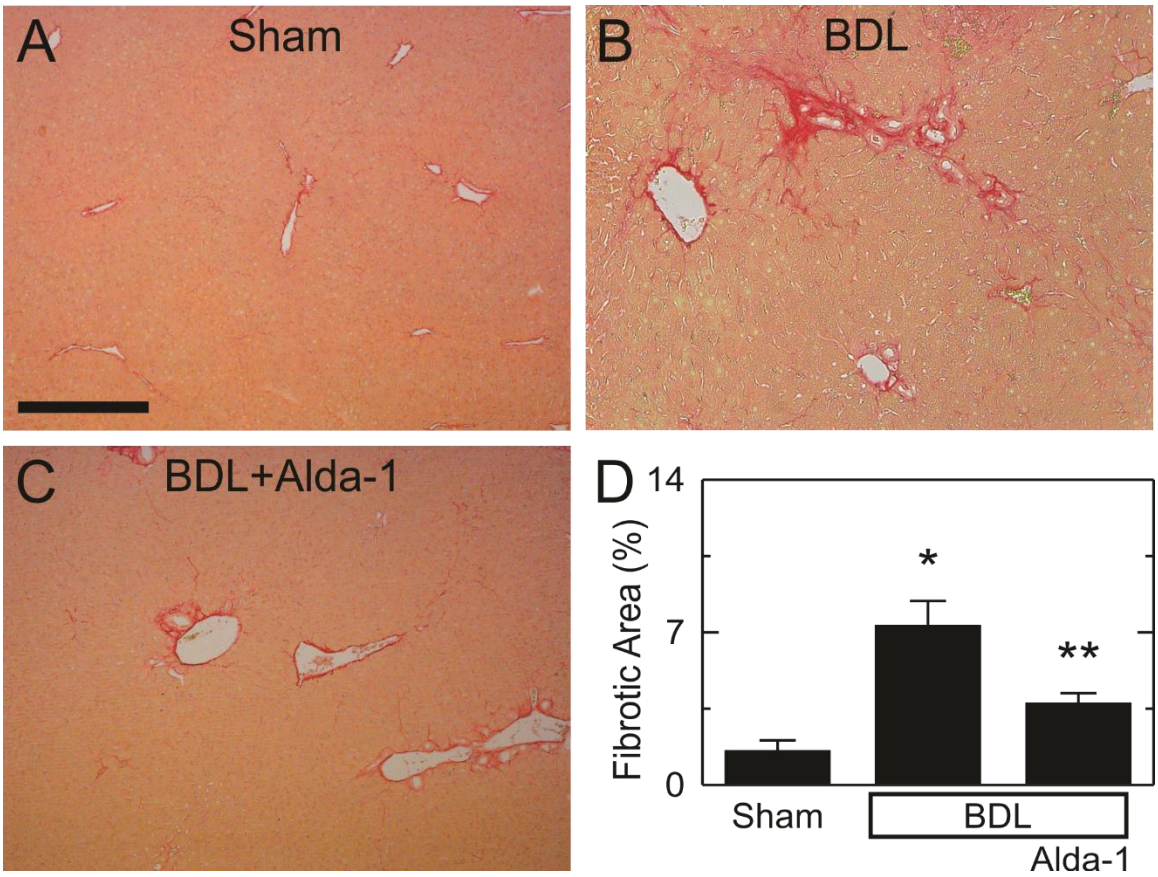

Figure 3-3. Alda-1 decreases picrosirius red staining after bile duct ligation.

Livers were harvested 14 days after sham operation plus vehicle treatment (**A**), BDL plus vehicle treatment (**B**) and BDL plus Alda-1 treatment (**C**), as described in Figure 2, fixed and subjected to picrosirius red staining as in Methods. Representative images are shown. The scale bar = 200 µm. Ten random images were collected per slide using a 10x objective, and picrosirius red-positive areas were quantified (**D**). Values are mean ± SEM (n = 6, 5 and 6, respectively, for sham, BDL and BDL plus Alda-1; *, $p<0.01$ vs. sham; **, $p<0.05$ vs. BDL; BDL plus Alda-1 is not statistically different compared to sham).

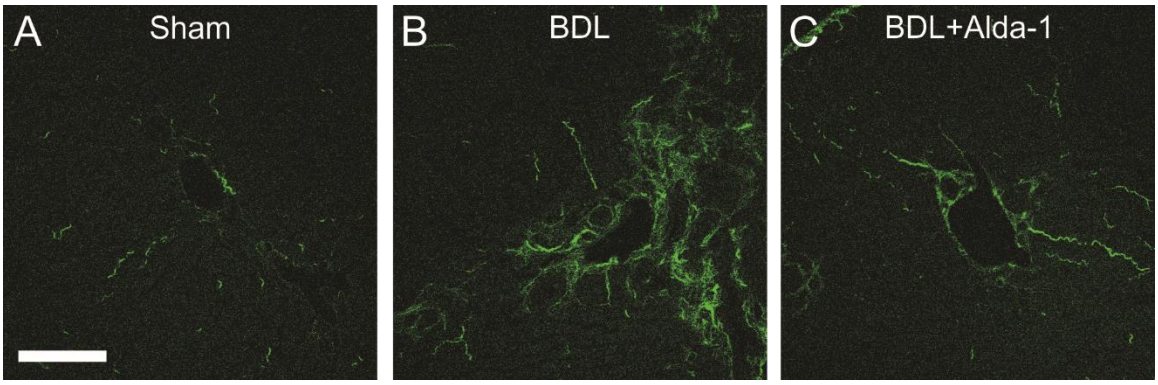

Figure 3-4. Alda-1 decreases second harmonic generation signals after bile duct ligation.

Livers were harvested 14 days after sham operation plus vehicle treatment (**A**), BDL with vehicle treatment (**B**) and BDL with Alda-1 treatment (**C**), as described in Figure 2. SHG images were collected from paraffin sections after H&E staining, as described in **EXPERIMENTAL PROCEDURES**. Representative images are shown. Bar is 100 μm.

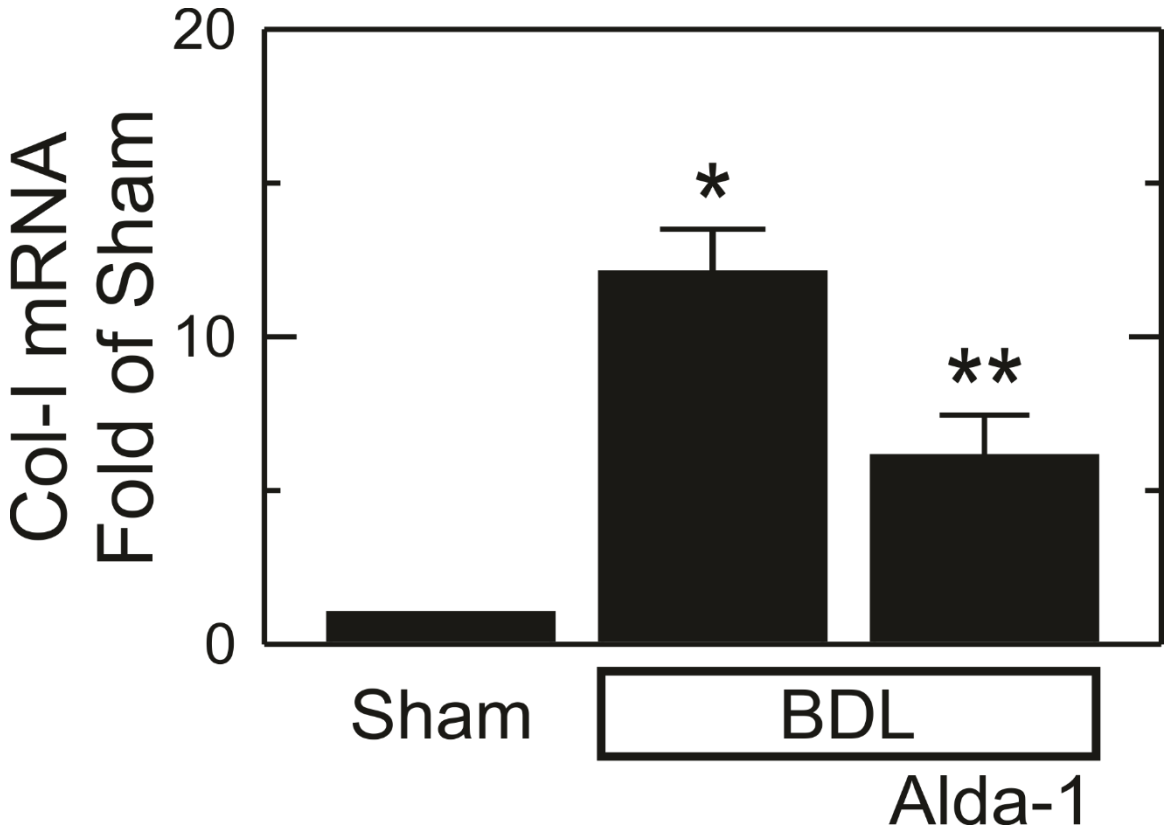

Figure 3-5. Alda-1 decreases collagen-I mRNA expression after bile duct ligation.

Livers were harvested 14 days after sham operation with vehicle treatment, BDL with vehicle treatment and BDL with Alda-1 treatment, as described in Figure 2. Col-I mRNA was assessed by qPCR as in Methods. Values are means ± SEM (n =4/group; *, $p<0.01$ vs. Sham, **$p<0.05$ vs. BDL).

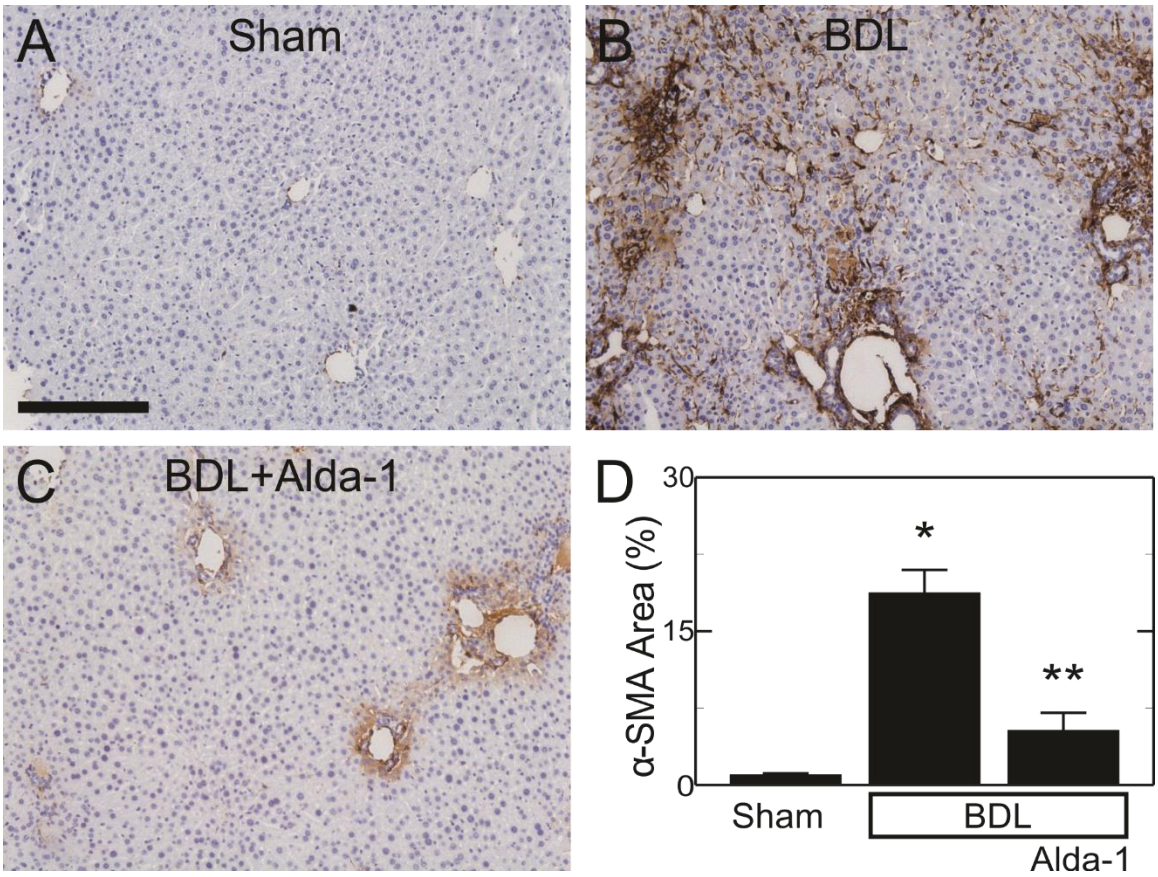

Figure 3-6. Alda-1 decreases myofibroblast-like cells after bile duct ligation.

Livers were harvested 14 days after sham operation plus vehicle treatment (**A**), BDL with vehicle treatment (**B**) and BDL with Alda-1 treatment (**C**), as described in Figure 2, and subjected to immunohistochemical analysis to detect α-SMA. Representative images are shown. The scale bar = 200 μm. Ten random images were collected per slide using a 10x objective, and the area containing α-SMA labeling was quantified morphometrically (D). Values are means ± SEM (n = 5, 5 and 5, respectively, for sham, BDL and BDL plus Alda-1; *, $p<0.01$ vs. sham; **, $p<0.01$ vs. BDL).

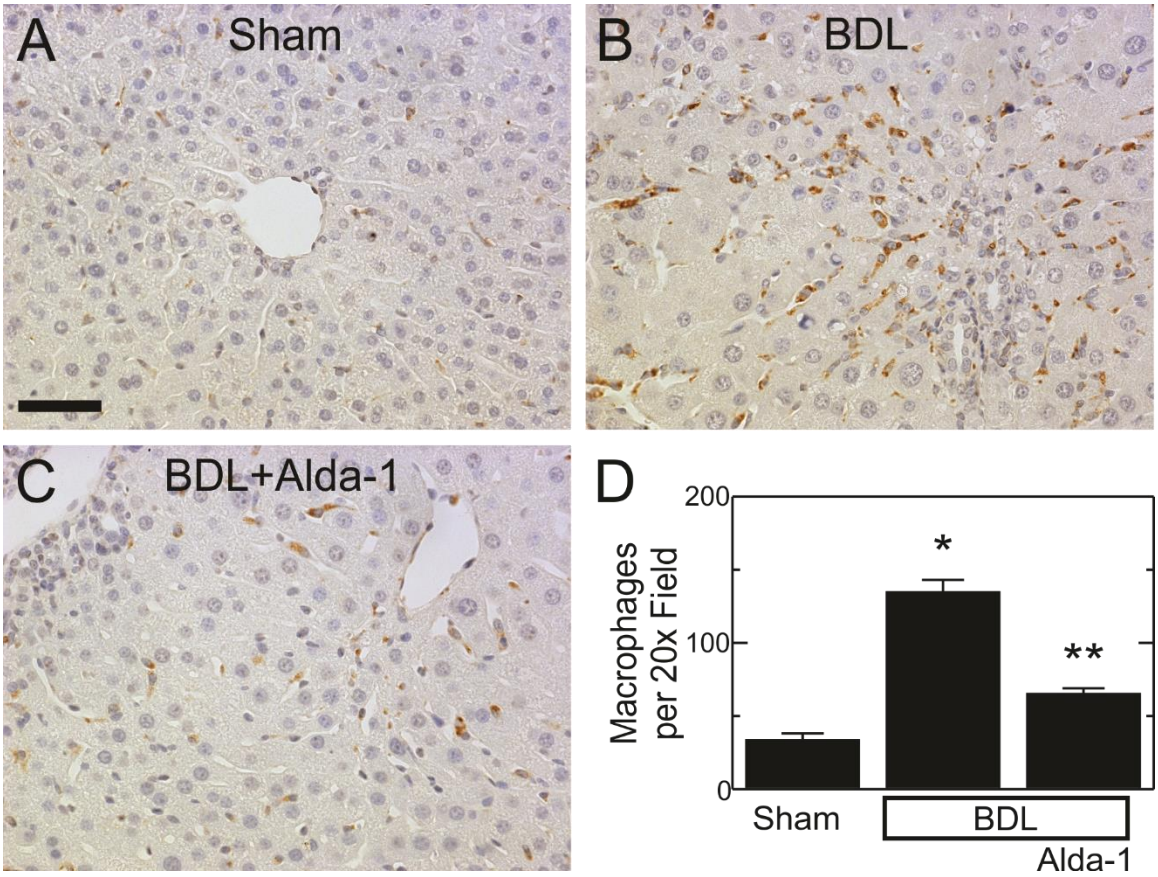

Figure 3-7. Alda-1 decreases macrophage infiltration after bile duct ligation.

Livers were harvested 14 days after sham operation with vehicle treatment (**A**), BDL with vehicle treatment (**B**) and BDL with Alda-1 treatment (**C**), as described in Figure 2. The macrophage marker CD68 was detected immunohistologically. Representative images are shown. The scale bar = 200 μm. For quantification, 10 random images were collected per slide using a 20x objective, and CD68 positive cells were counted. Values

are means ± SEM (n = 6, 5 and 6, respectively, for sham, BDL and BDL plus Alda-1; *, $p<0.01$ vs. sham; **, $p<0.01$ vs. sham and BDL).

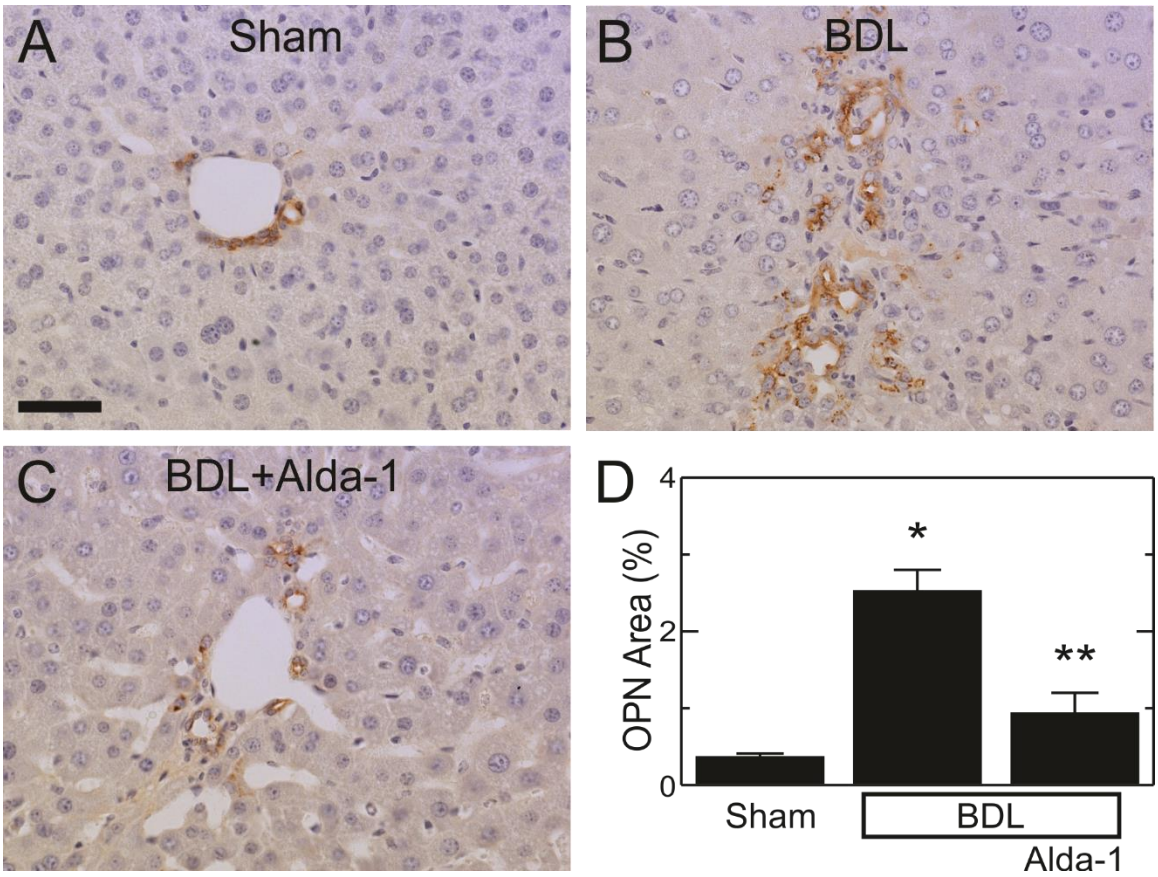

Figure 3-8. Alda-1 decreases osteopontin expression after bile duct ligation.

Livers were harvested 14 days after sham operation with vehicle treatment (A), BDL with vehicle treatment (B) and BDL with Alda-1 treatment (C), as described in Figure 2, and OPN was detected immunohistochemically. Representative images are shown. The scale bar = 200 µm. For quantification, 10 random images were collected per slide under a 20x objective (D). Values are means ± SEM (n = 6, 5 and 6, respectively, for sham, BDL and BDL plus Alda-1; *, $p<0.01$ vs. sham; **, $p<0.01$ vs. BDL).

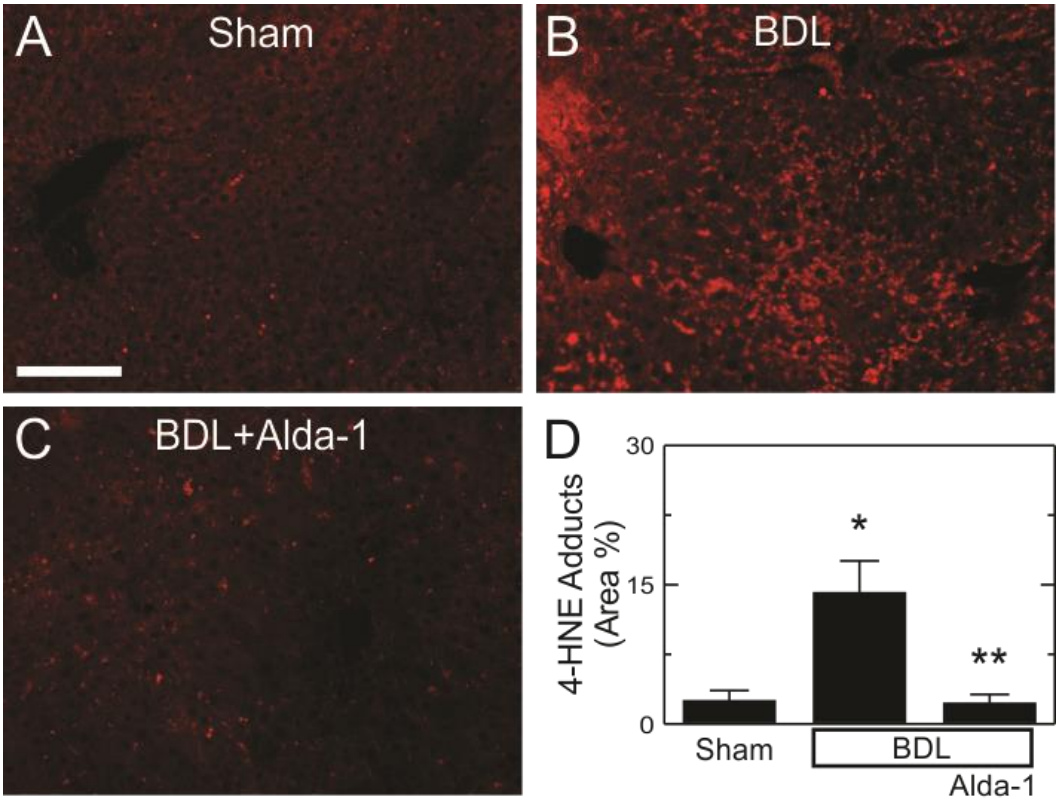

Figure 3-9. Alda-1 decreases 4-HNE adducts after bile duct ligation.

Livers were harvested 14 days after sham operation with vehicle treatment (**A**), BDL with vehicle treatment (**B**) and BDL with Alda-1 treatment (**C**), as described in Figure 2, and 4-HNE adducts were revealed by immunofluorescence labeling. Representative images are shown. The scale bar = 100 µm. Ten random images were collected per slide using a 20x objective, and 4-HNE positive areas were quantified (**D**). Values are means ± SEM (n = 5, 5, and 6, respectively, for sham, BDL and BDL plus Alda-1; *, $p<0.01$ vs. sham; **, $p<0.01$ vs. BDL).

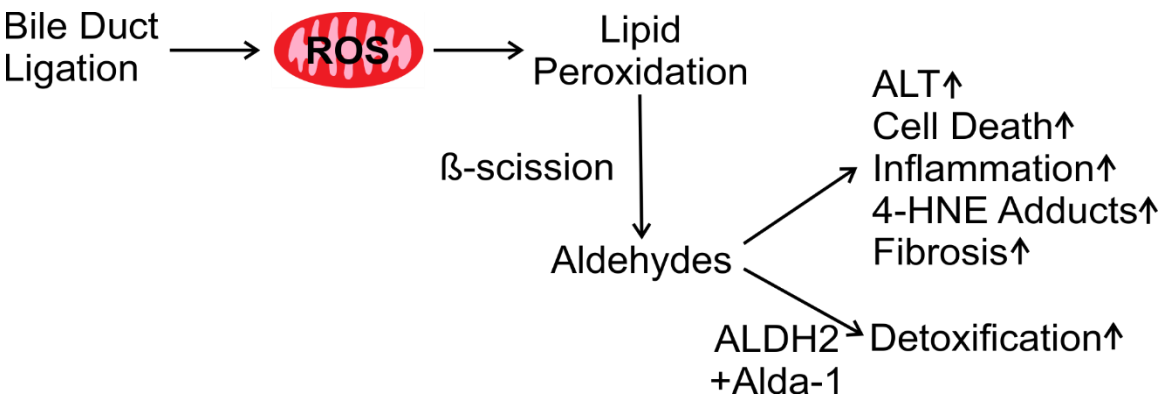

Figure 3-10. Aldehyde detoxification by aldehyde dehydrogenase-2 activation by Alda-1 decreases liver injury and fibrosis after bile duct ligation.

After bile duct ligation, mitochondrial ROS generate aldehydes by lipid peroxidation that are detoxified by ALDH2 activated by Alda-1. The result is a blunting of ALT, cell death, inflammation, aldehyde adduct formation, and fibrosis.

Table 3-1. Antibodies and Immunohistochemical Protocols.

	Osteopontin	α-SMA	CD-68	4-HNE Adducts
Antigen Retrieval	0.5% pepsin, 37°C, 10 min	citrate buffer/ heat, 30 minutes		none
Blocking	DAKO serum free protein block		2.5% normal horse serum	
Primary Ab	R&D AF808, goat anti-OPN, 1:1000 4°C, overnight	Abcam ab124964 rabbit anti-α-SMA, 1:1000, 4°C, overnight	Abcam ab125212 rabbit anti-CD68, 1:1000, 4°C, overnight	Alpha Diagnostics HNE11-S rabbit anti-4-HNE, 1:600, 4°C, overnight
Secondary Ab/Amplification	Santa Cruz sc-2020 donkey anti-goat 1:200, 23°C, 1 h	DAKO Envision+ Rabbit HRP Kit, 23°C, 1 h	Vector IMMPress HRP polymer kit, 23°C, 30min	
Visualization/ Tertriary Fluorescent Antibody	DAKO DAB kit, 3 min		Vector DAB kit, 2 min	Jackson Immuno 123-165-021 Cy3 anti-HRP, 1:500, 23°C, 1 h

Deparaffinized tissue sections were immunostained for OPN, α-SMA, CD68 and 4-HNE using the listed protocols. HRP, horseradish peroxidase.

Chapter 4: Summary and Conclusions

Oxidative stress, in particular mitochondrial oxidative stress, plays an important role in the pathogenesis of liver disease and fibrosis, as reviewed in Chapter 1 [18-28]. Oxidative stress leads to lipid peroxidation, which produces reactive aldehydes, but the role of these aldehydes in liver diseases remain unclear. In this study, I tested the central hypotheses that aldehydes are important mediators of liver injury and fibrosis and that acceleration of aldehyde degradation decreases liver injury and fibrosis.

The aldehyde dehydrogenase (ALDH) family of enzymes detoxifies aldehydes by oxidizing them to the corresponding organic acid. ALDH2 is of particular importance as a mitochondrial isoform abundant in the liver [64]. The small molecule Alda-1 activates ALDH2, thus increasing the clearance of MDA and 4-HNE, the substrates of ALDH2 [61, 69, 73]. Alda-1 is protective in several in vitro and in vivo models of I/R injury and radiation dermatitis involving oxidative stress [65-67, 84-88]. In liver, Alda-1 is protective against I/R injury and alcoholic liver disease in animal models [86, 87]. Here, I show benefits of Alda-1 administration against APAP hepatotoxicity, a model of acute liver injury, and cholestatic liver fibrosis, which causes chronic liver failure.

ACETAMINOPHEN HEPATOTOXICITY

Significance of my study

APAP intoxication is a leading cause of DILI and ALF in US and worldwide [181, 296]. The only clinically proven antidote for APAP intoxication is NAC, which is most effective if administered with 8 h of intoxication. Therefore, additional therapeutics are much needed. Previous studies show that APAP overdose increases the proportion of APAP metabolized by the P450 system, especially CYP2E1 [159, 179, 183]. NAPQI, the

metabolite of cytochrome P450, is detoxified by GSH conjugation. When the GSH pool is depleted, NAPQI forms adducts with mitochondrial proteins [156, 191]. These adducts cause increased production of ROS in the mitochondria. Oxidative stress, JNK activation, and mitochondrial dysfunction all contribute to cell death caused by APAP [159, 179, 183-185].

While the pathogenesis of APAP hepatotoxicity has been described in detail, the role of aldehydes generated by lipid peroxidation has not been previously explored. My goal in this study was to determine the role of aldehydes in APAP hepatotoxicity to identify aldehydes as a possible new therapeutic target and to evaluate aldehyde detoxification as a new method to prevent/treat APAP hepatotoxicity. Alda-1 provides a useful tool as a pharmacological activator of ALDH2 that is less expensive and more easily to be used than ALDH2 genetic knock-in or viral upregulation in experiments. More importantly, my data demonstrate that Alda-1 is a promising drug candidate that has the potential to be translated to clinical use.

My Findings and Contributions

4-HNE is one of the major products of lipid peroxidation that readily forms adducts with proteins [44, 53, 58, 59]. Therefore, 4-HNE protein adducts are used widely as a surrogate for reactive aldehyde production. 4-HNE is degraded by ALDH2 [61]. In my experiments, 4-HNE protein adducts markedly increased after APAP treatment (**Figure 2-5)**, demonstrating reactive aldehydes are indeed formed after APAP exposure, consistent with my central hypothesis. Alda-1 decreased these adducts by almost 90% after APAP administration, indicating ALDH2 activation is a highly effective way to decrease reactive aldehydes after APAP intoxication.

I further demonstrated that Alda-1 treatment decreased ALT release. ALT is released into blood when the plasma membrane permeability barrier fails due to hepatic injury and is well correlated with the extent of necrosis. Currently, ALT is the most widely accepted clinical marker of liver injury, although some biological changes (e.g., mitochondrial dysfunction) may occur before ALT increases and necrosis develops. However, ALT does not reflect the extent of apoptosis. After APAP, ALT was decreased by two-thirds by Alda-1 treatment compared to APAP with vehicle only, indicating hepatoprotection using a clinically relevant marker of liver damage. This result was further confirmed by histopathology, which showed a decrease in liver necrosis of 56% with Alda-1 treatment vs. APAP with vehicle only. Decreased ALT and improved histology by Alda-1 treatment indicated that the development of APAP hepatotoxicity, at least in part, is due to production of reactive aldehydes.

Once protection was established, I focused my experiments on mechanisms of APAP hepatotoxicity to determine at what point aldehydes act. Previous studies show that APAP hepatotoxicity is directly due to the formation of NAPQI adducts [159, 183, 185]. I demonstrated that Alda-1 did not change NAPQI adduct formation. Therefore, Alda-1 did not protect against APAP hepatotoxicity through an alteration of in the formation of the toxic APAP metabolite. JNK activation is also implicated in APAP hepatotoxicity, and previous studies show that JNK activation is in response to ROS formation mediated through ROS-sensitive ASK1 and MLK3 protein kinase activation [159, 185, 196-199, 246]. We demonstrated that JNK activation was unchanged by Alda-1 treatment. This finding suggests that Alda-1 possibly did not change ROS production. Rather, Alda-1 enhances detoxification of aldehydes downstream of oxidative stress and lipid

peroxidation. JNK is important for both the extrinsic and intrinsic pathways of apoptosis and for TNFα-stimulated necrosis as a central control protein in cell death [297, 298]. My results demonstrate that JNK activation is not the only mechanism of cell death in APAP toxicity.

Knowing that Alda-1 did not affect formation of NAPQI-protein adducts or JNK activation after APAP treatment, I explored the effects of Alda-1 on mitochondrial function after APAP. Using Rh123 fluorescence, I evaluated mitochondrial polarization status by intravital multiphoton microscopy. Mitochondrial depolarization decreased by ~50% after APAP, which was consistent with its protection against ALT release and necrosis detected by histology. These findings indicated that Alda-1 decreased APAP hepatotoxicity by prevention of mitochondrial dysfunction. This was especially significant because ROS, JNK activation, and aldehydes are implicated in causing the MPT [144, 257]. My result is consistent with the conclusion that aldehydes directly trigger mitochondrial depolarization in APAP intoxication and underlie, at least in part, the induction of the MPT by ROS. My results also indicated that acceleration of aldehyde degradation by ALDH2 activation can effectively protect mitochondria. Together, the results of my study not only identified a new therapeutic target and potential new treatment for APAP intoxication but also elucidated the mechanism of protection.

Limitations and Future Directions

While promising, the proposed mechanism must be confirmed. The MPT is a common mechanism for necrosis, apoptosis, and perhaps necroptosis. Previous studies show that apoptosis is limited in APAP hepatotoxicity [299, 300]. However, necrosis and necroptosis are histologically similar. It is unknown whether aldehydes also affect

necroptotic signaling. Necroptosis occurs through RIPK1, RIPK3, and mixed lineage kinase domain-like protein (MLKL) signaling. Future experiments should be performed to explore if these signaling molecules are activated by APAP and whether Alda-1 decreases their activation. These experiments will determine if aldehydes also alter necroptosis signaling. Further, the effects of aldehydes on other causes that can trigger the MPT onset should be explored, e.g., alterations in calcium and iron homeostasis.

Another limitation of this study is that mice were only treated with Alda-1 once before APAP, which showed that Alda-1 was effective in prevention of APAP hepatotoxicity. However, in humans, treatment for APAP hepatotoxicity typically starts after APAP overdose and often after symptoms of APAP hepatotoxicity have already developed. Accordingly, future studies are needed to determine whether Alda-1 treatment given some time after an APAP overdose is protective against hepatic injury. Also, Alda-1 may have off-target effects other than ALDH2 activation. Future studies with administration of Alda-1 in ALDH2-deficeint mice would clarify this. Since my experiments were done only in mice, caution should be exercised in extrapolating our conclusions from mice to human. *In vitro* studies comparing the effects of Alda-1 in mouse and human cells may provide some useful information in this aspect. Translational research and finally clinical trials should begin after Alda-1 is proven safe in toxicological studies. Aldea pharmaceuticals was founded in 2014 by the team that discovered Alda-1 with the goal of developing Alda-1 for clinical use, though no results have yet been reported.

FIBROSIS

Significance of my study

Liver fibrosis causes loss of parenchyma, distortion of liver morphology and loss of function as it progresses to cirrhosis, which leads to chronic liver failure end-stage liver disease, and death [214-217]. Chronic liver disease and cirrhosis are the 12th leading cause of death in the United States and worldwide [221].

Although recent studies have demonstrated the reversibility of fibrosis/cirrhosis in instances in which the initial insult (e.g., hepatitis C viral infection) has been eliminated, treatments for many causes of hepatic fibrosis are not available [233, 234]. Moreover, the onset of fibrosis is often insidious, and many patients are unaware that they have advanced liver fibrosis until it has reached advanced stages [214]. The only treatment for advanced cirrhosis is transplantation [214, 215]. Therefore, mechanism-based antifibrotic drugs are urgently needed. Unfortunately, the majority of antifibrotic drugs studied have been ineffective in clinical trials [215]. Therefore, identification of new therapeutic targets is essential.

Previous studies show that oxidative stress, particularly mitochondrial ROS, plays essential role in fibrosis, as reviewed in Chapter 1 [25-28, 226-229, 231]. Mitochondrial stress/dysfunction is also known to cause cell death and inflammation [29, 127, 131, 295]. However, the role of oxidative stress-induced aldehyde production in fibrosis remains unclear. My experiments were directed at determining if aldehydes played a causative role in liver injury and fibrosis caused by cholestasis after BDL, and whether aldehyde detoxification with Alda-1 was protective and anti-fibrotic in this injury.

My Findings and Contributions

Many models may cause hepatic fibrosis. I decided to use the model of experimental cholestasis in mice because it is clinically relevant and produces fibrosis

quickly. After BDL, 4-HNE protein adducts markedly increased (**Figure 3-9**), demonstrating increased production of reactive aldehydes. Moreover, ALT and biliary infarcts increased markedly after BDL, indicating liver injury caused by cholestasis (**Figure 3-1, Figure 3-2**). Alda-1 decreased 4-HNE adducts by 84%, ALT release by ~50% and biliary infarcts by ~75% after BDL, indicating that Alda-1 both decreased reactive aldehyde formation after BDL and decreased liver injury. These results strongly implied that aldehydes played a causative role in cholestatic liver injury after BDL.

I also measured fibrosis by picrosirius red staining, second-harmonic generation microscopy and COL-I mRNA expression after BDL. All these fibrotic endpoints were markedly increased 2 weeks after BDL, indicating development of liver fibrosis. Importantly, Alda-1 decreased fibrosis by about half. These data clearly demonstrated that aldehydes also play an important role in fibrosis and therefore are a potential therapeutic target. A previous study also revealed that Alda-1 decreases some molecular markers of fibrosis after chronic ethanol treatment, which is most likely due to decreasing acetaldehyde [132]. My new findings demonstrated that accelerating degradation of ROS-generated reactive aldehydes decreases fibrogenesis after cholestasis, and therefore could be a new therapeutic strategy.

I then explored the effect of aldehyde detoxification on several molecular/cellular events that can lead to or promote fibrosis. OPN is a protein that is proinflammatory and can stimulate HSC activation [287, 288, 301]. Inflammation is also known to promote fibrosis process. Myofibroblast activation leads to production of ECM and fibrosis. I observed that OPN expression in cholangiocytes and hepatocytes increased after BDL (**Figure 3-8**), which was associated with infiltration of macrophages as detected by CD-

68 immunohistochemistry (**Figure 3-7**) and myofibroblast activation as detected by increased α-SMA expression (**Figure 3-6**). All these changes were blunted by enhanced aldehyde degradation with Alda-1. These data suggested that aldehydes increased pro-inflammatory and pro-fibrotic signaling thus leading to myofibroblast activation of the fibrotic effector cells thus causing fibrosis.

Limitations/Future Directions

Although I have demonstrated that aldehydes play an important role in cholestatic liver injury and liver fibrosis, the exact molecular mechanisms that bridge increased reactive aldehydes to liver fibrosis need to be more fully explored. An interesting finding in my study suggests that cholestasis increases expression of the proinflammatory and profibrotic protein, OPN, in cholangiocytes and to a less extent in hepatocytes. Further, OPN appears to stimulate inflammation and HSC activation. Increased aldehyde degradation by Alda-1 decreased OPN expression, inflammation and myofibroblast activation **Figure 3-8, Figure 3-7, Figure 3-6**. Therefore, it is possible that OPN is an important link between aldehydes and fibrosis. The critical role of OPN can be determined by examining whether OPN deficiency decreases fibrosis after BDL and whether aldehyde (e.g. acrolein) treatment causes fibrosis in OPN knockout mice. Whether Alda-1 decreases aldehyde formation and OPN expression in different cell types (hepatocytes, cholangiocytes, and HSC) after bile acid or oxidant stimulation should also be explored in cell culture.

Hepatocytes have abundant mitochondria and are likely the source of most aldehydes. Aldehydes released by hepatocytes may then stimulate Kupffer cells and activate HSC, leading to proinflammatory and profibrogenic effects. Future studies can

test this hypothesis by 1) examining aldehydes in the conditioned media from hepatocyte cultured with bile acids or oxidants with and without Alda-1, and 2) examining if Kupffer cells and HSC activate and produce proinflammatory or profibrotic cytokines after co-culture with hepatocytes (or conditioned medium) that were stimulated with bile acids or oxidants in the presence or absence of Alda-1.

Conclusion

To my knowledge, these are the first studies to show that enhanced aldehyde detoxification by ALDH2 activation with Alda-1 decreases APAP hepatotoxicity and experimental fibrosis. My experiments suggest that increased aldehyde production is likely to be a key player in the pathogenesis of liver injury and/or fibrosis. Therefore, we conclude that aldehydes are an important therapeutic target in oxidative stress-related acute and chronic liver diseases. Moreover, these studies also demonstrated that activation of ALDH2 to enhance aldehyde degradation is a promising strategy that could be used in the clinical setting of liver injury and cirrhosis.

REFERENCES

[1] E. Birben, U.M. Sahiner, C. Sackesen, S. Erzurum, O. Kalayci, Oxidative stress and antioxidant defense, World Allergy Organ J 5(1) (2012) 9-19.

[2] S. Di Meo, T.T. Reed, P. Venditti, V.M. Victor, Role of ROS and RNS Sources in Physiological and Pathological Conditions, Oxid Med Cell Longev 2016 (2016) 1245049.

[3] E. Novo, M. Parola, Redox mechanisms in hepatic chronic wound healing and fibrogenesis, Fibrogenesis Tissue Repair 1(1) (2008) 5.

[4] J. Zhang, X. Wang, V. Vikash, Q. Ye, D. Wu, Y. Liu, W. Dong, ROS and ROS-Mediated Cellular Signaling, Oxid Med Cell Longev 2016 (2016) 4350965.

[5] C.L. Bigarella, R. Liang, S. Ghaffari, Stem cells and the impact of ROS signaling, Development 141(22) (2014) 4206-18.

[6] L.O. Klotz, H. Steinbrenner, Cellular adaptation to xenobiotics: Interplay between xenosensors, reactive oxygen species and FOXO transcription factors, Redox Biol 13 (2017) 646-654.

[7] W. Ahmad, B. Ijaz, K. Shabbiri, F. Ahmed, S. Rehman, Oxidative toxicity in diabetes and Alzheimer's disease: mechanisms behind ROS/ RNS generation, J Biomed Sci 24(1) (2017) 76.

[8] P. Davalli, T. Mitic, A. Caporali, A. Lauriola, D. D'Arca, ROS, Cell Senescence, and Novel Molecular Mechanisms in Aging and Age-Related Diseases, Oxid Med Cell Longev 2016 (2016) 3565127.

[9] J.N. Moloney, T.G. Cotter, ROS signalling in the biology of cancer, Semin Cell Dev Biol 80 (2018) 50-64.

[10] A.J. Kattoor, N.V.K. Pothineni, D. Palagiri, J.L. Mehta, Oxidative Stress in Atherosclerosis, Curr Atheroscler Rep 19(11) (2017) 42.

[11] A. Agita, M.T. Alsagaff, Inflammation, Immunity, and Hypertension, Acta Med Indones 49(2) (2017) 158-165.

[12] G. Aviello, U.G. Knaus, ROS in gastrointestinal inflammation: Rescue Or Sabotage?, Br J Pharmacol 174(12) (2017) 1704-1718.

[13] H. Blaser, C. Dostert, T.W. Mak, D. Brenner, TNF and ROS Crosstalk in Inflammation, Trends Cell Biol 26(4) (2016) 249-261.

[14] E.T. Chouchani, V.R. Pell, A.M. James, L.M. Work, K. Saeb-Parsy, C. Frezza, T. Krieg, M.P. Murphy, A Unifying Mechanism for Mitochondrial Superoxide Production during Ischemia-Reperfusion Injury, Cell Metab 23(2) (2016) 254-63.

[15] G. Katwal, D. Baral, X. Fan, H. Weiyang, X. Zhang, L. Ling, Y. Xiong, Q. Ye, Y. Wang, SIRT3 a Major Player in Attenuation of Hepatic Ischemia-Reperfusion Injury by Reducing ROS via Its Downstream Mediators: SOD2, CYP-D, and HIF-1alpha, Oxid Med Cell Longev 2018 (2018) 2976957.

[16] X. Xu, L. Zhang, X. Ye, Q. Hao, T. Zhang, G. Cui, M. Yu, Nrf2/ARE pathway inhibits ROS-induced NLRP3 inflammasome activation in BV2 cells after cerebral ischemia reperfusion, Inflamm Res 67(1) (2018) 57-65.

[17] T. Zhou, E.R. Prather, D.E. Garrison, L. Zuo, Interplay between ROS and Antioxidants during Ischemia-Reperfusion Injuries in Cardiac and Skeletal Muscle, Int J Mol Sci 19(2) (2018).

[18] M.L. Bajt, Y.S. Ho, S.L. Vonderfecht, H. Jaeschke, Reactive oxygen as modulator of TNF and fas receptor-mediated apoptosis in vivo: studies with glutathione peroxidase-deficient mice, Antioxid Redox Signal 4(5) (2002) 733-40.

[19] K. Du, A. Ramachandran, H. Jaeschke, Oxidative stress during acetaminophen hepatotoxicity: Sources, pathophysiological role and therapeutic potential, Redox Biol 10 (2016) 148-156.

[20] K. Du, C.D. Williams, M.R. McGill, Y. Xie, A. Farhood, M. Vinken, H. Jaeschke, The gap junction inhibitor 2-aminoethoxy-diphenyl-borate protects against acetaminophen hepatotoxicity by inhibiting cytochrome P450 enzymes and c-jun N-terminal kinase activation, Toxicol Appl Pharmacol 273(3) (2013) 484-91.

[21] H. Jaeschke, Reactive oxygen and mechanisms of inflammatory liver injury, J Gastroenterol Hepatol 15(7) (2000) 718-24.

[22] H. Jaeschke, G.J. Gores, A.I. Cederbaum, J.A. Hinson, D. Pessayre, J.J. Lemasters, Mechanisms of hepatotoxicity, Toxicol Sci 65(2) (2002) 166-76.

[23] J.J. Lemasters, T.P. Theruvath, Z. Zhong, A.L. Nieminen, Mitochondrial calcium and the permeability transition in cell death, Biochim Biophys Acta 1787(11) (2009) 1395-401.

[24] C.D. Williams, M.R. McGill, A. Farhood, H. Jaeschke, Fas receptor-deficient lpr mice are protected against acetaminophen hepatotoxicity due to higher glutathione synthesis and enhanced detoxification of oxidant stress, Food Chem Toxicol 58 (2013) 228-35.

[25] M. Parola, G. Robino, Oxidative stress-related molecules and liver fibrosis, J Hepatol 35(2) (2001) 297-306.

[26] V. Sanchez-Valle, N.C. Chavez-Tapia, M. Uribe, N. Mendez-Sanchez, Role of oxidative stress and molecular changes in liver fibrosis: a review, Curr Med Chem 19(28) (2012) 4850-60.

[27] Z. Zhong, M. Froh, M. Lehnert, R. Schoonhoven, L. Yang, H. Lind, J.J. Lemasters, R.G. Thurman, Polyphenols from Camellia sinenesis attenuate experimental cholestasis-induced liver fibrosis in rats, Am J Physiol Gastrointest Liver Physiol 285(5) (2003) G1004-13.

[28] Z. Zhong, M. Froh, M.D. Wheeler, O. Smutney, T.G. Lehmann, R.G. Thurman, Viral gene delivery of superoxide dismutase attenuates experimental cholestasis-induced liver fibrosis in the rat, Gene Ther 9(3) (2002) 183-91.

[29] E.J. Anderson, L.A. Katunga, M.S. Willis, Mitochondria as a source and target of lipid peroxidation products in healthy and diseased heart, Clin Exp Pharmacol Physiol 39(2) (2012) 179-93.

[30] R. Kumar, G. Joshi, H. Kler, S. Kalra, M. Kaur, R. Arya, Toward an Understanding of Structural Insights of Xanthine and Aldehyde Oxidases: An Overview of their Inhibitors and Role in Various Diseases, Med Res Rev 38(4) (2018) 1073-1125.

[31] J. Hu, A. Kholmukhamedov, C.C. Lindsey, C.C. Beeson, H. Jaeschke, J.J. Lemasters, Translocation of iron from lysosomes to mitochondria during acetaminophen-induced hepatocellular injury: Protection by starch-desferal and minocycline, Free Radic Biol Med 97 (2016) 418-426.

[32] G. Calabrese, B. Morgan, J. Riemer, Mitochondrial Glutathione: Regulation and Functions, Antioxid Redox Signal 27(15) (2017) 1162-1177.

[33] A.O. Oyewole, M.A. Birch-Machin, Mitochondria-targeted antioxidants, FASEB J 29(12) (2015) 4766-71.

[34] H. Vakifahmetoglu-Norberg, A.T. Ouchida, E. Norberg, The role of mitochondria in metabolism and cell death, Biochem Biophys Res Commun 482(3) (2017) 426-431.

[35] M.D. Brand, The sites and topology of mitochondrial superoxide production, Exp Gerontol 45(7-8) (2010) 466-72.

[36] M. Jastroch, A.S. Divakaruni, S. Mookerjee, J.R. Treberg, M.D. Brand, Mitochondrial proton and electron leaks, Essays Biochem 47 (2010) 53-67.

[37] C. Brenner, L. Galluzzi, O. Kepp, G. Kroemer, Decoding cell death signals in liver inflammation, J Hepatol 59(3) (2013) 583-94.

[38] B. Chakravarti, D.N. Chakravarti, Protein Tyrosine Nitration: Role in Aging, Curr Aging Sci 10(4) (2017) 246-262.

[39] M. Galicia-Moreno, G. Gutierrez-Reyes, The role of oxidative stress in the development of alcoholic liver disease, Rev Gastroenterol Mex 79(2) (2014) 135-44.

[40] N. He, J.J. Jia, J.H. Li, Y.F. Zhou, B.Y. Lin, Y.F. Peng, J.J. Chen, T.C. Chen, R.L. Tong, L. Jiang, H.Y. Xie, L. Zhou, S.S. Zheng, Remote ischemic perconditioning prevents liver transplantation-induced ischemia/reperfusion injury in rats: Role of ROS/RNS and eNOS, World J Gastroenterol 23(5) (2017) 830-841.

[41] S. Joshi-Barve, I. Kirpich, M.C. Cave, L.S. Marsano, C.J. McClain, Alcoholic, Nonalcoholic, and Toxicant-Associated Steatohepatitis: Mechanistic Similarities and Differences, Cell Mol Gastroenterol Hepatol 1(4) (2015) 356-367.

[42] S.K. Kim, H. Takeda, A. Takai, T. Matsumoto, N. Kakiuchi, A. Yokoyama, K. Yoshida, T. Kaido, S. Uemoto, S. Minamiguchi, H. Haga, Y. Shiraishi, S. Miyano, H. Seno, S.

Ogawa, H. Marusawa, Comprehensive analysis of genetic aberrations linked to tumorigenesis in regenerative nodules of liver cirrhosis, J Gastroenterol 54(7) (2019) 628-640.

[43] N. Zheng, L. Liu, W.W. Liu, F. Li, T. Hayashi, S.I. Tashiro, S. Onodera, T. Ikejima, Crosstalk of ROS/RNS and autophagy in silibinin-induced apoptosis of MCF-7 human breast cancer cells in vitro, Acta Pharmacol Sin 38(2) (2017) 277-289.

[44] S. Pizzimenti, E. Ciamporcero, M. Daga, P. Pettazzoni, A. Arcaro, G. Cetrangolo, R. Minelli, C. Dianzani, A. Lepore, F. Gentile, G. Barrera, Interaction of aldehydes derived from lipid peroxidation and membrane proteins, Front Physiol 4 (2013) 242.

[45] J.P. Castro, T. Jung, T. Grune, W. Siems, 4-Hydroxynonenal (HNE) modified proteins in metabolic diseases, Free Radic Biol Med 111 (2017) 309-315.

[46] J. Chen, G.I. Henderson, G.L. Freeman, Role of 4-hydroxynonenal in modification of cytochrome c oxidase in ischemia/reperfused rat heart, J Mol Cell Cardiol 33(11) (2001) 1919-27.

[47] J. Chen, N.C. Robinson, S. Schenker, T.A. Frosto, G.I. Henderson, Formation of 4-hydroxynonenal adducts with cytochrome c oxidase in rats following short-term ethanol intake, Hepatology 29(6) (1999) 1792-8.

[48] B.G. Hill, B.P. Dranka, L. Zou, J.C. Chatham, V.M. Darley-Usmar, Importance of the bioenergetic reserve capacity in response to cardiomyocyte stress induced by 4-hydroxynonenal, Biochem J 424(1) (2009) 99-107.

[49] B.S. Kristal, B.K. Park, B.P. Yu, 4-Hydroxyhexenal is a potent inducer of the mitochondrial permeability transition, J Biol Chem 271(11) (1996) 6033-8.

[50] V.R. Mali, S.S. Palaniyandi, Regulation and therapeutic strategies of 4-hydroxy-2-nonenal metabolism in heart disease, Free Radic Res 48(3) (2014) 251-63.

[51] G. Robino, E. Zamara, E. Novo, M.U. Dianzani, M. Parola, 4-Hydroxy-2,3-alkenals as signal molecules modulating proliferative and adaptative cell responses, Biofactors 15(2-4) (2001) 103-6.

[52] Y. Wang, W. Wang, H. Yang, D. Shao, X. Zhao, G. Zhang, Intraperitoneal injection of 4-hydroxynonenal (4-HNE), a lipid peroxidation product, exacerbates colonic inflammation through activation of Toll-like receptor 4 signaling, Free Radic Biol Med 131 (2018) 237-242.

[53] Y. Yang, R. Sharma, A. Sharma, S. Awasthi, Y.C. Awasthi, Lipid peroxidation and cell cycle signaling: 4-hydroxynonenal, a key molecule in stress mediated signaling, Acta Biochim Pol 50(2) (2003) 319-36.

[54] N. Moretto, G. Volpi, F. Pastore, F. Facchinetti, Acrolein effects in pulmonary cells: relevance to chronic obstructive pulmonary disease, Ann N Y Acad Sci 1259 (2012) 39-46.

[55] M. Shamoto-Nagai, W. Maruyama, Y. Hashizume, M. Yoshida, T. Osawa, P. Riederer, M. Naoi, In parkinsonian substantia nigra, alpha-synuclein is modified by acrolein, a lipid-peroxidation product, and accumulates in the dopamine neurons with inhibition of proteasome activity, J Neural Transm (Vienna) 114(12) (2007) 1559-67.

[56] J.F. Stevens, C.S. Maier, Acrolein: sources, metabolism, and biomolecular interactions relevant to human health and disease, Mol Nutr Food Res 52(1) (2008) 7-25.

[57] K. Uchida, M. Kanematsu, Y. Morimitsu, T. Osawa, N. Noguchi, E. Niki, Acrolein is a product of lipid peroxidation reaction. Formation of free acrolein and its conjugate with

lysine residues in oxidized low density lipoproteins, J Biol Chem 273(26) (1998) 16058-66.

[58] J.E. Cebak, I.N. Singh, R.L. Hill, J.A. Wang, E.D. Hall, Phenelzine Protects Brain Mitochondrial Function In Vitro and In Vivo following Traumatic Brain Injury by Scavenging the Reactive Carbonyls 4-Hydroxynonenal and Acrolein Leading to Cortical Histological Neuroprotection, J Neurotrauma 34(7) (2017) 1302-1317.

[59] M. Dodson, W.Y. Wani, M. Redmann, G.A. Benavides, M.S. Johnson, X. Ouyang, S.S. Cofield, K. Mitra, V. Darley-Usmar, J. Zhang, Regulation of autophagy, mitochondrial dynamics, and cellular bioenergetics by 4-hydroxynonenal in primary neurons, Autophagy 13(11) (2017) 1828-1840.

[60] L. Galam, A. Failla, R. Soundararajan, R.F. Lockey, N. Kolliputi, 4-hydroxynonenal regulates mitochondrial function in human small airway epithelial cells, Oncotarget 6(39) (2015) 41508-21.

[61] C.H. Chen, G.R. Budas, E.N. Churchill, M.H. Disatnik, T.D. Hurley, D. Mochly-Rosen, Activation of aldehyde dehydrogenase-2 reduces ischemic damage to the heart, Science 321(5895) (2008) 1493-5.

[62] B. Jackson, C. Brocker, D.C. Thompson, W. Black, K. Vasiliou, D.W. Nebert, V. Vasiliou, Update on the aldehyde dehydrogenase gene (ALDH) superfamily, Hum Genomics 5(4) (2011) 283-303.

[63] V. Koppaka, D.C. Thompson, Y. Chen, M. Ellermann, K.C. Nicolaou, R.O. Juvonen, D. Petersen, R.A. Deitrich, T.D. Hurley, V. Vasiliou, Aldehyde dehydrogenase inhibitors: a comprehensive review of the pharmacology, mechanism of action, substrate specificity, and clinical application, Pharmacol Rev 64(3) (2012) 520-39.

[64] C.H. Chen, J.C. Ferreira, E.R. Gross, D. Mochly-Rosen, Targeting aldehyde dehydrogenase 2: new therapeutic opportunities, Physiol Rev 94(1) (2014) 1-34.

[65] J. Ding, Q. Zhang, Q. Luo, Y. Ying, Y. Liu, Y. Li, W. Wei, F. Yan, H. Zhang, Alda-1 attenuates lung ischemia-reperfusion injury by reducing 4-hydroxy-2-nonenal in alveolar epithelial cells, Crit Care Med 44(7) (2016) e544-52.

[66] S.H. Fu, H.F. Zhang, Z.B. Yang, T.B. Li, B. Liu, Z. Lou, Q.L. Ma, X.J. Luo, J. Peng, Alda-1 reduces cerebral ischemia/reperfusion injury in rat through clearance of reactive aldehydes, Naunyn Schmiedebergs Arch Pharmacol 387(1) (2014) 87-94.

[67] S. Ning, G.R. Budas, E.N. Churchill, C.H. Chen, S.J. Knox, D. Mochly-Rosen, Mitigation of radiation-induced dermatitis by activation of aldehyde dehydrogenase 2 using topical alda-1 in mice, Radiat Res 178(1) (2012) 69-74.

[68] A. Panisello-Rosello, A. Lopez, E. Folch-Puy, T. Carbonell, A. Rolo, C. Palmeira, R. Adam, M. Net, J. Rosello-Catafau, Role of aldehyde dehydrogenase 2 in ischemia reperfusion injury: An update, World J Gastroenterol 24(27) (2018) 2984-2994.

[69] A.A. Klyosov, Kinetics and specificity of human liver aldehyde dehydrogenases toward aliphatic, aromatic, and fused polycyclic aldehydes, Biochemistry 35(14) (1996) 4457-67.

[70] R. Cui, Y. Kamatani, A. Takahashi, M. Usami, N. Hosono, T. Kawaguchi, T. Tsunoda, N. Kamatani, M. Kubo, Y. Nakamura, K. Matsuda, Functional variants in ADH1B and ALDH2 coupled with alcohol and smoking synergistically enhance esophageal cancer risk, Gastroenterology 137(5) (2009) 1768-75.

[71] H. Hoshi, W. Hao, Y. Fujita, A. Funayama, Y. Miyauchi, K. Hashimoto, K. Miyamoto, R. Iwasaki, Y. Sato, T. Kobayashi, H. Miyamoto, S. Yoshida, T. Mori, H. Kanagawa, E.

Katsuyama, A. Fujie, K. Kitagawa, K.I. Nakayama, T. Kawamoto, M. Sano, K. Fukuda, I. Ohsawa, S. Ohta, H. Morioka, M. Matsumoto, K. Chiba, Y. Toyama, T. Miyamoto, Aldehyde-stress resulting from Aldh2 mutation promotes osteoporosis due to impaired osteoblastogenesis, J Bone Miner Res 27(9) (2012) 2015-23.

[72] J.Y. Park, K. Matsuo, T. Suzuki, H. Ito, S. Hosono, T. Kawase, M. Watanabe, I. Oze, T. Hida, Y. Yatabe, T. Mitsudomi, T. Takezaki, K. Tajima, H. Tanaka, Impact of smoking on lung cancer risk is stronger in those with the homozygous aldehyde dehydrogenase 2 null allele in a Japanese population, Carcinogenesis 31(4) (2010) 660-5.

[73] S. Perez-Miller, H. Younus, R. Vanam, C.H. Chen, D. Mochly-Rosen, T.D. Hurley, Alda-1 is an agonist and chemical chaperone for the common human aldehyde dehydrogenase 2 variant, Nature structural & molecular biology 17(2) (2010) 159-64.

[74] J.S. Chang, J.R. Hsiao, C.H. Chen, ALDH2 polymorphism and alcohol-related cancers in Asians: a public health perspective, J Biomed Sci 24(1) (2017) 19.

[75] A. Matsumoto, D.C. Thompson, Y. Chen, K. Kitagawa, V. Vasiliou, Roles of defective ALDH2 polymorphism on liver protection and cancer development, Environ Health Prev Med 21(6) (2016) 395-402.

[76] A. Takada, M. Tsutsumi, Y. Kobayashi, Genotypes of ALDH2 related to liver and pulmonary diseases and other genetic factors related to alcoholic liver disease, Alcohol Alcohol 29(6) (1994) 719-27.

[77] H. Yang, Z. Song, G.P. Yang, B.K. Zhang, M. Chen, T. Wu, R. Guo, The ALDH2 rs671 polymorphism affects post-stroke epilepsy susceptibility and plasma 4-HNE levels, PLoS One 9(10) (2014) e109634.

[78] Q.Y. Li, N.M. Zhao, J.J. Ma, H.F. Duan, Y.C. Ma, W. Zhang, H.W. Zhao, Y.H. Qin, ALDH2*2 Allele is a Negative Risk Factor for Cerebral Infarction in Chinese Women, Biochem Genet 53(9-10) (2015) 260-7.

[79] Y. Mizuno, S. Hokimoto, E. Harada, K. Kinoshita, K. Nakagawa, M. Yoshimura, H. Ogawa, H. Yasue, Variant Aldehyde Dehydrogenase 2 (ALDH2*2) Is a Risk Factor for Coronary Spasm and ST-Segment Elevation Myocardial Infarction, J Am Heart Assoc 5(5) (2016).

[80] Y.F. Sung, C.C. Lu, J.T. Lee, Y.J. Hung, C.J. Hu, J.S. Jeng, H.Y. Chiou, G.S. Peng, Homozygous ALDH2*2 Is an Independent Risk Factor for Ischemic Stroke in Taiwanese Men, Stroke 47(9) (2016) 2174-9.

[81] K.K. Chaudhry, G. Samak, P.K. Shukla, H. Mir, R. Gangwar, B. Manda, T. Isse, T. Kawamoto, M. Salaspuro, P. Kaihovaara, P. Dietrich, I. Dragatsis, L.E. Nagy, R.K. Rao, ALDH2 Deficiency Promotes Ethanol-Induced Gut Barrier Dysfunction and Fatty Liver in Mice, Alcohol Clin Exp Res 39(8) (2015) 1465-75.

[82] Y.D. Kim, S.Y. Eom, M. Ogawa, T. Oyama, T. Isse, J.W. Kang, Y.W. Zhang, T. Kawamoto, H. Kim, Ethanol-induced oxidative DNA damage and CYP2E1 expression in liver tissue of Aldh2 knockout mice, J Occup Health 49(5) (2007) 363-9.

[83] H.J. Kwon, Y.S. Won, O. Park, B. Chang, M.J. Duryee, G.E. Thiele, A. Matsumoto, S. Singh, M.A. Abdelmegeed, B.J. Song, T. Kawamoto, V. Vasiliou, G.M. Thiele, B. Gao, Aldehyde dehydrogenase 2 deficiency ameliorates alcoholic fatty liver but worsens liver inflammation and fibrosis in mice, Hepatology 60(1) (2014) 146-57.

[84] X. Liu, G. Jin, B. Fan, Y. Xing, L. Wang, M. Wang, Y. Yuan, Q. Zhu, The impact of ALDH2 activation by Alda-1 on the expression of VEGF in the hippocampus of a rat model of post-MI depression, Neurosci Lett 674 (2018) 156-161.

[85] A. Stachowicz, K. Glombik, R. Olszanecki, A. Basta-Kaim, M. Suski, W. Lason, R. Korbut, The impact of mitochondrial aldehyde dehydrogenase (ALDH2) activation by Alda-1 on the behavioral and biochemical disturbances in animal model of depression, Brain Behav Immun 51 (2016) 144-53.

[86] T. Zhang, Q. Zhao, F. Ye, C.Y. Huang, W.M. Chen, W.Q. Huang, Alda-1, an ALDH2 activator, protects against hepatic ischemia/reperfusion injury in rats via inhibition of oxidative stress, Free Radic Res 52(6) (2018) 629-638.

[87] W. Zhong, W. Zhang, Q. Li, G. Xie, Q. Sun, X. Sun, X. Tan, X. Sun, W. Jia, Z. Zhou, Pharmacological activation of aldehyde dehydrogenase 2 by Alda-1 reverses alcohol-induced hepatic steatosis and cell death in mice, J Hepatol (2014).

[88] Q. Zhu, G. He, J. Wang, Y. Wang, W. Chen, Pretreatment with the ALDH2 agonist Alda-1 reduces intestinal injury induced by ischaemia and reperfusion in mice, Clin Sci (Lond) 131(11) (2017) 1123-1136.

[89] H.M. McBride, M. Neuspiel, S. Wasiak, Mitochondria: more than just a powerhouse, Curr Biol 16(14) (2006) R551-60.

[90] J.E. Vance, MAM (mitochondria-associated membranes) in mammalian cells: lipids and beyond, Biochim Biophys Acta 1841(4) (2014) 595-609.

[91] N. Wiedemann, N. Pfanner, Mitochondrial Machineries for Protein Import and Assembly, Annu Rev Biochem 86 (2017) 685-714.

[92] J.J. Lemasters, Evolution of voltage-dependent anion channel function: from molecular sieve to governator to actuator of ferroptosis, Front Oncol 7 (2017) 303.

[93] V. Shoshan-Barmatz, Y. Krelin, A. Shteinfer-Kuzmine, T. Arif, Voltage-dependent anion channel 1 as an emerging drug target for novel anti-cancer therapeutics, Frontiers in Oncology 7(154) (2017).

[94] M. Colombini, VDAC structure, selectivity, and dynamics, Biochim Biophys Acta 1818(6) (2012) 1457-65.

[95] V. Shoshan-Barmatz, D. Gincel, The voltage-dependent anion channel: characterization, modulation, and role in mitochondrial function in cell life and death, Cell Biochem Biophys 39(3) (2003) 279-92.

[96] S. Das, R. Wong, N. Rajapakse, E. Murphy, C. Steenbergen, Glycogen synthase kinase 3 inhibition slows mitochondrial adenine nucleotide transport and regulates voltage-dependent anion channel phosphorylation, Circ Res 103(9) (2008) 983-91.

[97] E. Holmuhamedov, J.J. Lemasters, Ethanol exposure decreases mitochondrial outer membrane permeability in cultured rat hepatocytes, Arch Biochem Biophys 481(2) (2009) 226-33.

[98] J.J. Lemasters, E. Holmuhamedov, Voltage-dependent anion channel (VDAC) as mitochondrial governator--thinking outside the box, Biochim Biophys Acta 1762(2) (2006) 181-90.

[99] M.G. Vander Heiden, N.S. Chandel, X.X. Li, P.T. Schumacker, M. Colombini, C.B. Thompson, Outer mitochondrial membrane permeability can regulate coupled respiration and cell survival, Proc Natl Acad Sci U S A 97(9) (2000) 4666-71.

[100] E.N. Maldonado, J.J. Lemasters, Warburg revisited: regulation of mitochondrial metabolism by voltage-dependent anion channels in cancer cells, J Pharmacol Exp Ther 342(3) (2012) 637-41.

[101] V. Shoshan-Barmatz, H. Kmita, J.J. Lemasters, Editorial: uncovering the function of the mitochondrial protein VDAC in health and disease: from structure-function to novel therapeutic strategies, Front Oncol 7 (2017) 320.

[102] S. Naghdi, G. Hajnoczky, VDAC2-specific cellular functions and the underlying structure, Biochim Biophys Acta 1863(10) (2016) 2503-14.

[103] S. Reina, F. Guarino, A. Magri, V. De Pinto, VDAC3 as a potential marker of mitochondrial status is involved in cancer and pathology, Front Oncol 6 (2016) 264.

[104] M. Habich, S.L. Salscheider, J. Riemer, Cysteine residues in mitochondrial intermembrane space proteins: more than just import, Br J Pharmacol 176(4) (2019) 514-531.

[105] S. Anderson, A.T. Bankier, B.G. Barrell, M.H. de Bruijn, A.R. Coulson, J. Drouin, I.C. Eperon, D.P. Nierlich, B.A. Roe, F. Sanger, P.H. Schreier, A.J. Smith, R. Staden, I.G. Young, Sequence and organization of the human mitochondrial genome, Nature 290(5806) (1981) 457-65.

[106] I. Kim, S. Rodriguez-Enriquez, J.J. Lemasters, Selective degradation of mitochondria by mitophagy, Arch Biochem Biophys 462(2) (2007) 245-53.

[107] B.J. Greber, N. Ban, Structure and function of the mitochondrial ribosome, Annu Rev Biochem 85 (2016) 103-32.

[108] C. Artus, H. Boujrad, A. Bouharrour, M.N. Brunelle, S. Hoos, V.J. Yuste, P. Lenormand, J.C. Rousselle, A. Namane, P. England, H.K. Lorenzo, S.A. Susin, AIF

promotes chromatinolysis and caspase-independent programmed necrosis by interacting with histone H2AX, EMBO J 29(9) (2010) 1585-99.

[109] C.P. Baines, Role of the mitochondrion in programmed necrosis, Front Physiol 1 (2010) 156.

[110] R.W. Birkinshaw, P.E. Czabotar, The BCL-2 family of proteins and mitochondrial outer membrane permeabilisation, Semin Cell Dev Biol 72 (2017) 152-162.

[111] D.R. Green, J.C. Reed, Mitochondria and apoptosis, Science 281(5381) (1998) 1309-12.

[112] H. Kim, H.C. Tu, D. Ren, O. Takeuchi, J.R. Jeffers, G.P. Zambetti, J.J. Hsieh, E.H. Cheng, Stepwise activation of BAX and BAK by tBID, BIM, and PUMA initiates mitochondrial apoptosis, Mol Cell 36(3) (2009) 487-99.

[113] C.R. Hackenbrock, Chemical and physical fixation of isolated mitochondria in low-energy and high-energy states, Proc Natl Acad Sci U S A 61(2) (1968) 598-605.

[114] P. Neupane, S. Bhuju, N. Thapa, H.K. Bhattarai, ATP synthase: structure, function and inhibition, Biomol Concepts 10(1) (2019) 1-10.

[115] K.S. McCommis, B.N. Finck, Mitochondrial pyruvate transport: a historical perspective and future research directions, Biochem J 466(3) (2015) 443-54.

[116] L.R. Gray, S.C. Tompkins, E.B. Taylor, Regulation of pyruvate metabolism and human disease, Cell Mol Life Sci 71(14) (2014) 2577-604.

[117] S.M. Houten, R.J. Wanders, A general introduction to the biochemistry of mitochondrial fatty acid beta-oxidation, J Inherit Metab Dis 33(5) (2010) 469-77.

[118] H.M. van Rossum, B.U. Kozak, M.S. Niemeijer, J.C. Dykstra, M.A. Luttik, J.M. Daran, A.J. van Maris, J.T. Pronk, Requirements for Carnitine Shuttle-Mediated Translocation of Mitochondrial Acetyl Moieties to the Yeast Cytosol, MBio 7(3) (2016).

[119] K. Lee, J. Kerner, C.L. Hoppel, Mitochondrial carnitine palmitoyltransferase 1a (CPT1a) is part of an outer membrane fatty acid transfer complex, J Biol Chem 286(29) (2011) 25655-62.

[120] M. Saraste, Oxidative phosphorylation at the fin de siecle, Science 283(5407) (1999) 1488-93.

[121] G. Lenaz, R. Fato, M.L. Genova, C. Bergamini, C. Bianchi, A. Biondi, Mitochondrial Complex I: structural and functional aspects, Biochim Biophys Acta 1757(9-10) (2006) 1406-20.

[122] J. Nedergaard, D. Ricquier, L.P. Kozak, Uncoupling proteins: current status and therapeutic prospects, EMBO Rep 6(10) (2005) 917-21.

[123] R.J. Kessler, C.A. Tyson, D.E. Green, Mechanism of uncoupling in mitochondria: uncouplers as ionophores for cycling cations and protons, Proc Natl Acad Sci U S A 73(9) (1976) 3141-5.

[124] H.S. Wong, P.A. Dighe, V. Mezera, P.A. Monternier, M.D. Brand, Production of superoxide and hydrogen peroxide from specific mitochondrial sites under different bioenergetic conditions, J Biol Chem 292(41) (2017) 16804-16809.

[125] L. Zhang, A. Reyes, X. Wang, The Role of DNA Repair in Maintaining Mitochondrial DNA Stability, Adv Exp Med Biol 1038 (2017) 85-105.

[126] T. Ozawa, Mechanism of somatic mitochondrial DNA mutations associated with age and diseases, Biochim Biophys Acta 1271(1) (1995) 177-89.

[127] J.B. Hoek, A. Cahill, J.G. Pastorino, Alcohol and mitochondria: a dysfunctional relationship, Gastroenterology 122(7) (2002) 2049-63.

[128] K.G. Ishak, H.J. Zimmerman, M.B. Ray, Alcoholic liver disease: pathologic, pathogenetic and clinical aspects, Alcohol Clin Exp Res 15(1) (1991) 45-66.

[129] T. Matsuhashi, M. Karbowski, X. Liu, J. Usukura, M. Wozniak, T. Wakabayashi, Complete suppresion of ethanol-induced formation of megamitochondria by 4-hydroxy-2,2,6,6-tetramethyl-piperidine-1-oxyl (4-OH-TEMPO), Free Radic Biol Med 24(1) (1998) 139-47.

[130] B. Fromenty, S. Grimbert, A. Mansouri, M. Beaugrand, S. Erlinger, A. Rotig, D. Pessayre, Hepatic mitochondrial DNA deletion in alcoholics: association with microvesicular steatosis, Gastroenterology 108(1) (1995) 193-200.

[131] I. Larosche, P. Letteron, A. Berson, B. Fromenty, T.T. Huang, R. Moreau, D. Pessayre, A. Mansouri, Hepatic mitochondrial DNA depletion after an alcohol binge in mice: probable role of peroxynitrite and modulation by manganese superoxide dismutase, J Pharmacol Exp Ther 332(3) (2010) 886-97.

[132] Z. Zhong, J.J. Lemasters, A Unifying Hypothesis Linking Hepatic Adaptations for Ethanol Metabolism to the Proinflammatory and Profibrotic Events of Alcoholic Liver Disease, Alcohol Clin Exp Res 42(11) (2018) 2072-2089.

[133] N.E. Sunny, F. Bril, K. Cusi, Mitochondrial Adaptation in Nonalcoholic Fatty Liver Disease: Novel Mechanisms and Treatment Strategies, Trends Endocrinol Metab 28(4) (2017) 250-260.

[134] M. Cannistra, M. Ruggiero, A. Zullo, G. Gallelli, S. Serafini, M. Maria, A. Naso, R. Grande, R. Serra, B. Nardo, Hepatic ischemia reperfusion injury: A systematic review of

literature and the role of current drugs and biomarkers, Int J Surg 33 Suppl 1 (2016) S57-70.

[135] R. Heidari, H. Niknahad, The Role and Study of Mitochondrial Impairment and Oxidative Stress in Cholestasis, Methods Mol Biol 1981 (2019) 117-132.

[136] K. Tsuneyama, H. Baba, Y. Morimoto, T. Tsunematsu, H. Ogawa, Primary Biliary Cholangitis: Its Pathological Characteristics and Immunopathological Mechanisms, J Med Invest 64(1.2) (2017) 7-13.

[137] Z. Zhong, V.K. Ramshesh, H. Rehman, R.T. Currin, V. Sridharan, T.P. Theruvath, I. Kim, G.L. Wright, J.J. Lemasters, Activation of the oxygen-sensing signal cascade prevents mitochondrial injury after mouse liver ischemia-reperfusion, Am J Physiol Gastrointest Liver Physiol 295(4) (2008) G823-32.

[138] N.S. Chandel, Mitochondria as signaling organelles, BMC Biol 12 (2014) 34.

[139] G. Kroemer, L. Galluzzi, P. Vandenabeele, J. Abrams, E.S. Alnemri, E.H. Baehrecke, M.V. Blagosklonny, W.S. El-Deiry, P. Golstein, D.R. Green, M. Hengartner, R.A. Knight, S. Kumar, S.A. Lipton, W. Malorni, G. Nunez, M.E. Peter, J. Tschopp, J. Yuan, M. Piacentini, B. Zhivotovsky, G. Melino, D. Nomenclature Committee on Cell, Classification of cell death: recommendations of the Nomenclature Committee on Cell Death 2009, Cell Death Differ 16(1) (2009) 3-11.

[140] Y. Li, M. Zhou, Q. Hu, X.C. Bai, W. Huang, S.H. Scheres, Y. Shi, Mechanistic insights into caspase-9 activation by the structure of the apoptosome holoenzyme, Proc Natl Acad Sci U S A 114(7) (2017) 1542-1547.

[141] A. Ashkenazi, W.J. Fairbrother, J.D. Leverson, A.J. Souers, From basic apoptosis discoveries to advanced selective BCL-2 family inhibitors, Nat Rev Drug Discov 16(4) (2017) 273-284.

[142] M.Y. Yoon, S.J. Kim, B.H. Lee, J.H. Chung, Y.C. Kim, Effects of dimethylsulfoxide on metabolism and toxicity of acetaminophen in mice, Biol Pharm Bull 29(8) (2006) 1618-24.

[143] S. Zaman, R. Wang, V. Gandhi, Targeting the apoptosis pathway in hematologic malignancies, Leuk Lymphoma 55(9) (2014) 1980-92.

[144] J.J. Lemasters, V. Necrapoptosis and the mitochondrial permeability transition: shared pathways to necrosis and apoptosis, Am J Physiol 276(1) (1999) G1-6.

[145] J.J. Lemasters, Modulation of mitochondrial membrane permeability in pathogenesis, autophagy and control of metabolism, J Gastroenterol Hepatol 22 Suppl 1 (2007) S31-7.

[146] J.J. Lemasters, A.L. Nieminen, T. Qian, L.C. Trost, S.P. Elmore, Y. Nishimura, R.A. Crowe, W.E. Cascio, C.A. Bradham, D.A. Brenner, B. Herman, The mitochondrial permeability transition in cell death: a common mechanism in necrosis, apoptosis and autophagy, Biochim Biophys Acta 1366(1-2) (1998) 177-96.

[147] J.J. Lemasters, T. Qian, C.A. Bradham, D.A. Brenner, W.E. Cascio, L.C. Trost, Y. Nishimura, A.L. Nieminen, B. Herman, Mitochondrial dysfunction in the pathogenesis of necrotic and apoptotic cell death, J Bioenerg Biomembr 31(4) (1999) 305-19.

[148] J.J. Lemasters, T. Qian, S.P. Elmore, L.C. Trost, Y. Nishimura, B. Herman, C.A. Bradham, D.A. Brenner, A.L. Nieminen, Confocal microscopy of the mitochondrial

permeability transition in necrotic cell killing, apoptosis and autophagy, Biofactors 8(3-4) (1998) 283-5.

[149] J.J. Lemasters, T. Qian, L. He, J.S. Kim, S.P. Elmore, W.E. Cascio, D.A. Brenner, Role of mitochondrial inner membrane permeabilization in necrotic cell death, apoptosis, and autophagy, Antioxid Redox Signal 4(5) (2002) 769-81.

[150] T. Miura, M. Tanno, The mPTP and its regulatory proteins: final common targets of signalling pathways for protection against necrosis, Cardiovasc Res 94(2) (2012) 181-9.

[151] J.S. Kim, L. He, J.J. Lemasters, Mitochondrial permeability transition: a common pathway to necrosis and apoptosis, Biochem Biophys Res Commun 304(3) (2003) 463-70.

[152] D. Siemen, M. Ziemer, What is the nature of the mitochondrial permeability transition pore and what is it not?, IUBMB Life 65(3) (2013) 255-62.

[153] M. Juhaszova, S. Wang, D.B. Zorov, H.B. Nuss, M. Gleichmann, M.P. Mattson, S.J. Sollott, The identity and regulation of the mitochondrial permeability transition pore: where the known meets the unknown, Ann N Y Acad Sci 1123 (2008) 197-212.

[154] F. Fakharnia, F. Khodagholi, L. Dargahi, A. Ahmadiani, Prevention of Cyclophilin D-Mediated mPTP Opening Using Cyclosporine-A Alleviates the Elevation of Necroptosis, Autophagy and Apoptosis-Related Markers Following Global Cerebral Ischemia-Reperfusion, J Mol Neurosci 61(1) (2017) 52-60.

[155] J. Hu, V.K. Ramshesh, M.R. McGill, H. Jaeschke, J.J. Lemasters, Low dose acetaminophen induces rerversible mitochondrial dysfunction associated with transient c-Jun n-terminal kinase activation in mouse liver, Toxicol Sci 150(1) (2016) 204-15.

[156] H. Jaeschke, M.R. McGill, A. Ramachandran, Oxidant stress, mitochondria, and cell death mechanisms in drug-induced liver injury: lessons learned from acetaminophen hepatotoxicity, Drug Metab Rev 44(1) (2012) 88-106.

[157] J.S. Kim, J.H. Wang, J.J. Lemasters, Mitochondrial permeability transition in rat hepatocytes after anoxia/reoxygenation: role of Ca2+-dependent mitochondrial formation of reactive oxygen species, Am J Physiol Gastrointest Liver Physiol 302(7) (2012) G723-31.

[158] K. Kon, J.S. Kim, H. Jaeschke, J.J. Lemasters, Mitochondrial permeability transition in acetaminophen-induced necrosis and apoptosis of cultured mouse hepatocytes, Hepatology 40(5) (2004) 1170-9.

[159] A. Ramachandran, H. Jaeschke, Mechanisms of acetaminophen hepatotoxicity and their translation to the human pathophysiology, J Clin Transl Res 3(Suppl 1) (2017) 157-169.

[160] A. Ramachandran, M. Lebofsky, C.P. Baines, J.J. Lemasters, H. Jaeschke, Cyclophilin D deficiency protects against acetaminophen-induced oxidant stress and liver injury, Free Radic Res 45(2) (2011) 156-64.

[161] T. Vanden Berghe, A. Linkermann, S. Jouan-Lanhouet, H. Walczak, P. Vandenabeele, Regulated necrosis: the expanding network of non-apoptotic cell death pathways, Nat Rev Mol Cell Biol 15(2) (2014) 135-47.

[162] H. Wang, L. Sun, L. Su, J. Rizo, L. Liu, L.F. Wang, F.S. Wang, X. Wang, Mixed lineage kinase domain-like protein MLKL causes necrotic membrane disruption upon phosphorylation by RIP3, Mol Cell 54(1) (2014) 133-146.

[163] D.C. Wallace, Mitochondrial diseases in man and mouse, Science 283(5407) (1999) 1482-8.

[164] Q. Zhang, M. Raoof, Y. Chen, Y. Sumi, T. Sursal, W. Junger, K. Brohi, K. Itagaki, C.J. Hauser, Circulating mitochondrial DAMPs cause inflammatory responses to injury, Nature 464(7285) (2010) 104-7.

[165] C.S. Calfee, M.A. Matthay, Clinical immunology: culprits with evolutionary ties, Nature 464(7285) (2010) 41-2.

[166] A.P. West, I.E. Brodsky, C. Rahner, D.K. Woo, H. Erdjument-Bromage, P. Tempst, M.C. Walsh, Y. Choi, G.S. Shadel, S. Ghosh, TLR signalling augments macrophage bactericidal activity through mitochondrial ROS, Nature 472(7344) (2011) 476-80.

[167] Q. Hu, C.R. Wood, S. Cimen, A.B. Venkatachalam, I.P. Alwayn, Mitochondrial Damage-Associated Molecular Patterns (MTDs) Are Released during Hepatic Ischemia Reperfusion and Induce Inflammatory Responses, PLoS One 10(10) (2015) e0140105.

[168] P.E. Marques, S.S. Amaral, D.A. Pires, L.L. Nogueira, F.M. Soriani, B.H. Lima, G.A. Lopes, R.C. Russo, T.V. Avila, J.G. Melgaco, A.G. Oliveira, M.A. Pinto, C.X. Lima, A.M. De Paula, D.C. Cara, M.F. Leite, M.M. Teixeira, G.B. Menezes, Chemokines and mitochondrial products activate neutrophils to amplify organ injury during mouse acute liver failure, Hepatology 56(5) (2012) 1971-82.

[169] K. Nakahira, S. Hisata, A.M. Choi, The Roles of Mitochondrial Damage-Associated Molecular Patterns in Diseases, Antioxid Redox Signal 23(17) (2015) 1329-50.

[170] K. Schroder, J. Tschopp, The inflammasomes, Cell 140(6) (2010) 821-32.

[171] P. Gurung, J.R. Lukens, T.D. Kanneganti, Mitochondria: diversity in the regulation of the NLRP3 inflammasome, Trends Mol Med 21(3) (2015) 193-201.

[172] H.B. Yu, B.B. Finlay, The caspase-1 inflammasome: a pilot of innate immune responses, Cell Host Microbe 4(3) (2008) 198-208.

[173] R. Zhou, A.S. Yazdi, P. Menu, J. Tschopp, A role for mitochondria in NLRP3 inflammasome activation, Nature 469(7329) (2011) 221-5.

[174] T. Csak, M. Ganz, J. Pespisa, K. Kodys, A. Dolganiuc, G. Szabo, Fatty acid and endotoxin activate inflammasomes in mouse hepatocytes that release danger signals to stimulate immune cells, Hepatology 54(1) (2011) 133-44.

[175] J. Petrasek, S. Bala, T. Csak, D. Lippai, K. Kodys, V. Menashy, M. Barrieau, S.Y. Min, E.A. Kurt-Jones, G. Szabo, IL-1 receptor antagonist ameliorates inflammasome-dependent alcoholic steatohepatitis in mice, J Clin Invest 122(10) (2012) 3476-89.

[176] G. Szabo, J. Petrasek, Inflammasome activation and function in liver disease, Nat Rev Gastroenterol Hepatol 12(7) (2015) 387-400.

[177] C.M. Herndon, D.M. Dankenbring, Patient perception and knowledge of acetaminophen in a large family medicine service, J Pain Palliat Care Pharmacother 28(2) (2014) 109-16.

[178] D.S. Budnitz, M.C. Lovegrove, A.E. Crosby, Emergency department visits for overdoses of acetaminophen-containing products, Am J Prev Med 40(6) (2011) 585-92.

[179] C. Bunchorntavakul, K.R. Reddy, Acetaminophen (APAP or N-Acetyl-p-Aminophenol) and Acute Liver Failure, Clin Liver Dis 22(2) (2018) 325-346.

[180] E.M. Lancaster, J.R. Hiatt, A. Zarrinpar, Acetaminophen hepatotoxicity: an updated review, Arch Toxicol 89(2) (2015) 193-9.

[181] M. Blieden, L.C. Paramore, D. Shah, R. Ben-Joseph, A perspective on the epidemiology of acetaminophen exposure and toxicity in the United States, Expert Rev Clin Pharmacol 7(3) (2014) 341-8.

[182] R.J. Fontana, Acute liver failure due to drugs, Semin Liver Dis 28(2) (2008) 175-87.

[183] E. Yoon, A. Babar, M. Choudhary, M. Kutner, N. Pyrsopoulos, Acetaminophen-induced hepatotoxicity: a comprehensive update, J Clin Transl Hepatol 4(2) (2016) 131-42.

[184] J.A. Hinson, D.W. Roberts, L.P. James, Mechanisms of acetaminophen-induced liver necrosis, Handb Exp Pharmacol (196) (2010) 369-405.

[185] H. Jaeschke, A. Ramachandran, Oxidant stress and lipid peroxidation in acetaminophen hepatotoxicity, React Oxyg Species (Apex) 5(15) (2018) 145-158.

[186] M.L. Bajt, T.R. Knight, J.J. Lemasters, H. Jaeschke, Acetaminophen-induced oxidant stress and cell injury in cultured mouse hepatocytes: protection by N-acetyl cysteine, Toxicol Sci 80(2) (2004) 343-9.

[187] H. Jaeschke, Glutathione disulfide formation and oxidant stress during acetaminophen-induced hepatotoxicity in mice in vivo: the protective effect of allopurinol, J Pharmacol Exp Ther 255(3) (1990) 935-41.

[188] M.A. Tirmenstein, S.D. Nelson, Acetaminophen-induced oxidation of protein thiols. Contribution of impaired thiol-metabolizing enzymes and the breakdown of adenine nucleotides, J Biol Chem 265(6) (1990) 3059-65.

[189] A.S. Burke, L.A. MacMillan-Crow, J.A. Hinson, Reactive nitrogen species in acetaminophen-induced mitochondrial damage and toxicity in mouse hepatocytes, Chem Res Toxicol 23(7) (2010) 1286-92.

[190] H. Jaeschke, J.J. Lemasters, Apoptosis versus oncotic necrosis in hepatic ischemia/reperfusion injury, Gastroenterology 125(4) (2003) 1246-57.

[191] Y. Qiu, L.Z. Benet, A.L. Burlingame, Identification of the hepatic protein targets of reactive metabolites of acetaminophen in vivo in mice using two-dimensional gel electrophoresis and mass spectrometry, J Biol Chem 273(28) (1998) 17940-53.

[192] H.M. Yan, A. Ramachandran, M.L. Bajt, J.J. Lemasters, H. Jaeschke, The oxygen tension modulates acetaminophen-induced mitochondrial oxidant stress and cell injury in cultured hepatocytes, Toxicol Sci 117(2) (2010) 515-23.

[193] R. Agarwal, L.A. MacMillan-Crow, T.M. Rafferty, H. Saba, D.W. Roberts, E.K. Fifer, L.P. James, J.A. Hinson, Acetaminophen-induced hepatotoxicity in mice occurs with inhibition of activity and nitration of mitochondrial manganese superoxide dismutase, J Pharmacol Exp Ther 337(1) (2011) 110-6.

[194] M.L. Bajt, T.R. Knight, A. Farhood, H. Jaeschke, Scavenging peroxynitrite with glutathione promotes regeneration and enhances survival during acetaminophen-induced liver injury in mice, J Pharmacol Exp Ther 307(1) (2003) 67-73.

[195] T.R. Knight, H. Jaeschke, Acetaminophen-induced inhibition of Fas receptor-mediated liver cell apoptosis: mitochondrial dysfunction versus glutathione depletion, Toxicol Appl Pharmacol 181(2) (2002) 133-41.

[196] K. Du, Y. Xie, M.R. McGill, H. Jaeschke, Pathophysiological significance of c-jun N-terminal kinase in acetaminophen hepatotoxicity, Expert Opin Drug Metab Toxicol 11(11) (2015) 1769-79.

[197] B.K. Gunawan, Z.X. Liu, D. Han, N. Hanawa, W.A. Gaarde, N. Kaplowitz, c-Jun N-terminal kinase plays a major role in murine acetaminophen hepatotoxicity, Gastroenterology 131(1) (2006) 165-78.

[198] N.C. Henderson, K.J. Pollock, J. Frew, A.C. Mackinnon, R.A. Flavell, R.J. Davis, T. Sethi, K.J. Simpson, Critical role of c-jun (NH2) terminal kinase in paracetamol- induced acute liver failure, Gut 56(7) (2007) 982-90.

[199] Y. Xie, M.R. McGill, K. Dorko, S.C. Kumer, T.M. Schmitt, J. Forster, H. Jaeschke, Mechanisms of acetaminophen-induced cell death in primary human hepatocytes, Toxicol Appl Pharmacol 279(3) (2014) 266-74.

[200] S. Fiorucci, E. Antonelli, E. Distrutti, A. Mencarelli, S. Farneti, P. Del Soldato, A. Morelli, Liver delivery of NO by NCX-1000 protects against acute liver failure and mitochondrial dysfunction induced by APAP in mice, Br J Pharmacol 143(1) (2004) 33-42.

[201] Z. Lin, F. Wu, S. Lin, X. Pan, L. Jin, T. Lu, L. Shi, Y. Wang, A. Xu, X. Li, Adiponectin protects against acetaminophen-induced mitochondrial dysfunction and acute liver injury by promoting autophagy in mice, J Hepatol 61(4) (2014) 825-31.

[202] C. Bunchorntavakul, K.R. Reddy, Acetaminophen-related hepatotoxicity, Clin Liver Dis 17(4) (2013) 587-607, viii.

[203] S.S. More, J. Nugent, A.P. Vartak, S.M. Nye, R. Vince, Hepatoprotective Effect of psi-Glutathione in a Murine Model of Acetaminophen-Induced Liver Toxicity, Chem Res Toxicol 30(3) (2017) 777-784.

[204] N.U. Nguyen, B.D. Stamper, Polyphenols reported to shift APAP-induced changes in MAPK signaling and toxicity outcomes, Chem Biol Interact 277 (2017) 129-136.

[205] M. Wei, Z. Zheng, L. Shi, Y. Jin, L. Ji, Natural Polyphenol Chlorogenic Acid Protects Against Acetaminophen-Induced Hepatotoxicity by Activating ERK/Nrf2 Antioxidative Pathway, Toxicol Sci 162(1) (2018) 99-112.

[206] M.R. McGill, H. Jaeschke, Animal models of drug-induced liver injury, Biochim Biophys Acta Mol Basis Dis 1865(5) (2019) 1031-1039.

[207] G.C. Boxill, C.B. Nash, A.G. Wheeler, Comparative pharmacological and toxicological evaluation of N-acetyl-p-aminophenol, salicylamide, and acetylsalicylic acid, J Am Pharm Assoc Am Pharm Assoc 47(7) (1958) 479-87.

[208] M.R. McGill, C.D. Williams, Y. Xie, A. Ramachandran, H. Jaeschke, Acetaminophen-induced liver injury in rats and mice: comparison of protein adducts, mitochondrial dysfunction, and oxidative stress in the mechanism of toxicity, Toxicol Appl Pharmacol 264(3) (2012) 387-94.

[209] H. Jaeschke, Y. Xie, M.R. McGill, Acetaminophen-induced Liver Injury: from Animal Models to Humans, J Clin Transl Hepatol 2(3) (2014) 153-61.

[210] K. Takemoto, E. Hatano, K. Iwaisako, M. Takeiri, N. Noma, S. Ohmae, K. Toriguchi, K. Tanabe, H. Tanaka, S. Seo, K. Taura, K. Machida, N. Takeda, S. Saji, S. Uemoto, M. Asagiri, Necrostatin-1 protects against reactive oxygen species (ROS)-induced hepatotoxicity in acetaminophen-induced acute liver failure, FEBS Open Bio 4 (2014) 777-87.

[211] E.H. Jeffery, K. Arndt, W.M. Haschek, The role of cytochrome P450IIE1 in bioactivation of acetaminophen in diabetic and acetone-treated mice, Adv Exp Med Biol 283 (1991) 249-51.

[212] L. Duan, J.S. Davis, B.L. Woolbright, K. Du, M. Cahkraborty, J. Weemhoff, H. Jaeschke, M. Bourdi, Differential susceptibility to acetaminophen-induced liver injury in sub-strains of C57BL/6 mice: 6N versus 6J, Food Chem Toxicol 98(Pt B) (2016) 107-118.

[213] H.C. Yohe, K.A. O'Hara, J.A. Hunt, T.J. Kitzmiller, S.G. Wood, J.L. Bement, W.J. Bement, J.G. Szakacs, S.A. Wrighton, J.M. Jacobs, V. Kostrubsky, P.R. Sinclair, J.F. Sinclair, Involvement of Toll-like receptor 4 in acetaminophen hepatotoxicity, Am J Physiol Gastrointest Liver Physiol 290(6) (2006) G1269-79.

[214] R. Bataller, D.A. Brenner, Liver fibrosis, Journal of Clinical Investigation 115(2) (2005) 209-218.

[215] D.C. Rockey, P.D. Bell, J.A. Hill, Fibrosis--a common pathway to organ injury and failure, N Engl J Med 373(1) (2015) 96.

[216] R.J. Sokol, Liver cell injury and fibrosis, J Pediatr Gastroenterol Nutr 35 Suppl 1 (2002) S7-10.

[217] P.P. Anthony, K.G. Ishak, N.C. Nayak, H.E. Poulsen, P.J. Scheuer, L.H. Sobin, The morphology of cirrhosis. Recommendations on definition, nomenclature, and classification by a working group sponsored by the World Health Organization, J Clin Pathol 31(5) (1978) 395-414.

[218] R. D'Ambrosio, A. Aghemo, M.G. Rumi, E. Degasperi, A. Sangiovanni, M. Maggioni, M. Fraquelli, R. Perbellini, W. Rosenberg, P. Bedossa, M. Colombo, P. Lampertico, Persistence of hepatocellular carcinoma risk in hepatitis C patients with a response to IFN and cirrhosis regression, Liver Int 38(8) (2018) 1459-1467.

[219] S. Scaglione, S. Kliethermes, G. Cao, D. Shoham, R. Durazo, A. Luke, M.L. Volk, The epidemiology of cirrhosis in the United States: a population-based study, J Clin Gastroenterol 49(8) (2015) 690-6.

[220] S.K. Asrani, H. Devarbhavi, J. Eaton, P.S. Kamath, Burden of liver diseases in the world, J Hepatol 70(1) (2019) 151-171.

[221] S.L. Murphy, J. Xu, K.D. Kochanek, S.C. Curtin, E. Arias, Deaths: final data for 2015, Natl Vital Stat Rep 66(6) (2017) 1-75.

[222] A. Pellicoro, P. Ramachandran, J.P. Iredale, J.A. Fallowfield, Liver fibrosis and repair: immune regulation of wound healing in a solid organ, Nat Rev Immunol 14(3) (2014) 181-94.

[223] D.C. Rockey, Translating an understanding of the pathogenesis of hepatic fibrosis to novel therapies, Clinical gastroenterology and hepatology : the official clinical practice journal of the American Gastroenterological Association 11(3) (2013) 224-31 e1-5.

[224] D.A. Brenner, T. Kisseleva, D. Scholten, Y.H. Paik, K. Iwaisako, S. Inokuchi, B. Schnabl, E. Seki, S. De Minicis, C. Oesterreicher, K. Taura, Origin of myofibroblasts in liver fibrosis, Fibrogenesis Tissue Repair 5(Suppl 1) (2012) S17.

[225] K. Iwaisako, C. Jiang, M. Zhang, M. Cong, T.J. Moore-Morris, T.J. Park, X. Liu, J. Xu, P. Wang, Y.H. Paik, F. Meng, M. Asagiri, L.A. Murray, A.F. Hofmann, T. Iida, C.K. Glass, D.A. Brenner, T. Kisseleva, Origin of myofibroblasts in the fibrotic liver in mice, Proc Natl Acad Sci U S A 111(32) (2014) E3297-305.

[226] B.L. Copple, H. Jaeschke, C.D. Klaassen, Oxidative stress and the pathogenesis of cholestasis, Semin Liver Dis 30(2) (2010) 195-204.

[227] J. Zhang, A. Yang, Y. Wu, W. Guan, B. Xiong, X. Peng, X. Wei, C. Chen, Z. Liu, Stachydrine ameliorates carbon tetrachloride-induced hepatic fibrosis by inhibiting inflammation, oxidative stress and regulating MMPs/TIMPs system in rats, Biomed Pharmacother 97 (2018) 1586-1594.

[228] R.J. Coffey, Jr., W.E. Russell, J.A. Barnard, Pharmacokinetics of TGF beta with emphasis on effects in liver and gut, Ann N Y Acad Sci 593 (1990) 285-91.

[229] H. Tilg, A.R. Moschen, G. Szabo, Interleukin-1 and inflammasomes in alcoholic liver disease/acute alcoholic hepatitis and nonalcoholic fatty liver disease/nonalcoholic steatohepatitis, Hepatology 64(3) (2016) 955-65.

[230] Y.H. Li, S.H. Woo, D.H. Choi, E.H. Cho, Succinate causes alpha-SMA production through GPR91 activation in hepatic stellate cells, Biochem Biophys Res Commun 463(4) (2015) 853-8.

[231] H. Rehman, Q. Liu, Y. Krishnasamy, Z. Shi, V.K. Ramshesh, K. Haque, R.G. Schnellmann, M.P. Murphy, J.J. Lemasters, D.C. Rockey, Z. Zhong, The mitochondria-targeted antioxidant MitoQ attenuates liver fibrosis in mice, Int J Physiol Pathophysiol Pharmacol 8(1) (2016) 14-27.

[232] Y.A. Lee, M.C. Wallace, S.L. Friedman, Pathobiology of liver fibrosis: a translational success story, Gut 64(5) (2015) 830-41.

[233] R. D'Ambrosio, A. Aghemo, M.G. Rumi, G. Ronchi, M.F. Donato, V. Paradis, M. Colombo, P. Bedossa, A morphometric and immunohistochemical study to assess the benefit of a sustained virological response in hepatitis C virus patients with cirrhosis, Hepatology 56(2) (2012) 532-43.

[234] A.J. van der Meer, B.J. Veldt, J.J. Feld, H. Wedemeyer, J.F. Dufour, F. Lammert, A. Duarte-Rojo, E.J. Heathcote, M.P. Manns, L. Kuske, S. Zeuzem, W.P. Hofmann, R.J. de Knegt, B.E. Hansen, H.L. Janssen, Association between sustained virological response and all-cause mortality among patients with chronic hepatitis C and advanced hepatic fibrosis, JAMA 308(24) (2012) 2584-93.

[235] A.M. Oseini, A.J. Sanyal, Therapies in non-alcoholic steatohepatitis (NASH), Liver Int 37 Suppl 1 (2017) 97-103.

[236] A.J. Sanyal, N. Chalasani, K.V. Kowdley, A. McCullough, A.M. Diehl, N.M. Bass, B.A. Neuschwander-Tetri, J.E. Lavine, J. Tonascia, A. Unalp, M. Van Natta, J. Clark, E.M. Brunt, D.E. Kleiner, J.H. Hoofnagle, P.R. Robuck, C.R.N. Nash, Pioglitazone, vitamin E, or placebo for nonalcoholic steatohepatitis, N Engl J Med 362(18) (2010) 1675-85.

[237] M. Malaguarnera, M. Motta, M. Vacante, G. Malaguarnera, F. Caraci, G. Nunnari, C. Gagliano, C. Greco, G. Chisari, F. Drago, G. Bertino, Silybin-vitamin E-phospholipids complex reduces liver fibrosis in patients with chronic hepatitis C treated with pegylated interferon alpha and ribavirin, Am J Transl Res 7(11) (2015) 2510-8.

[238] C. Liedtke, T. Luedde, T. Sauerbruch, D. Scholten, K. Streetz, F. Tacke, R. Tolba, C. Trautwein, J. Trebicka, R. Weiskirchen, Experimental liver fibrosis research: update on animal models, legal issues and translational aspects, Fibrogenesis Tissue Repair 6(1) (2013) 19.

[239] S.C. Yanguas, B. Cogliati, J. Willebrords, M. Maes, I. Colle, B. van den Bossche, C. de Oliveira, W. Andraus, V.A.F. Alves, I. Leclercq, M. Vinken, Experimental models of liver fibrosis, Arch Toxicol 90(5) (2016) 1025-1048.

[240] W.H. Tsai, A.B. DeAngelo, Responsiveness of hepatocytes from dichloroacetic acid or phenobarbital treated mice to growth factors in primary culture, Cancer Lett 99(2) (1996) 177-83.

[241] T.J. Caperna, M.L. Failla, Cadmium metabolism by rat liver endothelial and Kupffer cells, Biochem J 221(3) (1984) 631-6.

[242] Y.C. Koo, M.C. Pyo, M.H. Nam, C.O. Hong, S.Y. Yang, K.W. Lee, Chebulic acid prevents hepatic fibrosis induced by advanced glycation end-products in LX-2 cell by modulating Nrf2 translocation via ERK pathway, Toxicol In Vitro 34 (2016) 8-15.

[243] J. Lv, R. Bai, L. Wang, J. Gao, H. Zhang, Artesunate may inhibit liver fibrosis via the FAK/Akt/beta-catenin pathway in LX-2 cells, BMC Pharmacol Toxicol 19(1) (2018) 64.

[244] L. Xu, A.Y. Hui, E. Albanis, M.J. Arthur, S.M. O'Byrne, W.S. Blaner, P. Mukherjee, S.L. Friedman, F.J. Eng, Human hepatic stellate cell lines, LX-1 and LX-2: new tools for analysis of hepatic fibrosis, Gut 54(1) (2005) 142-51.

[245] D. Zhu, L. Lyu, P. Shen, J. Wang, J. Chen, X. Sun, L. Chen, L. Zhang, Q. Zhou, Y. Duan, rSjP40 protein promotes PPARgamma expression in LX-2 cells through microRNA-27b, FASEB J 32(9) (2018) 4798-4803.

[246] F.J. Cubero, M.E. Zoubek, W. Hu, J. Peng, G. Zhao, Y.A. Nevzorova, M. Al Masaoudi, L.P. Bechmann, M.V. Boekschoten, M. Muller, C. Preisinger, N. Gassler, A.E. Canbay, T. Luedde, R.J. Davis, C. Liedtke, C. Trautwein, Combined Activities of JNK1 and JNK2 in Hepatocytes Protect Against Toxic Liver Injury, Gastroenterology 150(4) (2016) 968-81.

[247] K.A. El-Mihi, H.I. Kenawy, A. El-Karef, N.M. Elsherbiny, L.A. Eissa, Naringin attenuates thioacetamide-induced liver fibrosis in rats through modulation of the PI3K/Akt pathway, Life Sci 187 (2017) 50-57.

[248] P.G. Traber, H. Chou, E. Zomer, F. Hong, A. Klyosov, M.I. Fiel, S.L. Friedman, Regression of fibrosis and reversal of cirrhosis in rats by galectin inhibitors in thioacetamide-induced liver disease, PLoS One 8(10) (2013) e75361.

[249] X. Liu, R. Dai, M. Ke, I. Suheryani, W. Meng, Y. Deng, Differential Proteomic Analysis of Dimethylnitrosamine (DMN)-Induced Liver Fibrosis, Proteomics 17(22) (2017).

[250] L.J. Su, S.L. Hsu, J.S. Yang, H.H. Tseng, S.F. Huang, C.Y. Huang, Global gene expression profiling of dimethylnitrosamine-induced liver fibrosis: from pathological and biochemical data to microarray analysis, Gene Expr 13(2) (2006) 107-32.

[251] C.G. Tag, S. Sauer-Lehnen, S. Weiskirchen, E. Borkham-Kamphorst, R.H. Tolba, F. Tacke, R. Weiskirchen, Bile duct ligation in mice: induction of inflammatory liver injury and fibrosis by obstructive cholestasis, J Vis Exp (96) (2015).

[252] G. Xu, Y. Shi, Apoptosis signaling pathways and lymphocyte homeostasis, Cell Res 17(9) (2007) 759-71.

[253] S. Chaudhuri, S.S. McCullough, L. Hennings, A.T. Brown, S.H. Li, P.M. Simpson, J.A. Hinson, L.P. James, Effect of trifluoperazine on toxicity, HIF-1alpha induction and hepatocyte regeneration in acetaminophen toxicity in mice, Toxicol Appl Pharmacol 264(2) (2012) 192-201.

[254] W. H.J., T. K., W. P.M., D.C. Rockey, J.J. Lemasters, Z. Zhong, Aldehyde dehydrogenase-2 activation by Alda-1 decreases necrosis and fibrosis after bile duct ligation in mice., (2019 submitted for publication) 28.

[255] J. Schindelin, I. Arganda-Carreras, E. Frise, V. Kaynig, M. Longair, T. Pietzsch, S. Preibisch, C. Rueden, S. Saalfeld, B. Schmid, J.Y. Tinevez, D.J. White, V. Hartenstein, K. Eliceiri, P. Tomancak, A. Cardona, Fiji: an open-source platform for biological-image analysis, Nat Methods 9(7) (2012) 676-82.

[256] Y. Krishnasamy, V.K. Ramshesh, M. Gooz, R.G. Schnellmann, J.J. Lemasters, Z. Zhong, Ethanol and high cholesterol diet causes severe steatohepatitis and early liver fibrosis in mice, PLoS One 11(9) (2016) e0163342.

[257] J.Y. Akakpo, A. Ramachandran, L. Duan, M.A. Schaich, M.W. Jaeschke, B.D. Freudenthal, W.X. Ding, B.H. Rumack, H. Jaeschke, Delayed Treatment with 4-Methylpyrazole Protects against Acetaminophen Hepatotoxicity in Mice by Inhibition of c-Jun N-Terminal Kinase, Toxicol Sci (2019).

[258] J.Y. Akakpo, A. Ramachandran, S.E. Kandel, H.M. Ni, S.C. Kumer, B.H. Rumack, H. Jaeschke, 4-Methylpyrazole protects against acetaminophen hepatotoxicity in mice and in primary human hepatocytes, Hum Exp Toxicol 37(12) (2018) 1310-1322.

[259] J.J. Ventura, P. Cogswell, R.A. Flavell, A.S. Baldwin, Jr., R.J. Davis, JNK potentiates TNF-stimulated necrosis by increasing the production of cytotoxic reactive oxygen species, Genes Dev 18(23) (2004) 2905-15.

[260] M.P. Murphy, How mitochondria produce reactive oxygen species, Biochem J 417(1) (2009) 1-13.

[261] R.S. Rahimi, D.C. Rockey, End-stage liver disease complications, Curr Opin Gastroenterol 29(3) (2013) 257-63.

[262] M. Blachier, H. Leleu, M. Peck-Radosavljevic, D.C. Valla, F. Roudot-Thoraval, The burden of liver disease in Europe: a review of available epidemiological data, J Hepatol 58(3) (2013) 593-608.

[263] L.B. Seeff, J.H. Hoofnagle, National Institutes of Health Consensus Development Conference: management of hepatitis C: 2002, Hepatology 36(5 Suppl 1) (2002) S1-2.

[264] J.L. Dienstag, Hepatitis B virus infection, N Engl J Med 359(14) (2008) 1486-500.

[265] J.M. Clark, F.L. Brancati, A.M. Diehl, Nonalcoholic fatty liver disease, Gastroenterology 122(6) (2002) 1649-57.

[266] D. Li, S.L. Friedman, Liver fibrogenesis and the role of hepatic stellate cells: new insights and prospects for therapy, J Gastroenterol Hepatol 14(7) (1999) 618-33.

[267] M. Setshedi, J.R. Wands, S.M. Monte, Acetaldehyde adducts in alcoholic liver disease, Oxid Med Cell Longev 3(3) (2010) 178-85.

[268] P.J. Campagnola, L.M. Loew, Second-harmonic imaging microscopy for visualizing biomolecular arrays in cells, tissues and organisms, Nat Biotechnol 21(11) (2003) 1356-60.

[269] Z. Shi, D.C. Rockey, Upregulation of the actin cytoskeleton via myocardin leads to increased expression of type 1 collagen, Lab Invest 97(12) (2017) 1412-1426.

[270] C.R. Drifka, A.G. Loeffler, K. Mathewson, G. Mehta, A. Keikhosravi, Y. Liu, S. Lemancik, W.A. Ricke, S.M. Weber, W.J. Kao, K.W. Eliceiri, Comparison of picrosirius red staining with second harmonic generation imaging for the quantification of clinically relevant collagen fiber features in histopathology samples, J Histochem Cytochem 64(9) (2016) 519-29.

[271] K. Iwaisako, D.A. Brenner, T. Kisseleva, What's new in liver fibrosis? The origin of myofibroblasts in liver fibrosis, J Gastroenterol Hepatol 27 Suppl 2 (2012) 65-8.

[272] M. Yang, A. Ramachandran, H.M. Yan, B.L. Woolbright, B.L. Copple, P. Fickert, M. Trauner, H. Jaeschke, Osteopontin is an initial mediator of inflammation and liver injury during obstructive cholestasis after bile duct ligation in mice, Toxicol Lett 224(2) (2014) 186-95.

[273] M. Sellinger, J.L. Boyer, Physiology of bile secretion and cholestasis, Prog Liver Dis 9 (1990) 237-59.

[274] B.L. Woolbright, H. Jaeschke, Novel insight into mechanisms of cholestatic liver injury, World J Gastroenterol 18(36) (2012) 4985-93.

[275] O.M. Lashin, P.A. Szweda, L.I. Szweda, A.M. Romani, Decreased complex II respiration and HNE-modified SDH subunit in diabetic heart, Free Radic Biol Med 40(5) (2006) 886-96.

[276] H. Rehman, V.K. Ramshesh, T.P. Theruvath, I. Kim, R.T. Currin, S. Giri, J.J. Lemasters, Z. Zhong, NIM811, a mitochondrial permeability transition inhibitor, attenuates cholestatic liver injury but not fibrosis in mice, The Journal of pharmacology and experimental therapeutics 327(3) (2008) 699-706.

[277] J.J. Maher, B.A. Neuschwander-Tetri, Manipulation of glutathione stores in rat hepatic stellate cells does not alter collagen synthesis, Hepatology 26(3) (1997) 618-23.

[278] S.L. Friedman, M.J. Arthur, Activation of cultured rat hepatic lipocytes by Kupffer cell conditioned medium. Direct enhancement of matrix synthesis and stimulation of cell proliferation via induction of platelet-derived growth factor receptors, J Clin Invest 84(6) (1989) 1780-5.

[279] R. Bataller, D.A. Brenner, Hepatic stellate cells as a target for the treatment of liver fibrosis, Semin Liver Dis 21(3) (2001) 437-51.

[280] A.M. Gressner, B. Lahme, A. Brenzel, Molecular dissection of the mitogenic effect of hepatocytes on cultured hepatic stellate cells, Hepatology 22(5) (1995) 1507-18.

[281] J.J. Maher, Leukocytes as Modulators of Stellate Cell Activation, Alcoholism: Clinical and Experimental Research 23(5) (1999) 917-921.

[282] J. Luan, D. Ju, Inflammasome: a double-edged sword in liver diseases, Front Immunol 9 (2018) 2201.

[283] A. Kauppinen, H. Niskanen, T. Suuronen, K. Kinnunen, A. Salminen, K. Kaarniranta, Oxidative stress activates NLRP3 inflammasomes in ARPE-19 cells--implications for age-related macular degeneration (AMD), Immunol Lett 147(1-2) (2012) 29-33.

[284] K.X. Wang, D.T. Denhardt, Osteopontin: role in immune regulation and stress responses, Cytokine Growth Factor Rev 19(5-6) (2008) 333-45.

[285] N. Clemente, D. Raineri, G. Cappellano, E. Boggio, F. Favero, M.F. Soluri, C. Dianzani, C. Comi, U. Dianzani, A. Chiocchetti, Osteopontin bridging innate and adaptive immunity in autoimmune diseases, J Immunol Res 2016 (2016) 7675437.

[286] C.M. Giachelli, D. Lombardi, R.J. Johnson, C.E. Murry, M. Almeida, Evidence for a role of osteopontin in macrophage infiltration in response to pathological stimuli in vivo, Am J Pathol 152(2) (1998) 353-8.

[287] D. Seth, A. Duly, P.C. Kuo, G.W. McCaughan, P.S. Haber, Osteopontin is an important mediator of alcoholic liver disease via hepatic stellate cell activation, World J Gastroenterol 20(36) (2014) 13088-104.

[288] R. Urtasun, A. Lopategi, J. George, T.M. Leung, Y. Lu, X. Wang, X. Ge, M.I. Fiel, N. Nieto, Osteopontin, an oxidant stress sensitive cytokine, up-regulates collagen-I via integrin alpha(V)beta(3) engagement and PI3K/pAkt/NFkappaB signaling, Hepatology 55(2) (2012) 594-608.

[289] C. Gao, H. Guo, Z. Mi, M.J. Grusby, P.C. Kuo, Osteopontin induces ubiquitin-dependent degradation of STAT1 in RAW264.7 murine macrophages, J Immunol 178(3) (2007) 1870-81.

[290] H. Guo, C.Q. Cai, R.A. Schroeder, P.C. Kuo, Osteopontin is a negative feedback regulator of nitric oxide synthesis in murine macrophages, J Immunol 166(2) (2001) 1079-86.

[291] S.A. Lund, C.M. Giachelli, M. Scatena, The role of osteopontin in inflammatory processes, J Cell Commun Signal 3(3-4) (2009) 311-22.

[292] E.E. Rollo, D.L. Laskin, D.T. Denhardt, Osteopontin inhibits nitric oxide production and cytotoxicity by activated RAW264.7 macrophages, J Leukoc Biol 60(3) (1996) 397-404.

[293] H. Guo, P.Y. Wai, Z. Mi, C. Gao, J. Zhang, P.C. Kuo, Osteopontin mediates Stat1 degradation to inhibit iNOS transcription in a cecal ligation and puncture model of sepsis, Surgery 144(2) (2008) 182-8.

[294] H.L. Kim, M.Y. Lee, Y.J. Shin, D.W. Song, J. Park, B.S. Chang, J.H. Lee, Increased expression of osteopontin in the degenerating striatum of rats treated with mitochondrial toxin 3-nitropropionic acid: a light and electron microscopy study, Acta Histochem Cytochem 48(5) (2015) 135-43.

[295] J. Zhang, Q. Wang, C. Xu, Y. Lu, H. Hu, B. Qin, Y. Wang, D. He, C. Li, X. Yu, S. Wang, J. Liu, MitoTEMPO prevents oxalate induced injury in NRK-52E cells via inhibiting mitochondrial dysfunction and modulating oxidative stress, Oxid Med Cell Longev 2017 (2017) 7528090.

[296] R.J. Fontana, Acute liver failure including acetaminophen overdose, Med Clin North Am 92(4) (2008) 761-94, viii.

[297] D.N. Dhanasekaran, E.P. Reddy, JNK signaling in apoptosis, Oncogene 27(48) (2008) 6245-51.

[298] Y. Xu, S. Huang, Z.G. Liu, J. Han, Poly(ADP-ribose) polymerase-1 signaling to mitochondria in necrotic cell death requires RIP1/TRAF2-mediated JNK1 activation, J Biol Chem 281(13) (2006) 8788-95.

[299] H. Jaeschke, M.L. Bajt, Intracellular signaling mechanisms of acetaminophen-induced liver cell death, Toxicol Sci 89(1) (2006) 31-41.

[300] H. Malhi, G.J. Gores, Cellular and molecular mechanisms of liver injury, Gastroenterology 134(6) (2008) 1641-54.

[301] J.D. Coombes, S.S. Choi, M. Swiderska-Syn, P. Manka, D.T. Reid, E. Palma, M.A. Briones-Orta, G. Xie, R. Younis, N. Kitamura, M. Della Peruta, S. Bitencourt, L. Dolle, Y.H. Oo, Z. Mi, P.C. Kuo, R. Williams, S. Chokshi, A. Canbay, L.C. Claridge, B. Eksteen, A.M. Diehl, W.K. Syn, Osteopontin is a proximal effector of leptin-mediated non-alcoholic steatohepatitis (NASH) fibrosis, Biochim Biophys Acta 1862(1) (2016) 135-44.